

## Supporting Information

# **Selective Multi-Electron Aggregation at a Hypervalent Iodine Center by Sequential Disproportionation**

Phong Thai,<sup>†</sup> Brandon L. Frey,<sup>†</sup> Matthew T. Figgins,<sup>†</sup>  
Richard R. Thompson,<sup>†</sup> Raanan Carmieli,<sup>#</sup> and David C. Powers<sup>†,\*</sup>

<sup>†</sup>Department of Chemistry, Texas A&M University, College Station, TX 77843, United States.

<sup>#</sup>Department of Chemical Research Support, Weizmann Institute of Science, Rehovot, Israel.

Email: [powers@chem.tamu.edu](mailto:powers@chem.tamu.edu)

## Table of Contents

A. General Considerations	
A.1 Materials	S3
A.2 Characterization Details	S3
A.3 X-ray Diffraction Details	S4
A.4 Computational Method Details	S4
B. Synthesis and Characterization	S5
B.1 Investigation of the Role of Methoxy Substitution	S10
B.2 Determination of $K_{eq}$ for TFE Binding to <b>3</b>	S15
C. Supporting Data	S16
D. Computational Data	S28
E. X-ray Diffraction Data	S34
F. Additional Data	S46
F.1 Impact of O <sub>2</sub> and H <sub>2</sub> O on the Synthesis of <b>2</b>	S46
F.2 Procedure for the Electrosynthesis of <b>3</b> , <b>3</b> ·HClO <sub>4</sub> , and <b>5</b>	S47
F.3 Optimization for the Electrosynthesis of <b>5</b>	S52
F.4 Control Reactions	S56
G. NMR Spectra for New Compounds	S59
H. References	S71

## A. General Considerations

**A.1 Materials** All chemicals and solvents were obtained as ACS reagent grade and used as received, unless otherwise noted. 2,4,6-Trimethylpyridine and sodium nitrite ( $\text{NaNO}_2$ ) were acquired from BeanTown Chemical (BTC). Potassium chlorate ( $\text{KClO}_3$ ) and silver nitrate ( $\text{AgNO}_3$ ) were purchased from Alfa Aesar. Potassium peroxymonosulfate (Oxone<sup>®</sup>) was purchased from Tokyo Chemical Industry (TCI). Potassium ethyl xanthate (KEX), 2,2,2-trifluoroethanol (TFE), sodium thiosulfate ( $\text{Na}_2\text{SO}_3$ ), lithium perchlorate ( $\text{LiClO}_4$ ), 1,1,1,3,3,3-hexafluoroisopropanol (HFIP), boron trifluoride diethyl etherate ( $\text{BF}_3 \cdot \text{OEt}_2$ ), bis(trifluoroacetoxy)iodobenzene (PIFA), and pyridine were acquired from Oakwood. Iodine ( $\text{I}_2$ ), *n*-butyllithium (*n*-BuLi), mesitylene, cobalt(II) chloride ( $\text{CoCl}_2 \cdot 6\text{H}_2\text{O}$ ), *tert*-butyl alcohol (*t*-BuOH), acetaldehyde, acetic anhydride ( $\text{Ac}_2\text{O}$ ), 2,6-lutidine, thiophenol (PhSH), hexanes, ethyl acetate (EtOAc), diethyl ether ( $\text{Et}_2\text{O}$ ), and dichloromethane were obtained from Sigma Aldrich. 2-Bromo-5-methoxyaniline was obtained from Ambeed, Inc. Glacial acetic acid (AcOH), perchloric acid ( $\text{HClO}_4$ , 70 wt% solution), hydrochloric acid (HCl), potassium hydroxide (KOH), sodium hydroxide (NaOH), and anhydrous magnesium sulfate ( $\text{MgSO}_4$ ) were obtained from VWR. Acetonitrile (MeCN), ethanol (EtOH), methanol (MeOH), tetrahydrofuran (THF, HPLC grade), and carbon tetrachloride ( $\text{CCl}_4$ ) were obtained from Fischer Scientific. Dry THF was obtained from a drying column and stored over activated 4 Å molecular sieves.<sup>1</sup> NMR solvents were purchased from Cambridge Isotope Laboratories (CIL) and were used as received. All reactions were carried out under ambient atmosphere unless otherwise noted. Pyridinium perchlorate ( $\text{Pyr} \cdot \text{HClO}_4$ ), 2,6-lutidinium perchlorate ( $\text{Lut} \cdot \text{HClO}_4$ ), 2,4,6-collidinium perchlorate ( $\text{Col} \cdot \text{HClO}_4$ ),<sup>1</sup> 2-(*tert*-butylsulfonyl)iodobenzene (**S1**),<sup>2</sup> 2-(*tert*-butylsulfonyl)iodosylbenzene (**S3**),<sup>2</sup> 2-(*tert*-butylsulfonyl)iodoxybenzene (**S5**),<sup>3</sup> 2-bromo-5-methoxybenzenethiol (**S6**),<sup>4</sup> and 2,2,2-trifluoroethoxide ( $\text{LiOCH}_2\text{CF}_3$ ) were synthesized according to literature methods.<sup>5</sup>

**A.2 Characterization Details** <sup>1</sup>H and <sup>13</sup>C NMR spectral acquisitions were recorded on an Inova 500 FT NMR (Varian), a VNMRs 500 FT NMR (Varian), or an Acsend<sup>™</sup> 400 NMR (Bruker) and were referenced against residual proteo solvent signals:  $\text{CDCl}_3$  (7.26 ppm, <sup>1</sup>H; 77.16 ppm, <sup>13</sup>C), acetonitrile-*d*<sub>3</sub> (1.94 ppm, <sup>1</sup>H, 1.32 ppm, <sup>13</sup>C), dimethylsulfoxide-*d*<sub>6</sub> (2.50 ppm, <sup>1</sup>H), and dichloromethane-*d*<sub>2</sub> (53.84 ppm, <sup>13</sup>C).<sup>6</sup> Proton (<sup>1</sup>H) NMR data are reported as follows: chemical shift ( $\delta$ , ppm), (multiplicity: s (singlet), d (doublet), t (triplet), q (quartet), m (multiplet), integration). <sup>13</sup>C NMR data are reported as follows: chemical shift ( $\delta$ , ppm). Mass spectrometry data were recorded on either Orbitrap Fusion<sup>™</sup> Tribrid<sup>™</sup> Mass Spectrometer or Q Exactive<sup>™</sup> Focus Hybrid Quadrupole-Orbitrap<sup>™</sup> Mass Spectrometer from ThermoFisher Scientific. UV-vis spectra were recorded at 23 °C in quartz cuvettes with 1.0 cm path length on an Ocean Optics Flame-S miniature spectrometer with DH-mini UV-vis NIR light source (200–900 nm) and were blanked against the appropriate solvent. Cyclic voltammetry (CV) experiments were carried out using CH Instruments Electrochemical Analyzer (Model CHI620A) in a three-electrode cell set-up. For CV experiments, a glassy carbon working electrode, Pt wire counter electrode, and Ag-reference electrode were used (obtained from CH Instruments). For constant potential electrolysis (CPE), Ag reference electrode, glassy carbon (GC), graphite (C), nickel (Ni), and platinum (Pt) electrodes were purchased from IKA. CPE experiments were carried out using CH Instruments

Electrochemical Analyzer (Model CHI620A or CHI620E) in a three-electrode cell set-up. All electrochemical experiments were carried out in a 10-mL Electrasyn glass vial (undivided cell set-up) or in a Pro-Divide electrochemical cell (divided cell set-up) purchased from IKA. Reference electrodes were prepared using a 0.10 M solution of [TBA]PF<sub>6</sub> in MeCN with 1.0 mM AgNO<sub>3</sub>. *In situ* EPR spectra were recorded at 295 K on a Bruker ELEXSYS E500 X-band spectrometer equipped with a ER4102ST resonator with a small electrochemical cell based on a Wilmad-LabGlass flat-cell for aqueous solutions (WG-808-A-Q) using the following experimental parameters: 1024 points with 20 mW microwave power, 0.01 mT modulation amplitude, 100 kHz modulation frequency, and a sweep range of 5 mT. A computer-controlled BioLogic SP-200 was used as potentiostat. Sample solutions were prepared under an N<sub>2</sub> atmosphere in a Sigma-Aldrich AtmosBag with 1 mM of appropriate analyte and 0.1 M of LiClO<sub>4</sub> as electrolyte in MeCN.

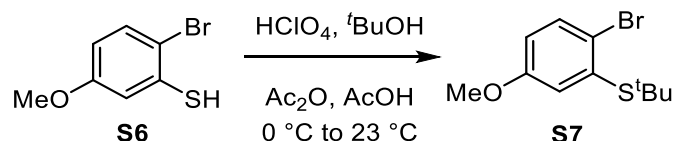
**A.3 X-Ray Diffraction Details** X-ray crystal structures of **1**, **3**, **3**·HClO<sub>4</sub>, **5**, **6**, and **S3**·HBF<sub>4</sub> were collected using a Bruker APEX 2 Duo X-ray (three-circle) diffractometer. Crystals were mounted on a MiTeGen dual-thickness micro-mount and placed under a cold N<sub>2</sub> stream (Oxford). The X-ray radiation employed was generated from a Mo sealed X-ray tube (K<sub>α</sub> = 0.70173 Å with a potential of 40 kV and a current of 40 mA). Bruker AXS APEX III software was used for data collection and reduction. Absorption corrections were applied using the program SADABS. A solution was obtained using XT/XS in APEX3 and refined in Olex2.<sup>7-9</sup> Hydrogen atoms were placed in idealized positions and were set riding on the respective parent atoms, unless otherwise stated. All non-hydrogen atoms were refined with anisotropic thermal parameters. The structure was refined (weighted least squares refinement on F<sup>2</sup>) to convergence.<sup>8</sup> The refinements for **1**, **3**, **3**·HClO<sub>4</sub>, **5**, **6**, and **S3**·HBF<sub>4</sub> have been deposited in the CCDC as (CCDC 2176972–2176975, 2189772, and 2234041).

**A.4 Computational Method Details** All computations were carried out using Revision C.01 of the Gaussian 16<sup>10</sup> suite of programs with the B3LYP<sup>11, 12</sup> functional in conjunction with Grimme's D3 empirical dispersion<sup>13</sup> and Becke-Johnson damping<sup>14</sup> [EMP = GD3BJ] The basis set combination (BS1) is as follows: def2-TZVPP+ECP<sup>15, 16</sup> for I and 6-31G(d')<sup>17</sup> (the 6-31G(d') basis set has the d polarization functions taken from the 6-311G(d)<sup>18</sup>) for H, B, C, O, F, and S. All computations were performed using an SMD<sup>18, 19</sup> implicit solvation model with parameters consistent with using 2-methyl-1-propanol as the solvent to better mimic the dielectric constant for HFIP. All minima were confirmed by an analytical frequency computation. UV-VIS absorption spectra were simulated by single point TD-DFT<sup>20</sup> calculations using the SMD- B3LYP-D3BJ/BS1 optimized geometry (SMD-TD-DFT// SMD-B3LYP-D3BJ/BS1) where the first 30 vertical excitations were solved iteratively. Orbital images were generated using GaussView6<sup>21</sup> with an isovalue of 0.02. GaussView6 was also used to visualize computed structures.

## B. Synthesis and Characterization

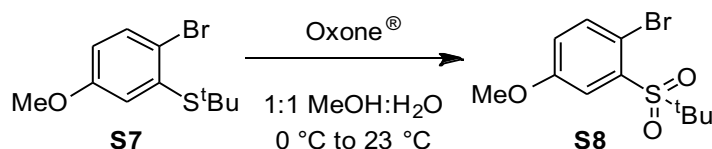
**SAFETY** Hypervalent iodine compounds and perchlorate salts can be explosive and should be treated with appropriate care. The authors did not encounter any issues working on the scales described in this document but have avoided heating the reported compounds in the absence of solvent.

### Synthesis of (2-bromo-5-methoxyphenyl)(tert-butyl)sulfane (**S7**)



A 100-mL round-bottomed flask was cooled to 0 °C and then charged with acetic acid (3.0 mL), perchloric acid (70 wt% solution, 1.74 mL), and acetic anhydride (1.0 mL). To this reaction mixture, 2-bromo-5-methoxybenzenethiol (**S6**, 3.17 g, 14.5 mmol, 1.00 equiv), *tert*-butanol (1.65 mL, 17.3 mmol, 1.20 equiv), and acetic acid (2.2 mL) were added. The reaction mixture was allowed to warm to 23 °C and was stirred overnight. The reaction mixture was poured into 30 mL of brine and extracted with diethyl ether (3 × 30 mL). The organic layers were combined, washed with saturated NaHCO<sub>3</sub> aqueous solution (until evolution of CO<sub>2</sub> ceased) and water, and were dried over Na<sub>2</sub>SO<sub>4</sub>. The solvent was removed *in vacuo* to afford a brown oil, which was used in the next step without further purification (3.56 g, 89% yield). A crude sample was characterized by NMR. <sup>1</sup>H NMR (δ 23 °C, 400 MHz, CDCl<sub>3</sub>): 7.55 (d, *J* = 8.71 Hz, 1H), 7.21 (d, *J* = 3.03 Hz, 1H), 6.77 (dd, *J* = 8.84, 3.11 Hz, 1H), 3.80 (s, 3H), 1.36 (s, 9H). <sup>13</sup>C NMR (δ 23 °C, 100 MHz, CDCl<sub>3</sub>): 158.5, 135.0, 133.9, 124.6, 123.0, 116.4, 55.7, 48.8, 31.2. HRMS-APCI: calculated for [M+H]<sup>+</sup> = 275.0100, 277.0079; observed [M+H]<sup>+</sup> = 275.0092, 277.0072.

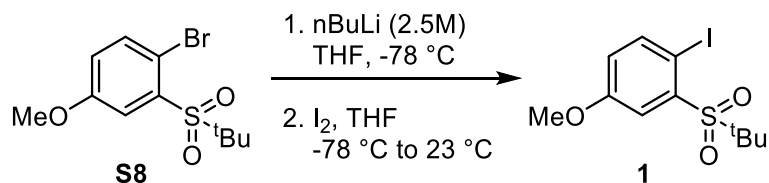
### Synthesis of 1-bromo-2-(tert-butylsulfonyl)-4-methoxybenzene (**S8**)



A 250-mL round-bottomed flask was charged with crude (2-bromo-5-methoxyphenyl)(*tert*-butyl)sulfane (**S7**, 3.56 g, 13.0 mmol, 1.00 equiv) from the previous reaction and methanol (60 mL) and was cooled to 0 °C. A solution of Oxone<sup>®</sup> (9.97 g, 32.4 mmol, 2.50 equiv) in water (60 mL) was added to the reaction mixture. The reaction mixture was allowed to warm to 23 °C and was stirred for 16 h. A second portion of Oxone<sup>®</sup> (797 mg, 2.59 mmol, 0.500 equiv) was added to the reaction mixture, which was allowed to stir for 16 h. Methanol was then removed under reduced pressure. Water (60 mL) was added to the residue, and the aqueous phase was extracted with diethyl ether (3 × 60 mL). The combined organic layers were washed with brine (60 mL) and dried over Na<sub>2</sub>SO<sub>4</sub>. The solvent was removed *in vacuo* and the residue was purified by SiO<sub>2</sub> chromatography (eluent 75:25 hexanes:ethyl acetate) to afford the title compound a yellow solid (1.90 g, 48% yield). <sup>1</sup>H NMR (δ, 23 °C, 400 MHz,

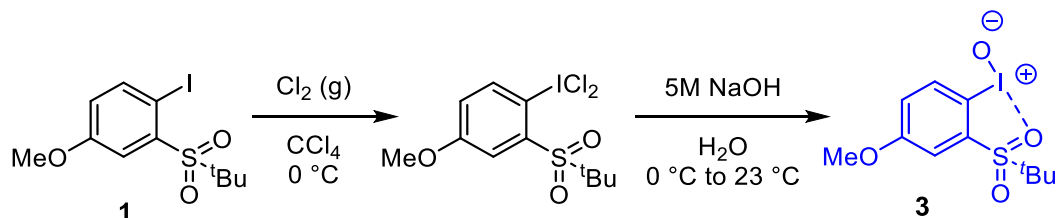
CDCl<sub>3</sub>): 7.64 (d, *J* = 8.78 Hz, 1H), 7.58 (d, *J* = 3.16 Hz, 1H), 6.99 (dd, *J* = 8.77, 3.11 Hz, 1H), 3.85 (s, 3H), 1.42 (s, 9H). <sup>13</sup>C NMR (δ 23 °C, 100 MHz, CDCl<sub>3</sub>): 158.8, 137.2, 135.7, 121.0, 120.0, 113.1, 62.8, 56.1, 24.2. HRMS-APCI: calculated for [M+H]<sup>+</sup> = 306.9998, 308.9978; observed [M+H]<sup>+</sup> = 306.9998, 308.9977.

### Synthesis of 2-(*tert*-butylsulfonyl)-1-iodo-4-methoxybenzene (**1**)



Under an N<sub>2</sub> atmosphere, a 150-mL Schlenk flask was charged with 1-bromo-2-(*tert*-butylsulfonyl)-4-methoxybenzene (**S8**, 1.90 g, 6.19 mmol, 1.00 equiv) and dry THF (12 mL) and was cooled to -78 °C. To this reaction solution, *n*-BuLi (2.5M in hexanes, 3.00 mL, 7.50 mmol, 1.21 equiv) was added dropwise, and the reaction mixture was stirred at -78 °C for 30 min before a solution I<sub>2</sub> (2.70 g, 10.6 mmol, 1.72 equiv) in dry THF (12 mL) was added. The reaction mixture was allowed to warm to 23 °C and was stirred overnight. The solvent was removed *in vacuo*, and saturated NH<sub>4</sub>Cl (30 mL) was added to the residue, and the aqueous layer was extracted with CH<sub>2</sub>Cl<sub>2</sub> (3 × 30 mL). The combined organic layers were washed with saturated Na<sub>2</sub>S<sub>2</sub>O<sub>3</sub> aqueous solution (20 mL) and dried over Na<sub>2</sub>SO<sub>4</sub>. The solvent was removed *in vacuo* and the residue was purified by SiO<sub>2</sub> chromatography (eluent 75:25 hexanes:ethyl acetate) to give a yellow solid, which was triturated in cold diethyl ether to afford the title compound as a white solid (1.86 g, 85% yield). <sup>1</sup>H NMR (δ, 23 °C, 400 MHz, CDCl<sub>3</sub>): 8.00 (d, *J* = 8.73 Hz, 1H), 7.62 (d, *J* = 3.04 Hz, 1H), 6.81 (dd, *J* = 8.69, 3.03 Hz, 1H), 3.84, (s, 3H), 1.43 (s, 9H). <sup>13</sup>C NMR (δ, 23 °C, 100 MHz, CDCl<sub>3</sub>): 159.8, 144.5, 138.5, 120.9, 120.0, 82.7, 62.8, 55.9, 24.4. HRMS-APCI: calculated for [M+H]<sup>+</sup> = 354.9859, observed [M+H]<sup>+</sup> = 354.9859. Colorless needle-like crystals suitable for single-crystal X-ray diffraction were grown by pentane vapor diffusion into a diethyl ether solution at 23 °C. The displacement ellipsoid plot is collected in Figure S18 and refinement details are collected in Table S7.

### Synthesis of 2-(*tert*-butylsulfonyl)-1-iodosyl-4-methoxybenzene (**3**)

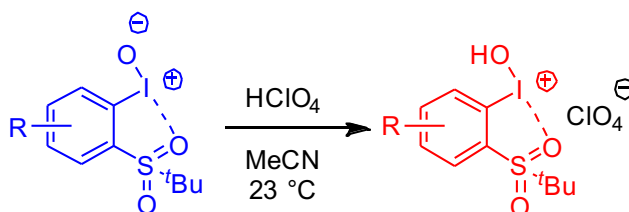


A 10-mL round-bottomed flask was charged with 2-(*tert*-butylsulfonyl)-1-iodo-4-methoxybenzene (**1**, 354 mg, 1.00 mmol, 1.00 equiv) and CCl<sub>4</sub> (1.50 mL), and the suspension was stirred at 0 °C. In another separate round-bottomed flask, conc. HCl (3.0 mL, 36 mmol, 36 equiv) was added in one portion to stirring solid potassium chlorate (735 mg, 6.00 mmol, 6.00 equiv). The generated Cl<sub>2</sub> gas was transferred to the reaction mixture using Tygon<sup>®</sup> tubing and glass fittings. This process was repeated two more times to afford a bright-yellow

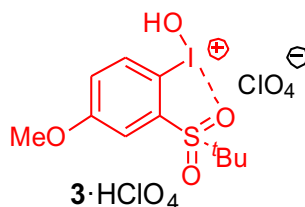
solid, which was isolated by filtration, washed with ice-cold water (20 mL), and used in the next reaction without further purification.

A 25-mL round-bottomed flask was charged with the yellow solid obtained from the previous step and was cooled to 0 °C. To this reaction vessel, an ice-cold aqueous NaOH solution (5.0 M, 1.5 mL, 7.5 mmol, 7.5 equiv) was added dropwise. The reaction mixture was stirred for 20 min at 0 °C before ice-cold water (2.0 mL) was added. The reaction mixture was allowed to warm to 23 °C and was stirred for 16 h. The obtained solid was isolated by filtration, washed with ice-cold water (20 mL), and obtained as a bright-yellow solid (201 mg, 54% yield). <sup>1</sup>H NMR (δ, 23 °C, 400 MHz, CD<sub>3</sub>CN): 7.75 (d, *J* = 8.87 Hz, 1H), 7.53 (dd, *J* = 9.12, 2.84 Hz, 1H), 7.42 (d, *J* = 2.90 Hz, 1H), 3.92 (s, 3H), 1.38 (s, 9H). <sup>13</sup>C NMR (δ, 23 °C, 100 MHz, CD<sub>2</sub>Cl<sub>2</sub>): 161.4, 132.7, 127.3, 121.0, 118.3, 104.4, 63.3, 56.3, 23.3. HRMS-APCI: calculated for [M+H]<sup>+</sup> = 370.9808, observed [M+H]<sup>+</sup> = 370.9791. Yellow crystals suitable for single-crystal X-ray diffraction were grown by diffusion of toluene into a CHCl<sub>3</sub> solution at -22 °C. The displacement ellipsoid plot is collected in Figure S19 and refinement details are collected in Table S8.

### Synthesis of (2-(*tert*-butylsulfonyl) phenyl)(hydroxy)iodonium perchlorate (3·HClO<sub>4</sub>) derivatives

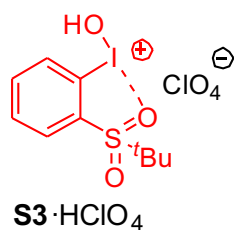


A 20-mL scintillation vial was charged with HClO<sub>4</sub> (70 wt% solution, 41.3 mg, 0.275 mmol, 1.10 equiv) and MeCN (2.00 mL) at 23 °C. To this stirring solution, a 2-(*tert*-butylsulfonyl)iodosylbenzene derivative (0.250 mmol, 1.00 equiv) was added slowly over 30 s. Cold ether (10 mL) was then added to the reaction mixture to induce precipitation of a solid, which was isolated by filtration and washed with cold ether (6.0 mL).



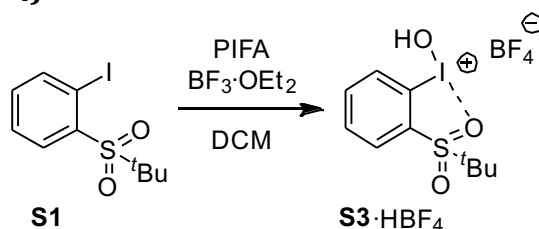
(2-(*tert*-butylsulfonyl)-4-methoxyphenyl)(hydroxy)iodonium perchlorate (3·HClO<sub>4</sub>). Prepared from 2-(*tert*-butylsulfonyl)-1-iodosyl-4-methoxybenzene **3** (92.5 mg) and obtained as a white solid (47 mg, 40% yield). <sup>1</sup>H NMR (δ, 23 °C, 400 MHz, CD<sub>3</sub>CN): 8.18 (br, 1H), 7.78 (d, *J* = 9.27 Hz, 1H), 7.73 (dd, *J* = 9.08, 2.63 Hz, 1H), 7.59 (d, *J* = 2.64 Hz, 1H), 4.01 (s, 3H), 1.51 (s, 9H). <sup>13</sup>C NMR (δ, 23 °C, 100 MHz, CD<sub>3</sub>CN): 164.1, 132.4, 129.3, 124.9, 120.3, 105.3, 67.2, 57.8, 23.3. HRMS-APCI: calculated for [M]<sup>+</sup> = 370.9808, observed [M]<sup>+</sup> = 370.9791. Colorless needle-like crystals suitable for single-crystal X-ray diffraction characterization were grown by diffusion of diethyl ether into an MeCN solution of 2-(*tert*-butylsulfonyl)-1-iodosyl-4-methoxybenzene (**3**, 35.4 mg, 0.100 mmol, 1.00 equiv) and HClO<sub>4</sub> (70 wt% solution, 25 μL,

1.0 equiv) at 23 °C. The displacement ellipsoid plot is collected in Figure S20 and refinement details are collected in Table S9.



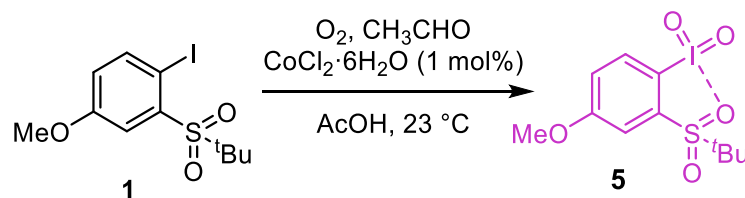
(2-(*tert*-butylsulfonyl)phenyl)(hydroxy)iodonium perchlorate (**S3·HClO<sub>4</sub>**). Prepared from 2-(*tert*-butylsulfonyl)iodosylbenzene **S3** (85.0 mg) and obtained as a white solid (84 mg, 76% yield). <sup>1</sup>H NMR (d, 23 °C, 400 MHz, CD<sub>3</sub>CN): 8.23 (td, *J* = 8.16, 1.51 Hz, 1H), 8.16 (dd, *J* = 8.07, 1.69 Hz, 1H), 8.07 (br, 1H), 7.97 (t, *J* = 7.89 Hz, 2H), 1.48 (s, 9H). <sup>13</sup>C NMR (δ, 23 °C, 100 MHz, CD<sub>3</sub>CN): 139.2, 135.3, 133.7, 131.1, 128.4, 117.5, 67.1, 23.2. HRMS-ESI: calculated for [M]<sup>+</sup> = 340.9703, observed [M]<sup>+</sup> = 340.9700.

### Characterization of (2-(*tert*-butylsulfonyl)phenyl)(hydroxy)iodonium tetrafluoroborate (**3·HBF<sub>4</sub>**)



A 20-mL scintillation vial was charged with 2-(*tert*-butylsulfonyl)iodobenzene **S1** (38.9 mg, 0.120 mmol, 1.00 equiv), PIFA (26.0 mg, 60.0 μmol, 0.500 equiv), and CH<sub>2</sub>Cl<sub>2</sub> (1.5 mL). The reaction mixture was cooled to -20 °C, and BF<sub>3</sub>·OEt<sub>2</sub> (15.2 μL, 0.120 mmol, 1.00 equiv) was added slowly. The mixture was further stirred at -20 °C for 3 h, then it was filtered through celite and cooled at -20 °C for 16 h, which resulted in colorless needle-like crystals suitable for single-crystal X-ray diffraction. The displacement ellipsoid plot is collected in Figure S23 and refinement details are collected in Table S12.

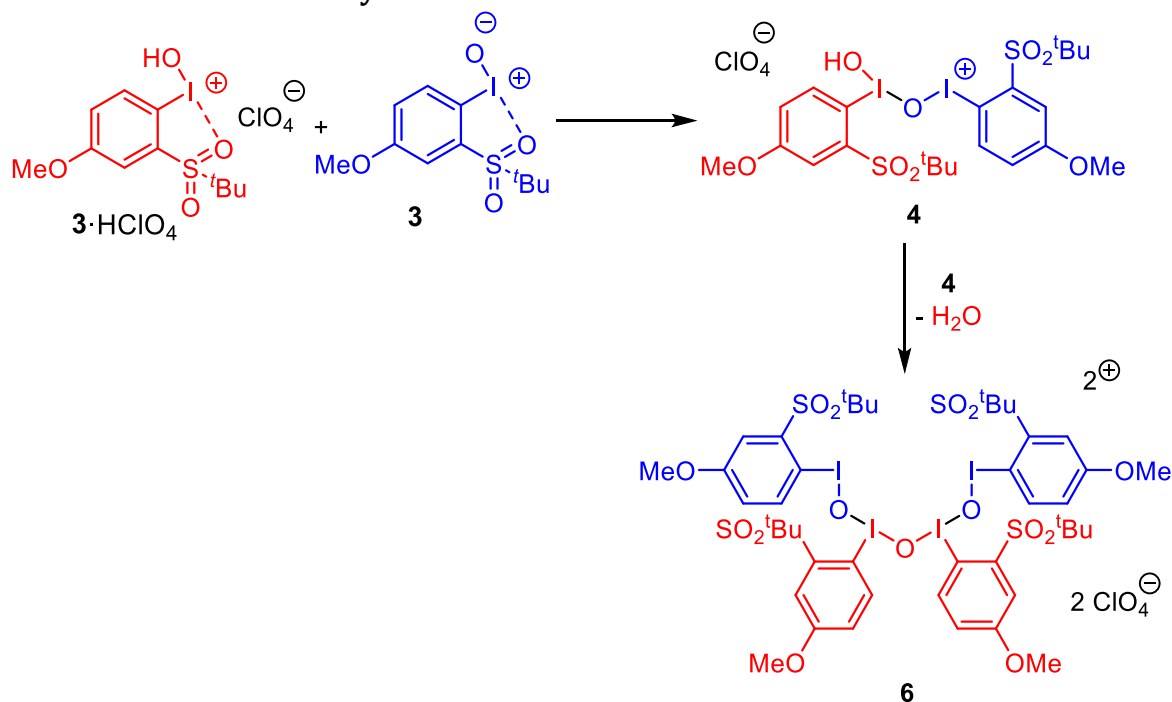
### Synthesis of 2-(*tert*-butylsulfonyl)-1-iodoxy-4-methoxybenzene (**5**)



A 20-mL scintillation vial was charged with 2-(*tert*-butylsulfonyl)-1-iodo-4-methoxybenzene (**1**, 142 mg, 0.400 mmol, 1.00 equiv), CoCl<sub>2</sub>·6H<sub>2</sub>O (0.9 mg, 4 μmol, 1 mol%),

and acetic acid (2.0 mL). The reaction vessel was fitted with a rubber septum and was purged with O<sub>2</sub> for 5 min before acetaldehyde (224 μL, 4.07 mmol, 10.0 equiv) was added in one portion. The reaction mixture was stirred under 1 atm O<sub>2</sub> delivered by an inflated balloon for 12 h at 23 °C. The solvent was removed *in vacuo*, and the residue was treated with 3:1 diethyl ether : CH<sub>2</sub>Cl<sub>2</sub> to induce precipitation. The solid was isolated by filtration, washed with cold hexanes, and dried *in vacuo* to afford a white solid (90 mg, 58% yield). <sup>1</sup>H NMR (δ, 23 °C, 400 MHz, (CD<sub>3</sub>)<sub>2</sub>SO): 8.37 (d, *J* = 8.81 Hz, 1H), 7.68 (dd, *J* = 8.86, 2.21 Hz, 1H), 7.30 (d, *J* = 2.61 Hz, 1H), 3.94 (s, 3H), 1.34 (s, 9H). <sup>13</sup>C NMR (δ, 23 °C, 100 MHz, (CD<sub>3</sub>)<sub>2</sub>SO): 161.6, 138.9, 133.8, 126.3, 119.8, 116.0, 61.4, 56.4, 23.2. HRMS-APCI: calculated for [M+H]<sup>+</sup> = 386.9758, observed [M+H]<sup>+</sup> = 386.9744. Yellow crystals suitable for single-crystal X-ray diffraction were grown by diffusion of pentane into a CH<sub>2</sub>Cl<sub>2</sub> solution at -22 °C. The displacement ellipsoid plot is collected in Figure S21 and refinement details are collected in Table S10.

### Characterization of Iodosylbenzene Tetramer 6

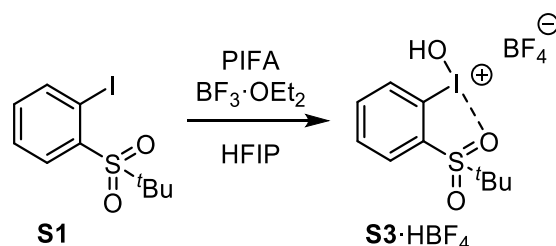


Yellow crystals of 6 suitable for characterization were grown from a 75% (v/v) TFE/MeCN solution consisting of equimolar 3 and 3·HClO<sub>4</sub> with ether slow diffusion at -22 °C. The displacement ellipsoid plot is collected in Figure S22 and refinement details are collected in Table S11.

## B.1 Investigation of the Role of Methoxy Substitution

The *para*-methoxy substituent in aryl iodide **1** stabilizes the resulting radical cation, which both facilitates electrolysis and enables observation of the transient iodanyl radical. In the absence of a methoxy group, no transient intermediate was observed in the oxidation of **S1** by PIFA/  $\text{BF}_3 \cdot \text{OEt}_2$  (Figure S1). The electrolysis of **S1** in TFE or MeCN to yield **S3** and **S3**· $\text{HClO}_4$ , respectively, was achievable, albeit at a higher potential (Figure S2–S4). In the electrolysis of **S1** in a TFE/MeCN solvent mixture, the product **S5** was not observed (Figure S4). Figure S5 depicts the cyclic voltammograms of aryl iodide **S1** in TFE and MeCN.

### Observation in the Oxidation of Aryl Iodide **S1** by PIFA and $\text{BF}_3 \cdot \text{OEt}_2$ .



A 20-mL scintillation vial was charged with 2-(*tert*-butylsulfonyl)iodobenzene **S1** (20.4 mg, 63.0  $\mu\text{mol}$ , 1.00 equiv),  $\text{BF}_3 \cdot \text{OEt}_2$  (8.0  $\mu\text{L}$ , 63  $\mu\text{mol}$ , 1.0 equiv), and HFIP (0.75 mL). To this colorless solution was added a solution of PIFA (27.1 mg, 63.0  $\mu\text{mol}$ , 1.00 equiv) dissolved in HFIP (0.25 mL) resulting in a faint yellow solution, which remained during the duration of the experiment. No transient absorption was observed even when the reaction was carried out at 0 °C. The reaction mixture was stirred at 23 °C for 30 min, then it was concentrated *in vacuo*. To the residual was added 1.0 mL of MeCN and mesitylene as an internal standard. An aliquot (0.10 mL) of the reaction mixture was taken, diluted with  $\text{CD}_3\text{CN}$  (0.50 mL), and analyzed by  $^1\text{H}$  NMR (41% yield of **S3**· $\text{HBF}_4$ ). The  $^1\text{H}$  NMR spectral data of the solution is in good agreement with an externally prepared sample of **S3**· $\text{HClO}_4$  in  $\text{CD}_3\text{CN}$  (Figure S1).

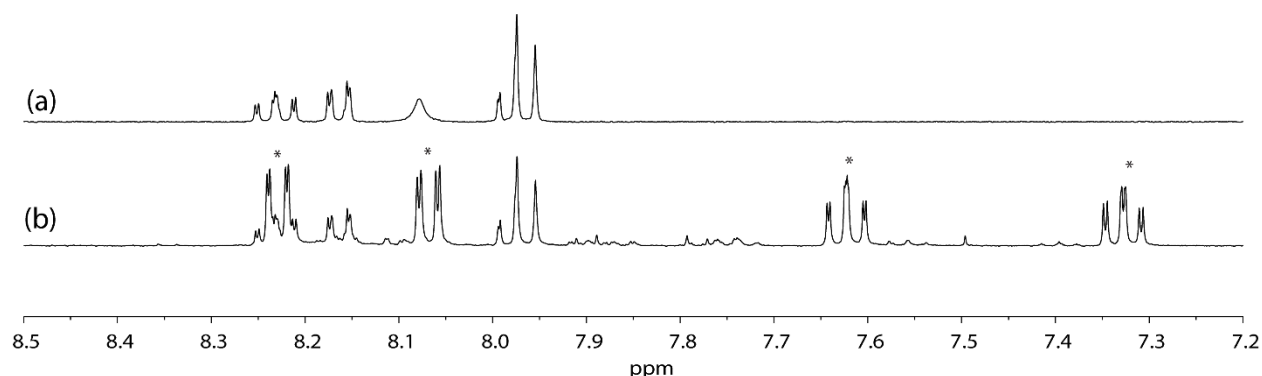
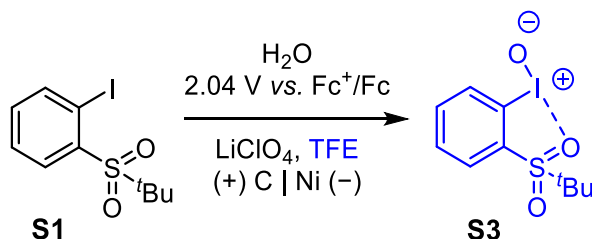


**Figure S1.** NMR spectra (23 °C, 400 MHz,  $\text{CD}_3\text{CN}$ ) of: (a) independently synthesized **S3**· $\text{HClO}_4$ , (b) aliquot of reaction mixture of **S1** in MeCN. The asterisk (\*) indicates signals associated with aryl iodide **S1**.

## Electrosynthesis of 2-(*tert*-butylsulfonyl)iodosylbenzene (**S3**)



A 10-mL glass vial was charged with 2-(*tert*-butylsulfonyl)iodobenzene (**S1**, 40.5 mg, 0.125 mmol, 1.00 equiv), water (4.50  $\mu$ L, 0.250 mmol, 2.00 equiv), lithium perchlorate (53.0 mg, 0.500 mmol, 4.00 equiv), and TFE (5.0 mL), and was fitted with a graphite anode, nickel cathode, and  $\text{Ag}^+/\text{Ag}$  reference electrode. A constant potential of 2.20 V vs.  $\text{Ag}^+/\text{Ag}$  (2.04 V vs.  $\text{Fc}^+/\text{Fc}$ ) was applied to the reaction mixture with stirring at 400 rpm, 23  $^\circ\text{C}$  until 30 C charge (2.5 F/mol) was passed. The electrolysis was then stopped, and mesitylene was added as an internal standard. An aliquot (0.10 mL) of the reaction mixture was taken, diluted with  $\text{CD}_3\text{CN}$  (0.50 mL), and analyzed by  $^1\text{H}$  NMR spectroscopy (60% yield, 48% faradaic efficiency). Spectral data obtained following electrolysis of **S1** is well-matched to that obtained for externally synthesized **S3** dissolved in TFE (Figure S2).

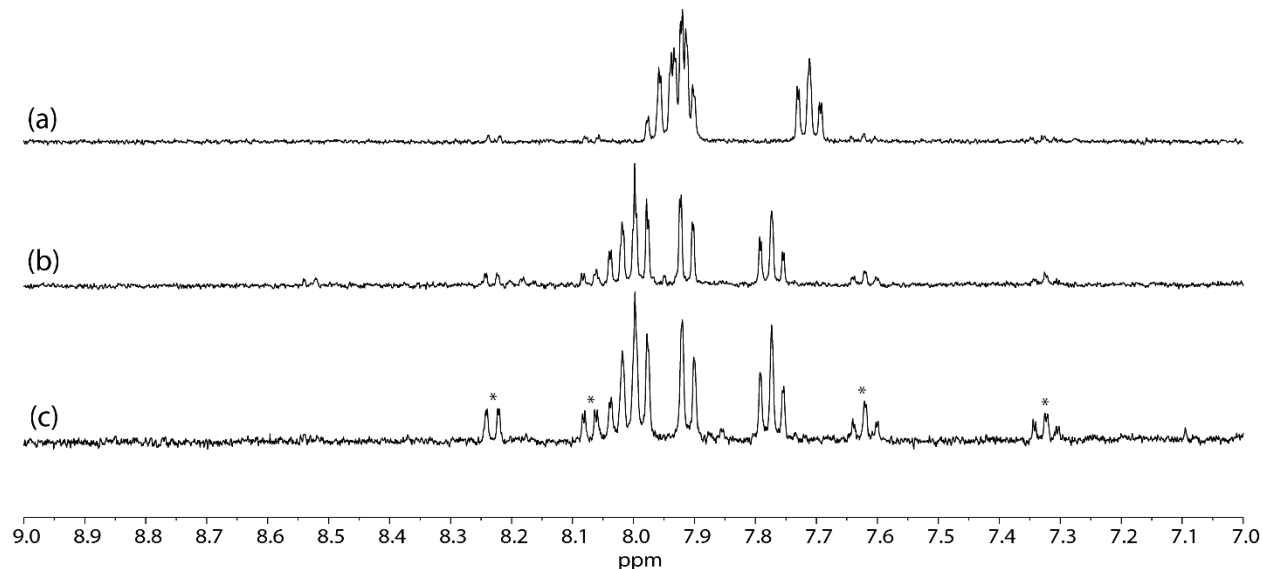
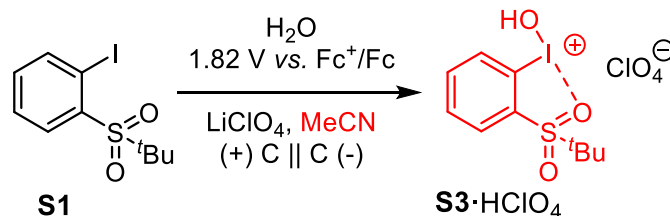


**Figure S2.** NMR spectra (23  $^\circ\text{C}$ , 400 MHz,  $\text{CD}_3\text{CN}$ ) of: (a) independently synthesized **S3** in the absence of TFE, (b) aliquot of independently synthesized **S3** in TFE, (c) aliquot of electrolysis mixture of **S1** in TFE. The asterisk (\*) indicates signals associated with aryl iodide **S1**.

## Electrosynthesis of (2-(*tert*-butylsulfonyl)phenyl)(hydroxy)iodonium perchlorate (**S3**·HClO<sub>4</sub>)



The anodic cell of a 5-mL divided cell was charged with 2-(*tert*-butylsulfonyl)-1-iodo-4-methoxybenzene (**1**, 40.5 mg, 0.125 mmol, 1.00 equiv), water (4.5  $\mu$ L, 0.25 mmol, 2.0 equiv), lithium perchlorate (106 mg, 1.00 mmol, 8.00 equiv), and MeCN (5.0 mL), and was fitted with a graphite electrode and an Ag<sup>+</sup>/Ag reference electrode. The cathodic cell was charged with lithium perchlorate (106 mg, 1.00 mmol, 8.00 equiv) and MeCN (5.0 mL), and was fitted with a graphite electrode. A constant potential of 1.96 V vs. Ag<sup>+</sup>/Ag (1.82 V vs. Fc<sup>+</sup>/Fc) was applied to the reaction mixture with stirring at 400 rpm, 23 °C until 27 C charge (3.5 F/mol) was passed. The electrolysis was then stopped, and mesitylene was added to the anodic cell as an internal standard. An aliquot (0.10 mL) of the reaction mixture in the anodic cell was taken, diluted with CD<sub>3</sub>CN (0.50 mL), and analyzed by NMR spectroscopy (78% yield, 454% faradaic efficiency). Spectral data obtained following electrolysis of **S1** is well-matched to that obtained for independently synthesized **S3**·HClO<sub>4</sub> (Figure S3).

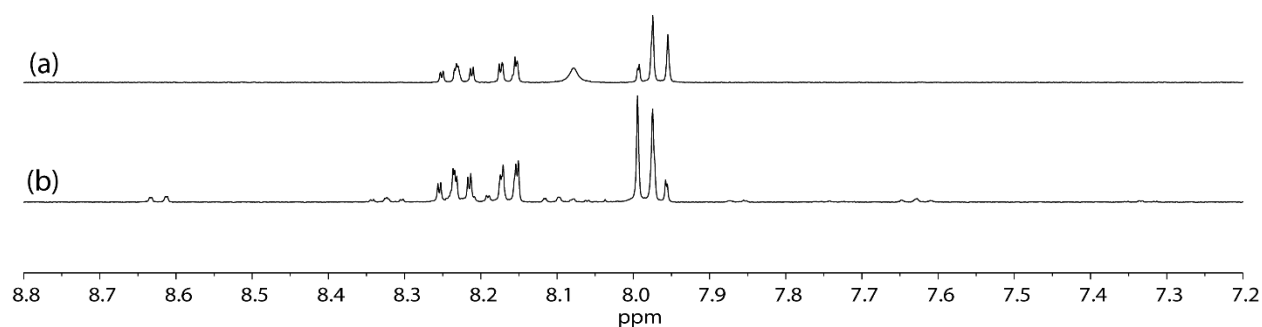
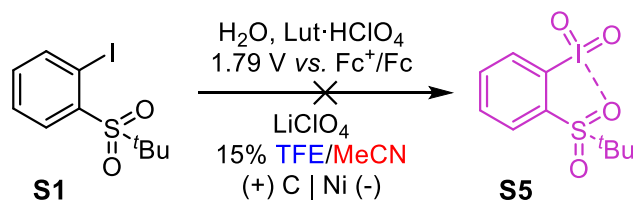


**Figure S3.** NMR spectra (23 °C, 400 MHz, CD<sub>3</sub>CN) of: (a) independently synthesized **S3**·HClO<sub>4</sub>, (b) aliquot of electrolysis mixture of **S1** in MeCN.

## Attempt at the Electrosynthesis of 2-(*tert*-butylsulfonyl)iodoxybenzene (**S5**)



A 10-mL glass vial was charged with 2-(*tert*-butylsulfonyl)iodobenzene (**S1**, 40.5 mg, 0.125 mmol, 1.00 equiv), lutidinium perchlorate (64.9 mg, 0.313 mmol, 2.50 equiv), water (4.50  $\mu\text{L}$ , 0.250 mmol, 2.00 equiv), lithium perchlorate (53.0 mg, 0.500 mmol, 4.00 equiv), MeCN (3.25 mL), and TFE (0.75 mL), and was fitted with a graphite anode, nickel cathode, and  $\text{Ag}^+/\text{Ag}$  reference electrode. A constant potential of 1.94 V vs.  $\text{Ag}^+/\text{Ag}$  (1.79 V vs.  $\text{Fc}^+/\text{Fc}$ ) was applied to the reaction mixture with stirring at 400 rpm, 23 °C until 48 C of charge (4.0 F/mol) was passed. Mesitylene was added as an internal standard. An aliquot (0.10 mL) of the reaction mixture was taken, diluted with  $\text{CD}_3\text{CN}$  (0.50 mL), and analyzed by  $^1\text{H}$  NMR spectroscopy. The product **S5** was not observed, while the decomposition product *tert*-butylsulfonylbenzene was detected in 19% NMR yield. The  $^1\text{H}$  NMR spectral data of the electrolysis solution lacks spectral features of **S5** when compared to that of an externally synthesized **S5** dissolved in  $\text{CD}_3\text{CN}$  (Figure S4).

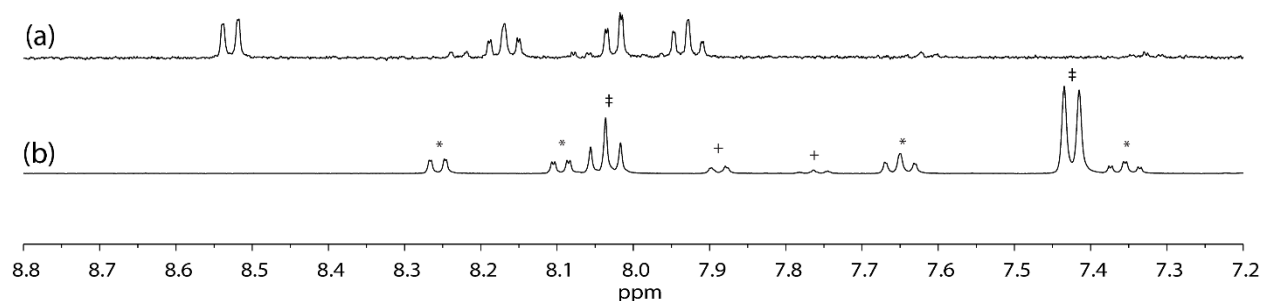


**Figure S4.** NMR spectra (23 °C, 400 MHz,  $\text{CD}_3\text{CN}$ ) of: (a) independently synthesized **S5**, (b) aliquot of electrolysis mixture of **S1** in 15% TFE/MeCN. The asterisk (\*) indicates signals associated with aryl iodide **S1**. The double dagger (‡) relates to signals of 2,6-lutidinium perchlorate. The plus sign (+) relates to signals of *tert*-butylsulfonylbenzene.

### Cyclic Voltammogram of Aryl Iodide S1

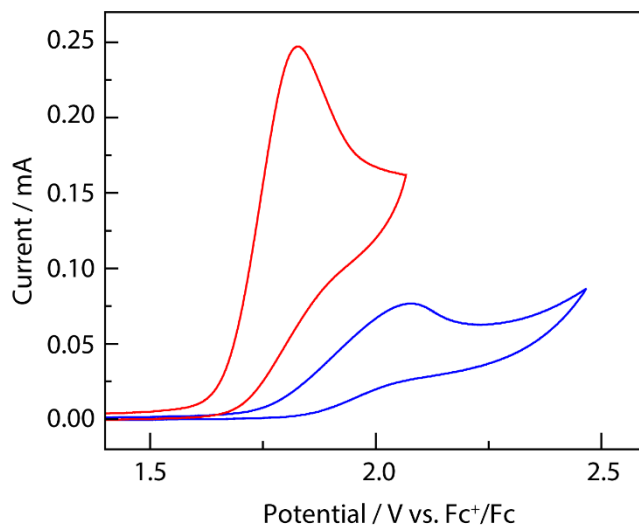


**Figure S5. CV of 2-(*tert*-butylsulfonyl)iodobenzene (S1) in TFE (—) and MeCN (—).** CV conditions: 5.0 mM of S1, 0.10 M LiClO<sub>4</sub> solution of TFE or MeCN, glassy carbon working electrode, Pt wire counter electrode, Ag<sup>+</sup>/Ag reference electrode, and scan rate 0.10 V/s. The CV was externally referenced to Fc<sup>+</sup>/Fc.

## B.2 Determination of $K_{eq}$ for TFE Binding to **3**

To determine the  $K_{eq}$  for the complexation of TFE to **3**, a test tube was charge with  $CD_3CN$  (0.60 mL), 2-(*tert*-butylsulfonyl)-1-iodosyl-4-methoxybenzene (**3**, 2.8 mg, 7.6  $\mu$ mol), and mesitylene (2.70 mg, 22.5  $\mu$ mol). The solution was filtered through Celite and the filtrate was added to an NMR tube. A  $^1H$  NMR spectrum was recorded. Then, TFE was added incrementally (1.0  $\mu$ L, 14  $\mu$ mol portions) via a 10  $\mu$ L syringe. The NMR cavity was maintained at 23.0  $^\circ$ C throughout the experiment. A visualization for the spectral changes is presented in Figure S15.

The equilibrium constant for adduct formation between **3** and TFE was calculated via Eqn S1.<sup>22</sup>

$$K_{eq} = \frac{\Delta\delta_{obs}}{(\Delta\delta_{CA} - \Delta\delta_{obs}) \left( [TFE] - \frac{[3]\Delta\delta_{obs}}{\Delta\delta_{CA}} \right)} \quad (S1)$$

where:

$\Delta\delta_{obs}$  = difference between the spectrum of **3** and the spectrum of **3** acquired with TFE  
 $\Delta\delta_{CA}$  = change in chemical shift between the completely complexed and uncomplexed **3**  
 $\Delta\delta_{CA}$  was determined by plugging in values for two measurements into equation S1 and setting them equal to each other. This was repeated for multiple measurements to ensure the consistency of the value.  $\Delta\delta_{CA}$  was determined to be 0.0336 ppm.  $K_{eq}$  was then calculated individually for 14 different concentrations of TFE. It was found that  $K_{eq} = 13.5 \pm 0.6$  and that  $\Delta G = -1.51 \pm 0.02$  kcal/mol.

### C. Supporting Data

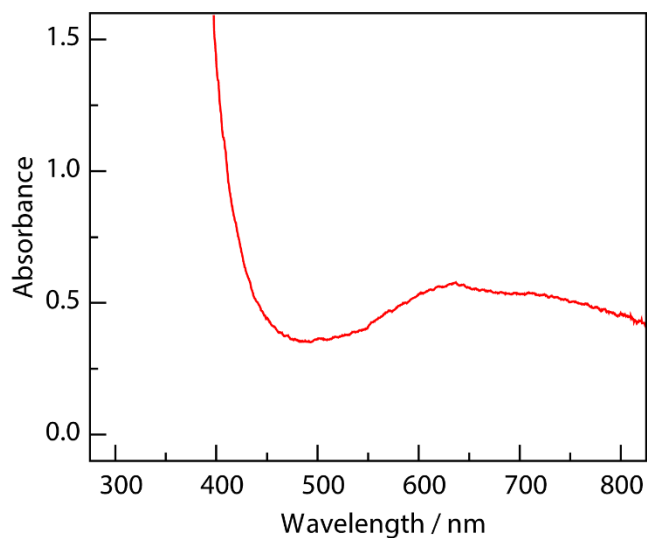
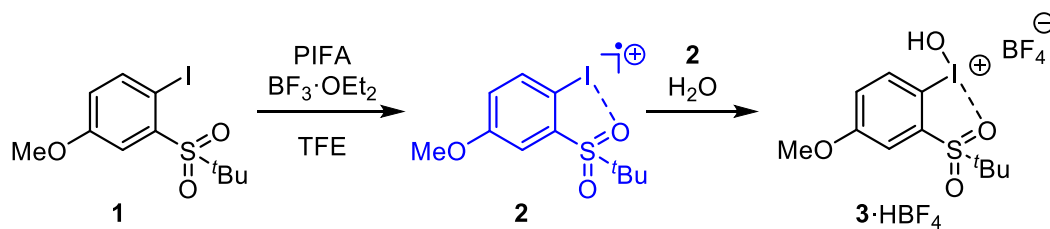


**Figure S6. UV-vis spectrum of the iodanyl radical **2** generated in TFE.** Procedure: A cuvette was charged with 2-(*tert*-butylsulfonyl)-1-iodo-4-methoxybenzene (**1**, 112 mg, 0.315 mmol, 1.00 equiv),  $\text{BF}_3 \cdot \text{OEt}_2$  (400  $\mu\text{L}$ , 0.320 mmol, 1.02 equiv), and HFIP (3.0 mL) at 23  $^\circ\text{C}$ . To this cuvette was added a solution of PIFA (70.0, 0.163 mmol, 0.517 equiv) dissolved in TFE (0.5 mL). A UV-vis spectrum of the solution was acquired immediately after the addition. The absorbance at 637 completely bleached after 10 s, which was too rapid to reliably collect kinetic data.

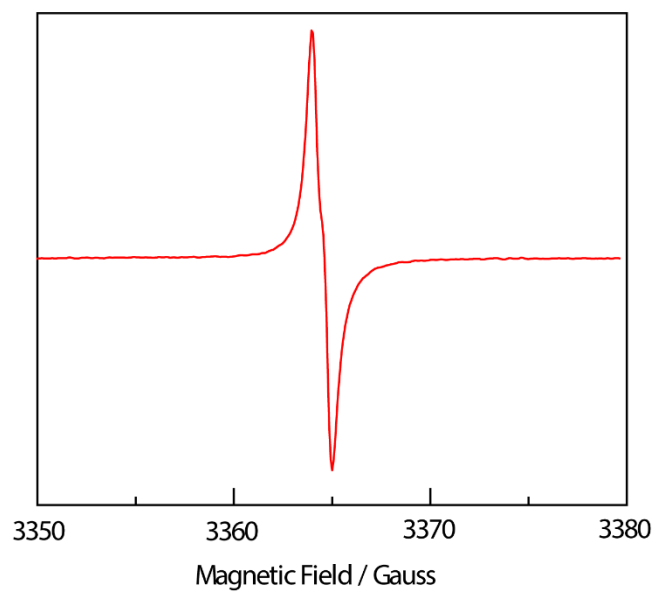
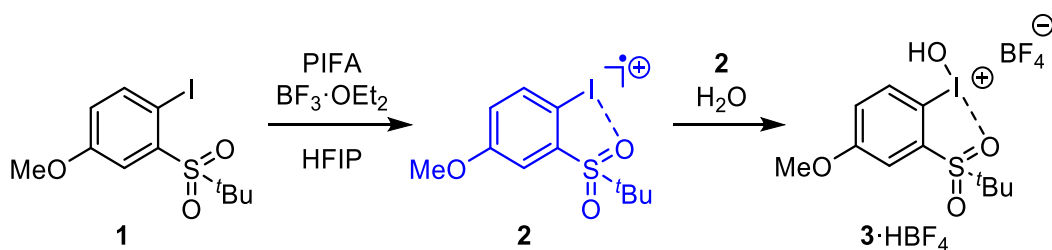


**Figure S7.** *In situ* EPR spectrum obtained from a 1.0 mM 2-(*tert*-butylsulfonyl)-1-iodo-4-methoxybenzene (**1**) in 0.10 M LiClO<sub>4</sub> solution of MeCN electrolyzed at 1.51 V vs Fc<sup>+</sup>/Fc.



A cuvette was charged with 2-(*tert*-butylsulfonyl)-1-iodo-4-methoxybenzene **1** (5.6 mg, 16  $\mu\text{mol}$ , 1.0 equiv),  $\text{BF}_3 \cdot \text{OEt}_2$  (2.0  $\mu\text{L}$ , 16  $\mu\text{mol}$ , 1.0 equiv), and HFIP (3.0 mL) at 23  $^\circ\text{C}$ . To this cuvette was added a solution of PIFA (3.5 mg, 8.1  $\mu\text{mol}$ , 0.50 equiv) dissolved in HFIP (0.5 mL). The cuvette was then capped, inverted twice to mix, and subjected to UV-Vis analysis. The spectral bleaching over time is depicted in Figure S7a. The kinetic plots of zeroth, first, and second order of absorbance at 647 nm versus time are detailed in Figure S7b–d.

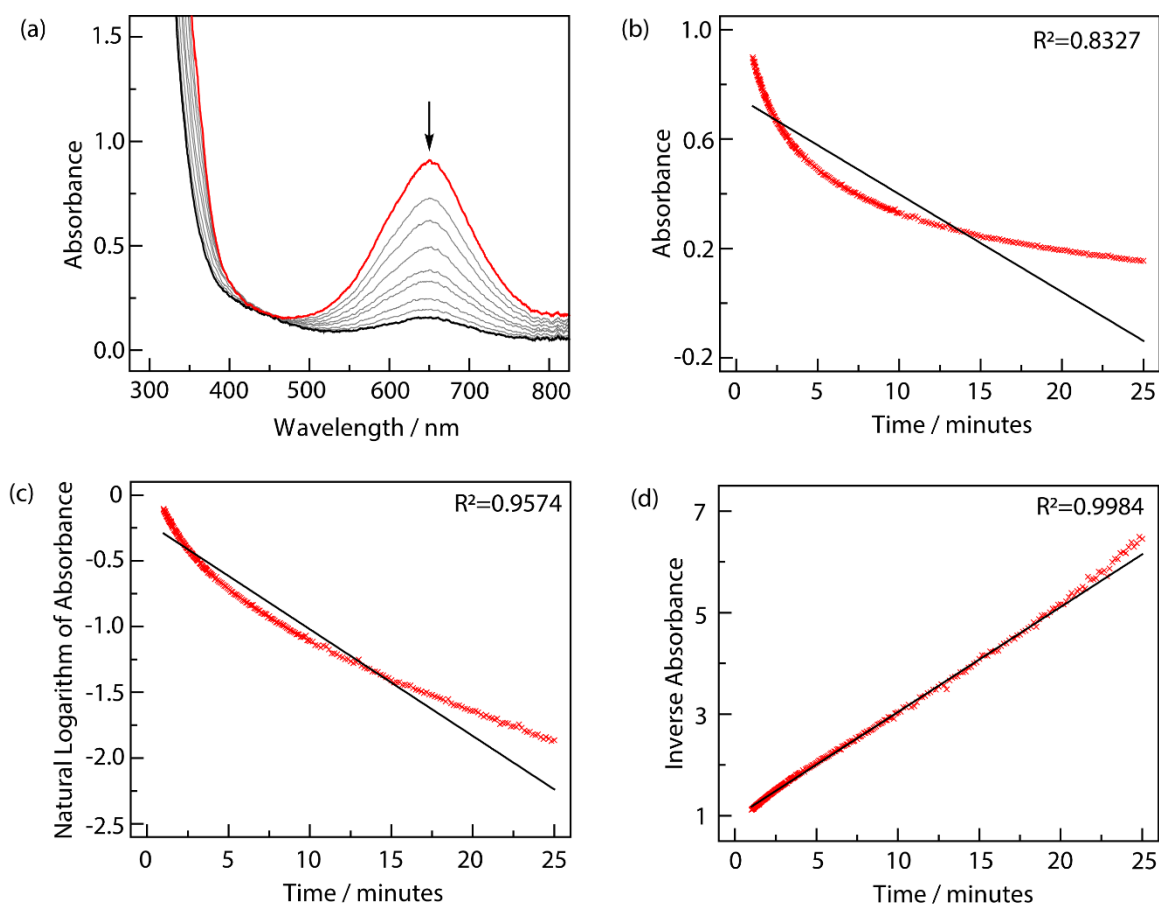
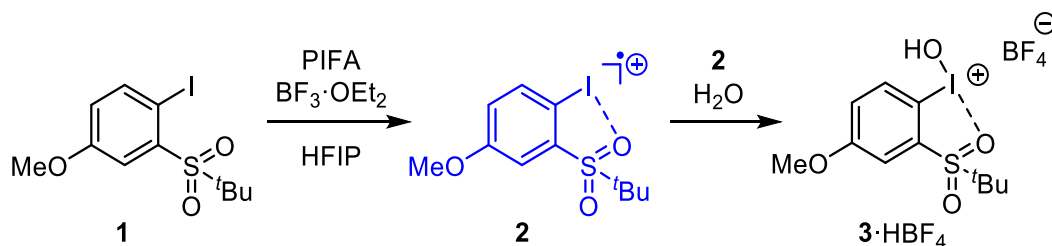
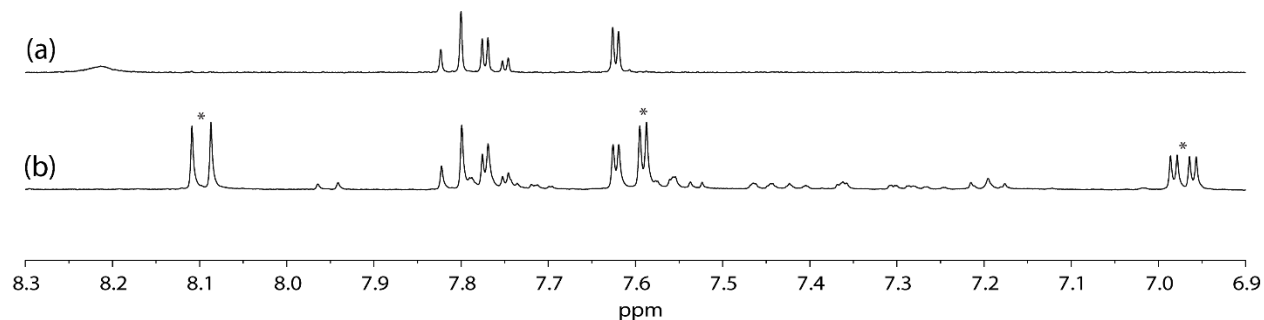


**Figure S8.** (a) UV-vis spectra depicting the color bleaching of a solution of iodanyl radical **2** obtained over 25 min. (b) Plot of  $\text{Abs}_{647}$  ( $\times$ ) and linear fit (—) vs. time. (c) Plot of  $\ln(\text{Abs}_{647})$  ( $\times$ ) and linear fit (—) vs. time. (d) Plot of  $(1/\text{Abs}_{647})$  ( $\times$ ) and linear fit (—) vs. time.

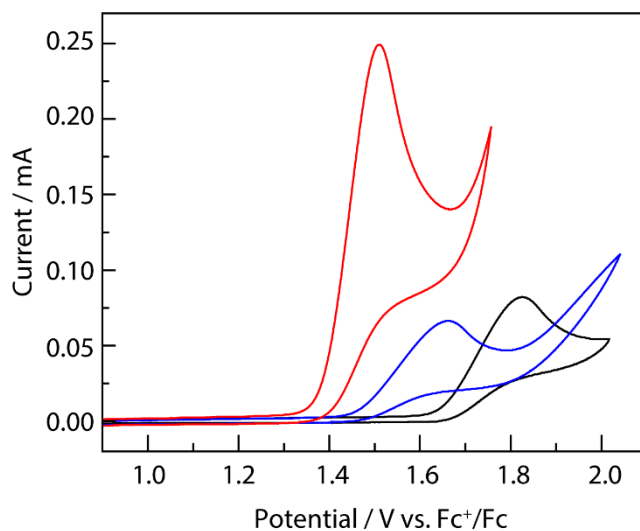
**Identification of the I(III) disproportionation product following the synthesis of iodanyl radical 2.**



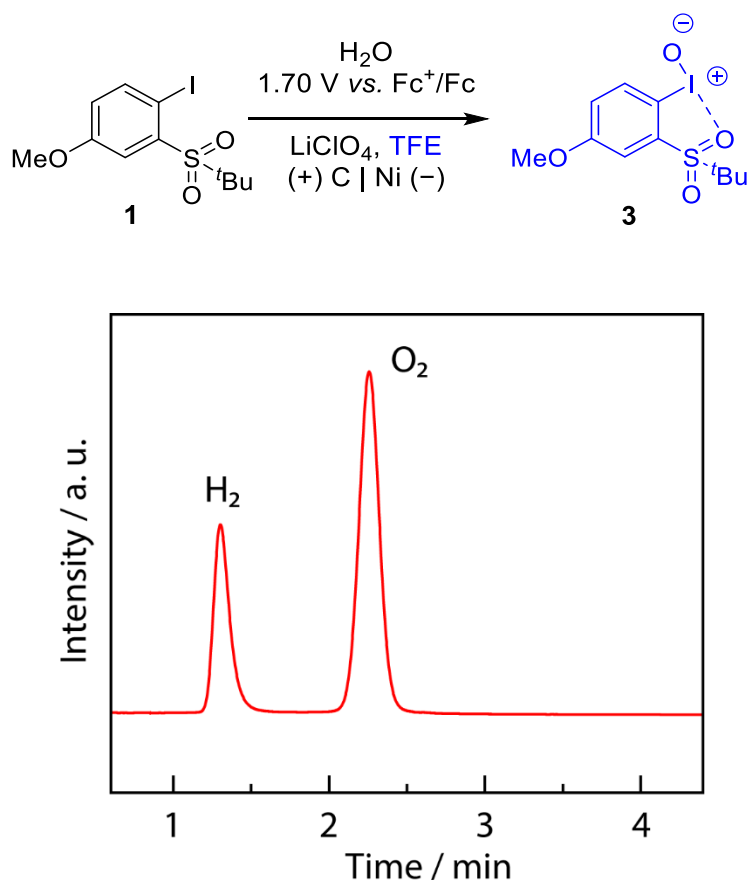
A 20-mL scintillation vial was charged with 2-(*tert*-butylsulfonyl)-1-iodo-4-methoxybenzene **1** (22.3 mg, 63.0  $\mu\text{mol}$ , 1.00 equiv),  $\text{BF}_3 \cdot \text{OEt}_2$  (8.0  $\mu\text{L}$ , 64  $\mu\text{mol}$ , 1.0 equiv), and HFIP (0.75 mL). To this cuvette was added a solution of PIFA (27.1 mg, 63.0  $\mu\text{mol}$ , 1.00 equiv) dissolved in HFIP (0.25 mL) resulting in an immediate blue color consistent with the spectral data represented in Figure S3a. The reaction mixture was stirred at 23 °C for 30 min, then the reaction mixture concentrated *in vacuo*. To the residual was added 1.0 mL of MeCN and mesitylene as an internal standard. An aliquot (0.10 mL) of the reaction mixture was taken, diluted with  $\text{CD}_3\text{CN}$  (0.50 mL), and analyzed by  $^1\text{H}$  NMR (41% yield of **3**· $\text{HBF}_4$  with 46% remaining **1**). The  $^1\text{H}$  NMR spectral data of the solution is in good agreement with an externally prepared sample of **3**· $\text{HClO}_4$  in  $\text{CD}_3\text{CN}$  (Figure S8).



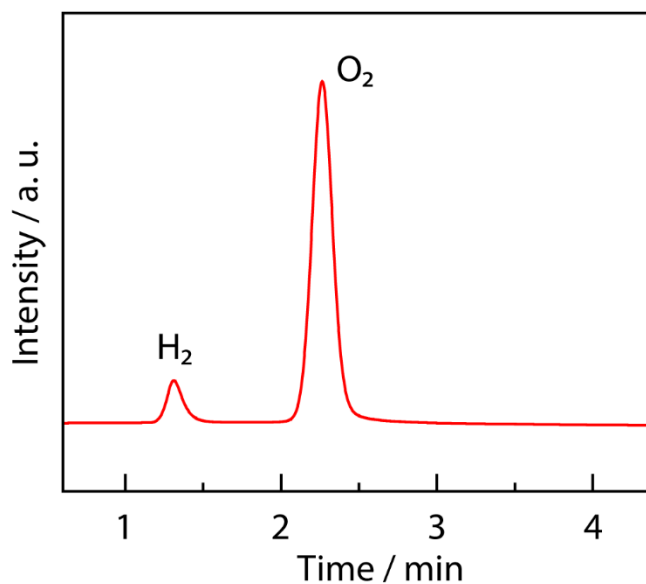
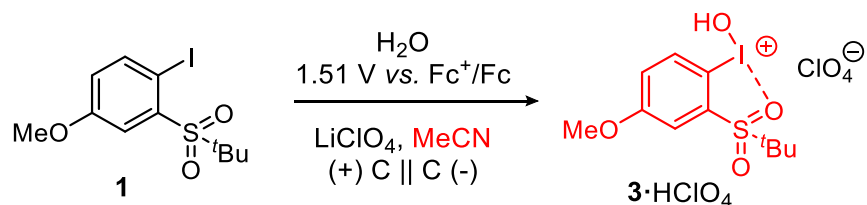
**Figure S9.** NMR spectra (23 °C, 400 MHz,  $\text{CD}_3\text{CN}$ ) of: (a) **3**· $\text{HClO}_4$ , (b) aliquot of reaction mixture of **1** in MeCN. The asterisk (\*) indicates signals associated with aryl iodide **1**.



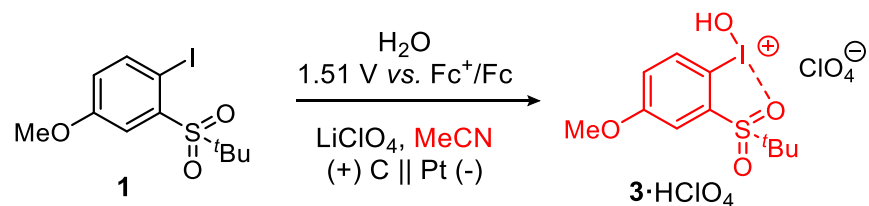
**Figure S10. CV of 2-(*tert*-butylsulfonyl)-1-iodo-4-methoxybenzene (**1**) in various solvents: HFIP (—), TFE (—), and MeCN (—). CV conditions: 5.0 mM of **1** in 10 mL solvent with 0.10 M of supporting electrolyte (HFIP: TBAPF<sub>6</sub>; TFE and MeCN: LiClO<sub>4</sub>), glassy carbon working electrode, Pt wire counter electrode, Ag<sup>+</sup>/Ag reference electrode, and scan rate 0.10 V/s. The CV was externally referenced to Fc<sup>+</sup>/Fc.**



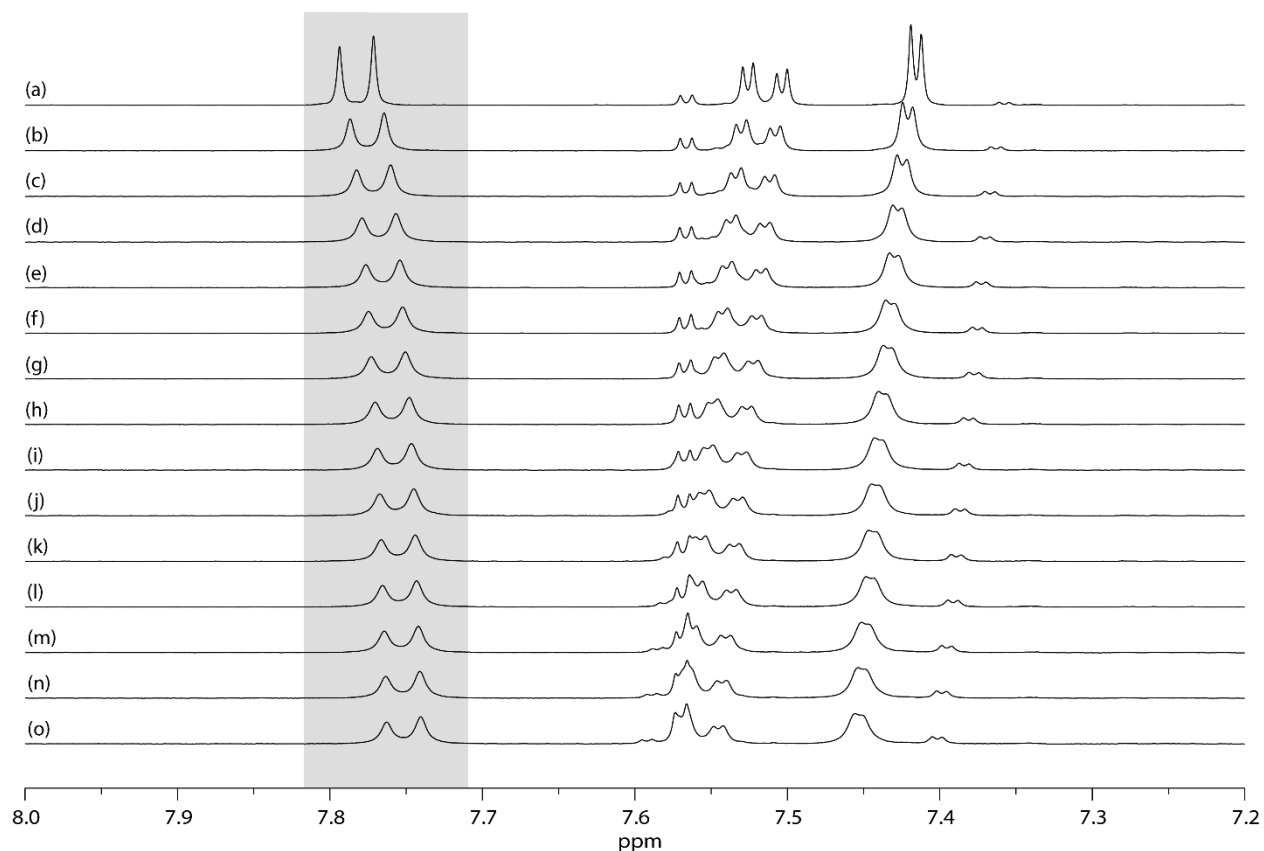
**Figure S11. Gas chromatograph of headspace of the electrolysis of **1** to generate **3** in TFE.** Procedure: A 10-mL glass vial was charged with 2-(*tert*-butylsulfonyl)-1-iodo-4-methoxybenzene (**1**, 44.3 mg, 0.125 mmol, 1.00 equiv), water (4.50  $\mu$ L, 0.250 mmol, 2.00 equiv), lithium perchlorate (53.0 mg, 0.500 mmol, 4.00 equiv), and TFE (5.0 mL), and was fitted with a graphite anode, nickel cathode, and Ag<sup>+</sup>/Ag reference electrode. A constant potential of 1.86 V vs. Ag<sup>+</sup>/Ag (1.70 V vs. Fc<sup>+</sup>/Fc) was applied to the reaction mixture with stirring at 400 rpm, 23 °C until 24 C charge (2.0 F/mol) was passed. The electrolysis was then stopped, and the headspace of the reaction mixture was analyzed by gas chromatography. The oxygen (O<sub>2</sub>) peak is due to the ambient conditions used for reaction set-up. The headspace volume was 9.5 cm<sup>3</sup>. The volume of the empty reaction chamber (14.5 cm<sup>3</sup>) was determined via measuring the volume of acetone needed to fill the chamber.



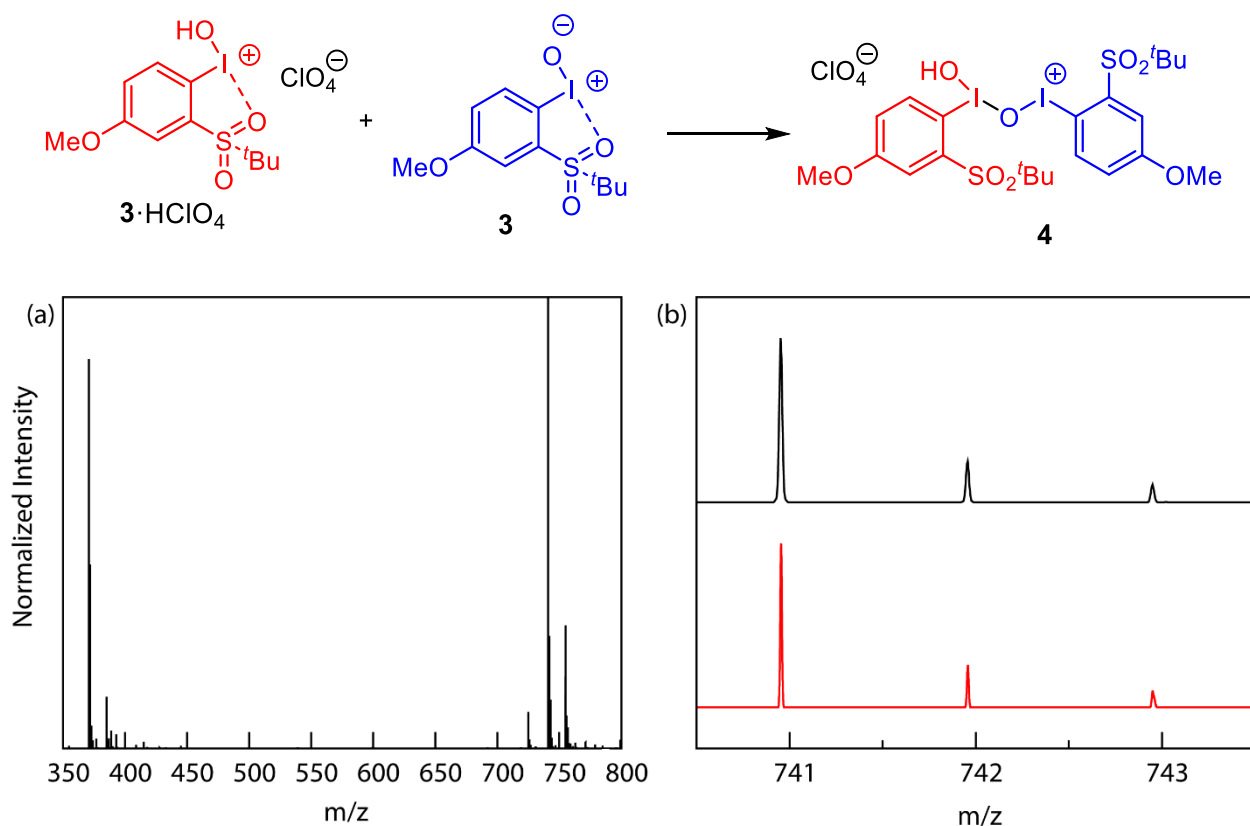
**Figure S12. Gas chromatograph of headspace of the electrolysis of 1 to generate 3·HClO<sub>4</sub> in MeCN.** Procedure: The anodic cell of a 5-mL divided cell fitted with a frit was charged with 2-(*tert*-butylsulfonyl)-1-iodo-4-methoxybenzene (**1**, 44.3 mg, 0.125 mmol, 1.00 equiv), water (4.5  $\mu$ L, 0.25 mmol, 2.0 equiv), lithium perchlorate (106 mg, 1.00 mmol, 8.00 equiv), and MeCN (5.0 mL), and was fitted with a graphite electrode and an Ag<sup>+</sup>/Ag reference electrode. The cathodic cell was charged with lithium perchlorate (106 mg, 1.00 mmol, 8.00 equiv) and MeCN (5.0 mL), and was fitted with a graphite electrode. A constant potential of 1.65V vs. Ag<sup>+</sup>/Ag (1.51 V vs. Fc<sup>+</sup>/Fc) was applied to the reaction mixture with stirring at 400 rpm, 23 °C until 27 C charge (2.3 F/mol) was passed. The electrolysis was then stopped, and the headspace of the reaction mixture was analyzed by gas chromatography. The oxygen (O<sub>2</sub>) peak is due to the ambient conditions used for reaction set-up. The headspace volume was 5.0 cm<sup>3</sup>. The volume of the empty cathodic chamber (10.0 cm<sup>3</sup>) was determined via measuring the volume of acetone needed to fill the chamber.



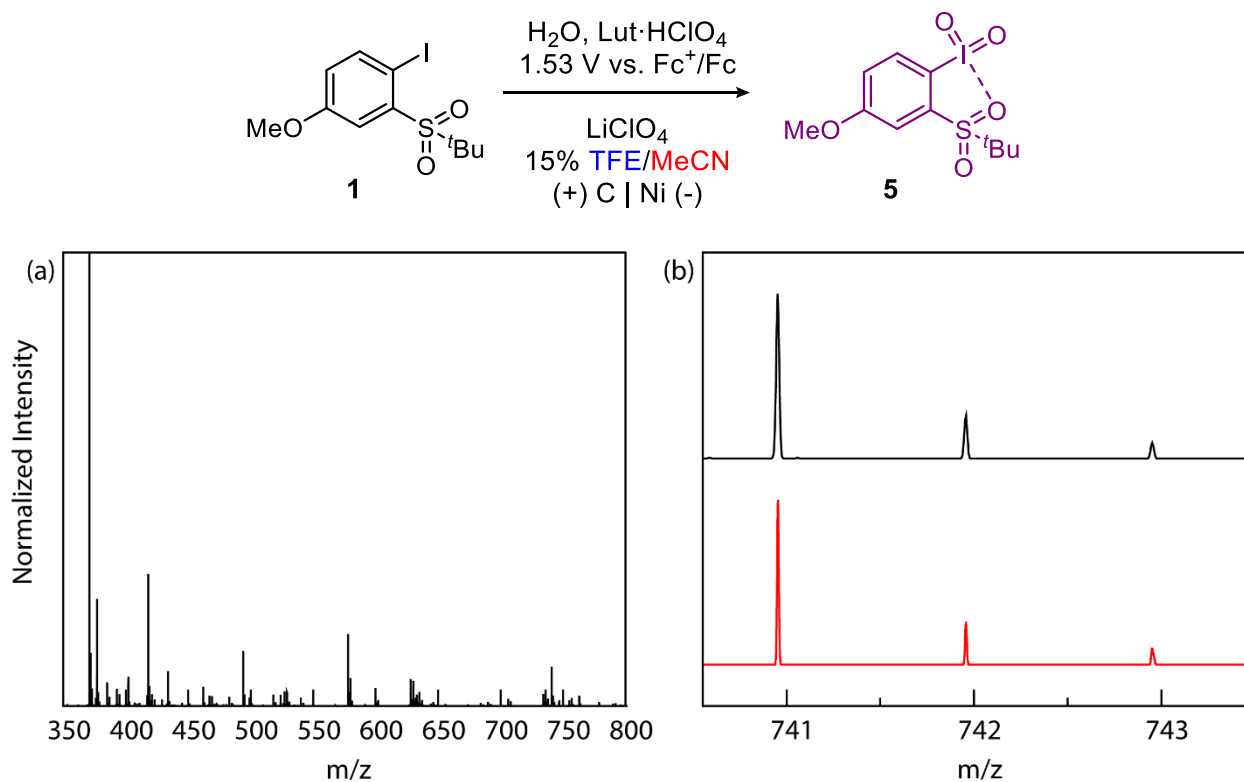
**Figure S13. Electrosynthesis of (2-(*tert*-butylsulfonyl)-4-methoxyphenyl)(hydroxy)iodonium perchlorate (3·HClO<sub>4</sub>) using platinum as the cathode instead of graphite.** Black deposition resulting from lithium cation reduction in the electrochemical synthesis of 3·HClO<sub>4</sub>.<sup>23</sup> Procedure: The anodic cell of a 5-mL divided cell fitted with a frit was charged with 2-(*tert*-butylsulfonyl)-1-iodo-4-methoxybenzene **1** (44.3 mg, 0.125 mmol, 1.00 equiv), water (4.5 μL, 0.25 mmol, 2.0 equiv), lithium perchlorate (106 mg, 1.00 mmol, 8.0 equiv), and MeCN (5.0 mL), and was fitted with a graphite electrode and an Ag<sup>+</sup>/Ag reference electrode. The cathodic cell was charged with lithium perchlorate (106 mg, 1.00 mmol, 8.00 equiv) and MeCN (5.0 mL), and was fitted with a platinum electrode. A constant potential of 1.65V vs. Ag<sup>+</sup>/Ag (1.51 V vs. Fc<sup>+</sup>/Fc) was applied to the reaction mixture with stirring at 400 rpm, 23 °C until 10 C charge (0.83 F/mol) was passed. The electrolysis was then stopped, and the platinum counter electrode was examined.



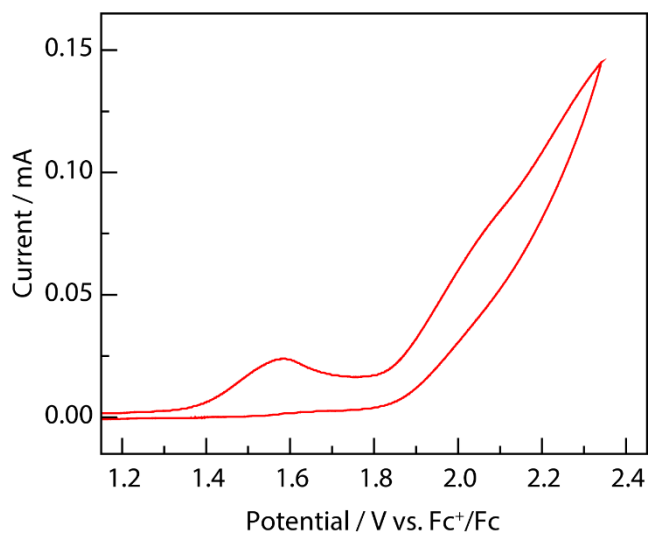
**Figure S14.**  $^1\text{H}$  NMR spectra of **3** in the presence of TFE obtained at 23.0 °C in  $\text{CD}_3\text{CN}$ . (a) 0  $\mu\text{L}$  TFE, (b) 1.0  $\mu\text{L}$  TFE, (c) 2.0  $\mu\text{L}$  TFE, (d) 3.0  $\mu\text{L}$  TFE, (e) 4.0  $\mu\text{L}$  TFE, (f) 5.0  $\mu\text{L}$  TFE, (g) 6.0  $\mu\text{L}$  TFE, (h) 8.0  $\mu\text{L}$  TFE, (i) 10.0  $\mu\text{L}$  TFE, (j) 12.0  $\mu\text{L}$  TFE, (k) 14.0  $\mu\text{L}$  TFE, (l) 16.0  $\mu\text{L}$  TFE, (m) 20.0  $\mu\text{L}$  TFE, (n) 24.0  $\mu\text{L}$  TFE, and (o) 28.0  $\mu\text{L}$  TFE. Monitoring the chemical shift as a function of  $[\text{TFE}]$  for the highlighted peak enabled determination of  $K_{\text{eq}}$  and  $\Delta G$  of TFE binding as described in Section B.2.



**Figure S15. Mass Spectrometric Analysis of a Mixture of **3** and **3**· $\text{HClO}_4$ .** Procedure: A test tube was charged with 2-(*tert*-butylsulfonyl)-1-iodosyl-4-methoxybenzene (**3**, 3.7 mg, 0.010 mmol, 1.0 equiv) and 15% TFE/ $\text{CD}_3\text{CN}$  (1.0 mL). A second test tube was charged with **3** (3.7 mg, 0.010 mmol, 1.0 equiv),  $\text{HClO}_4$  (70 wt% solution, 1.5 mg, 0.010 mmol, 1.0 equiv), and 15% TFE/ $\text{CD}_3\text{CN}$  (1.0 mL). The contents of the two test tubes are mixed, and an aliquot the resulting mixture was analyzed by mass spectrometry. (a) Positive-mode ESI-MS of a mixture of **3** and **3**· $\text{HClO}_4$ . (b) Expansion of the prospective region of the dimer **4** of the mass spectrum. HRMS-ESI: measured mass  $[\text{M}]^+ = 740.9526$  (—), and simulated mass  $[\text{M}]^+ = 740.9544$  (—).



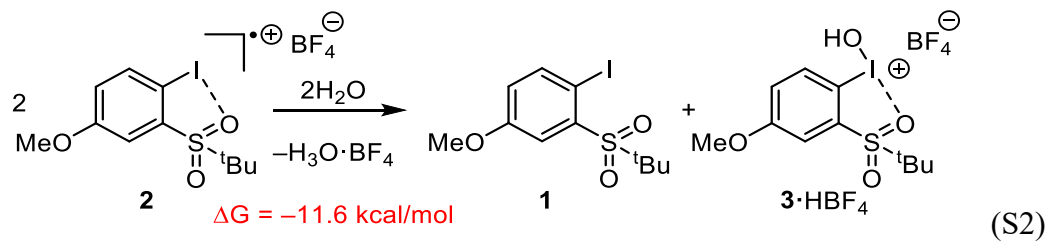
**Figure S16. Mass Spectrometric Analysis of the Electrochemical Synthesis of 2-(*tert*-butylsulfonyl)-1-iodoxy-4-methoxybenzene (**5**).** Procedure: A 10-mL glass vial was charged with 2-(*tert*-butylsulfonyl)-1-iodo-4-methoxybenzene (**1**, 44.3 mg, 0.125 mmol, 1.00 equiv), lutidinium perchlorate (64.9 mg, 0.313 mmol, 2.50 equiv), water (4.50  $\mu\text{L}$ , 0.250 mmol, 2.00 equiv), lithium perchlorate (53.0 mg, 0.500 mmol, 4.00 equiv), MeCN (3.25 mL), and TFE (0.75 mL), and was fitted with a graphite anode, nickel cathode, and  $\text{Ag}^+/\text{Ag}$  reference electrode. A constant potential of 1.68V vs.  $\text{Ag}^+/\text{Ag}$  (1.53 V vs.  $\text{Fc}^+/\text{Fc}$ ) was applied to the reaction mixture with stirring at 400 rpm, 23  $^\circ\text{C}$  until 60 C charge (5.0 F/mol) was passed. The electrolysis was then stopped, and an aliquot of the reaction mixture was analyzed by mass spectrometry. (a) Positive-mode ESI-MS flowing the electrolysis of 2-(*tert*-butylsulfonyl)-1-iodo-4-methoxybenzene **1**. The spectrum shows the presence of the I(III) products **3** and **3** $\cdot\text{HClO}_4$  (HRMS-ESI: measured mass  $[\text{M}]^+ = 370.9803$ , calculated for  $[\text{M}]^+ = 370.9808$ ), the I(V) product **5** (HRMS-ESI: measured mass  $[\text{M}+\text{H}]^+ = 386.9297$ , calculated for  $[\text{M}+\text{H}]^+ = 386.9758$ ), and the dimer **4** (see (b)). (b) Expansion of the prospective region of the dimer **4** of the mass spectrum. HRMS-ESI: measured mass  $[\text{M}]^+ = 740.9534$  (—), and simulated mass  $[\text{M}]^+ = 740.9544$  (—).



**Figure S17. CV of 2-(*tert*-butylsulfonyl)-1-iodosyl-4-methoxybenzene 3 in TFE.** CV conditions: 5.0 mM of **3**, 0.10 M LiClO<sub>4</sub> solution of TFE, glassy carbon working electrode, Pt wire counter electrode, Ag<sup>+</sup>/Ag reference electrode, and scan rate 0.10 V/s. The CV was externally referenced to Fc<sup>+</sup>/Fc.

## D. Computational Data

The disproportionation of **2** to generate **1** and **3**·HBF<sub>4</sub> is calculated to be favorable ( $\Delta G = -11.6$  kcal/mol, Eqn. S2).



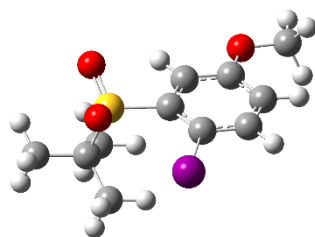


**Table S1.** Optimized Coordinates of **1**.

I	1.513312	-2.090723	0.025157
S	0.684736	1.464150	-0.824359
O	-4.189593	0.552089	-0.112081
O	1.858467	0.764666	-1.389097
O	0.015845	2.465223	-1.687369
C	-0.350272	-1.093912	-0.012617
C	-1.453559	-1.884145	0.327508
H	-1.299267	-2.923169	0.602758
C	-2.753687	-1.378806	0.315826
H	-3.574161	-2.033849	0.588407
C	-2.975980	-0.047816	-0.055237
C	-1.882460	0.755022	-0.402585
H	-2.064503	1.781248	-0.702340
C	-0.582508	0.246600	-0.375679
C	-5.338200	-0.226998	0.232091
H	-5.278019	-0.581152	1.269476
H	-6.192539	0.445734	0.123006
H	-5.452685	-1.081560	-0.447485
C	1.187790	2.321283	0.747909
C	1.747971	1.284919	1.721353
H	2.071912	1.811820	2.627501
H	2.612603	0.760907	1.303301
H	0.991285	0.548999	2.014205
C	2.264271	3.326049	0.316180
H	2.598866	3.869095	1.208250
H	3.131271	2.822814	-0.124883
H	1.870842	4.054287	-0.401330
C	-0.038883	3.030928	1.325422
H	-0.467916	3.743098	0.613199
H	-0.814155	2.321694	1.634485
H	0.280495	3.587359	2.215215

electronic energy = -1349.863334

sum of electronic and zero-point energies = -1349.617793

sum of electronic and thermal energy = -1349.600353

sum of electronic and thermal enthalpy = -1349.599409

sum of electronic and free energy = -1349.66348

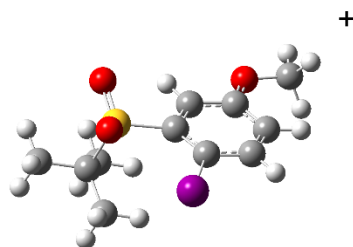


**Table S2.** Optimized Coordinates of **2**.

I	1.249991	-2.193008	0.019515
S	0.839119	1.403067	-0.822213
O	-4.074939	0.912127	-0.082216
O	1.881776	0.563505	-1.442319
O	0.227530	2.468633	-1.641829
C	-0.464465	-1.068183	-0.005249
C	-1.661730	-1.774323	0.323586
H	-1.588568	-2.826820	0.578822
C	-2.891440	-1.161574	0.323279
H	-3.780705	-1.726330	0.579987
C	-2.969094	0.209814	-0.025640
C	-1.781816	0.932501	-0.358864
H	-1.885114	1.975030	-0.641195
C	-0.553554	0.314695	-0.339037
C	-5.352740	0.295627	0.215029
H	-5.352384	-0.067250	1.247445
H	-6.083606	1.094166	0.085716
H	-5.538253	-0.520227	-0.490443
C	1.490214	2.173937	0.741988
C	2.015646	1.073103	1.661744
H	2.432813	1.555025	2.554353
H	2.810449	0.490515	1.185911
H	1.220038	0.395143	1.989905
C	2.620716	3.095096	0.262527
H	3.053438	3.579205	1.146084
H	3.413278	2.532539	-0.242417
H	2.248928	3.875491	-0.409677
C	0.354994	2.967199	1.391647
H	-0.054166	3.722632	0.713414
H	-0.454713	2.317107	1.740821
H	0.767785	3.482675	2.267241

electronic energy = -1349.649779

sum of electronic and zero-point energies = -1349.404134

sum of electronic and thermal energy = -1349.386639

sum of electronic and thermal enthalpy = -1349.385695

sum of electronic and free energy = -1349.450287

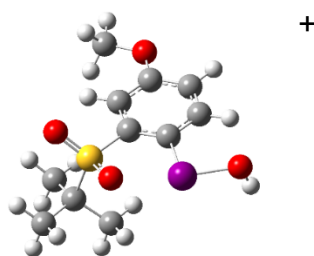


**Table S3.** Optimized Coordinates of  $3 \cdot H^+$ .

I	2.299187	-0.460923	-0.125121
S	-0.418682	1.451639	-0.729651
O	3.003460	-2.179886	0.501285
H	3.057404	-2.152089	1.474102
O	1.089003	1.448426	-0.905792
O	-1.221390	1.844836	-1.896984
O	-3.592959	-2.545100	0.129033
C	0.285086	-1.103311	0.021118
C	-0.764631	-0.241317	-0.285176
C	-2.092206	-0.677679	-0.274484
C	-2.886788	0.003964	-0.553887
C	-2.358890	-2.007623	0.079734
C	-1.294046	-2.867966	0.405101
H	-1.519601	-3.896545	0.672879
C	0.023651	-2.428343	0.367848
H	0.837180	-3.110267	0.592294
C	-4.710135	-1.712898	-0.207458
H	-4.781551	-0.859502	0.479027
H	-5.591026	-2.349412	-0.097935
H	-4.634848	-1.358888	-1.243308
C	-0.787890	2.556750	0.720296
C	-0.314360	3.947111	0.277979
H	0.758458	3.960194	0.059198
H	-0.504500	4.637682	1.107962
H	-0.867242	4.303531	-0.597654
C	-2.296909	2.524116	0.968820
H	-2.864443	2.807311	0.076282
H	-2.514957	3.254922	1.756719
H	-2.633778	1.543498	1.320497
C	0.006710	2.030480	1.916543
H	-0.291310	1.013174	2.194070
H	-0.209954	2.685494	2.768882
H	1.085778	2.057457	1.734427

electronic energy = -1425.458782

sum of electronic and zero-point energies = -1425.198937

sum of electronic and thermal energy = -1425.179912

sum of electronic and thermal enthalpy = -1425.178968

sum of electronic and free energy = -1425.245997

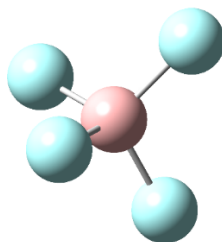


**Table S4.** Optimized Coordinates of  $\text{BF}_4^-$ .

B	0.000000	0.000000	0.000000
F	0.813973	0.813973	0.813973
F	-0.813973	-0.813973	0.813973
F	0.813973	-0.813973	-0.813973
F	-0.813973	0.813973	-0.813973

electronic energy = -424.579539

sum of electronic and zero-point energies = -424.565433

sum of electronic and thermal energies = -424.561016

sum of electronic and thermal enthalpies = -424.560072

sum of electronic and free energies = -424.590736

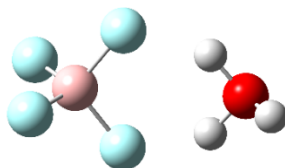


**Table S5.** Optimized Coordinates of  $\text{H}_3\text{O}\cdot\text{BF}_4$ .

B	-0.673173	-0.000097	0.007705
F	0.186941	1.159892	-0.068927
F	-1.323962	-0.005507	1.226737
F	0.186609	-1.159405	-0.078963
F	-1.542150	0.004996	-1.065385
H	1.773875	-0.778530	-0.073830
O	2.409843	0.000485	-0.090952
H	2.975513	-0.001821	0.708074
H	1.770792	0.777165	-0.066320

electronic energy = -501.448077

sum of electronic and zero-point energies = -501.396602

sum of electronic and thermal energies = -501.389455

sum of electronic and thermal enthalpies = -501.388511

sum of electronic and free energies = -501.427847

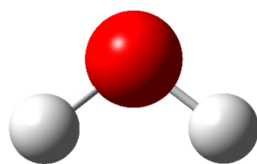


**Table S6.** Optimized Coordinates of H<sub>2</sub>O.

O	0.000000	0.000000	0.118679
H	0.000000	0.764025	-0.474715
H	0.000000	-0.764025	-0.474715

electronic energy = -76.417106

sum of electronic and zero-point energies = -76.396134

sum of electronic and thermal energy = -76.393299

sum of electronic and thermal enthalpy = -76.392355

sum of electronic and free energy = -76.413795

## E. X-ray Diffraction Data

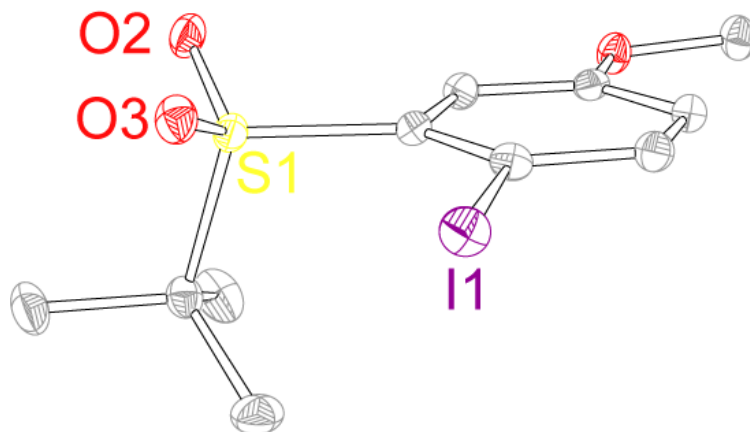


**Figure S18.** Displacement ellipsoid plot of **1** plotted at 50% probability. H-atoms are removed for clarity.

**Table S7.** X-ray experimental details for **1** (CCDC 2176972)

Crystal data	
Chemical formula	C <sub>11</sub> H <sub>15</sub> IO <sub>3</sub> S
<i>M</i> <sub>r</sub>	354.19
Crystal system, space group	Orthorhombic, <i>Pbca</i>
Temperature (K)	110
<i>a</i> , <i>b</i> , <i>c</i> (Å)	11.9016(5), 9.6956(5), 21.935(1)
<i>V</i> (Å <sup>3</sup> )	2531.1(2)
<i>Z</i>	8
Radiation type	Mo <i>K</i> α
μ (mm <sup>-1</sup> )	2.69
Crystal size (mm)	0.16 × 0.08 × 0.06
Data collection	
Diffractometer	Bruker <i>APEX-II</i> CCD Multi-scan
Absorption correction	<i>SADABS2016/2</i> (Bruker,2016/2) was used for absorption correction. <i>wR2(int)</i> was 0.0783 before and 0.0595 after correction. The Ratio of minimum to maximum transmission is 0.8167. The λ/2 correction factor is not present.
<i>T</i> <sub>min</sub> , <i>T</i> <sub>max</sub>	0.609, 0.746
No. of measured, independent and observed [ <i>I</i> > 2σ( <i>I</i> )] reflections	44111, 4226, 3200
<i>R</i> <sub>int</sub>	0.058
(sin θ/λ) <sub>max</sub> (Å <sup>-1</sup> )	0.735
Refinement	
<i>R</i> [ <i>F</i> <sup>2</sup> > 2σ( <i>F</i> <sup>2</sup> )], <i>wR</i> ( <i>F</i> <sup>2</sup> ), <i>S</i>	0.027, 0.58, 1.07
No. of reflections	4226
No. of parameters	149
H-atom treatment	H-atom parameters constrained
Δρ <sub>max</sub> , Δρ <sub>min</sub> (e Å <sup>-3</sup> )	0.97, -0.65

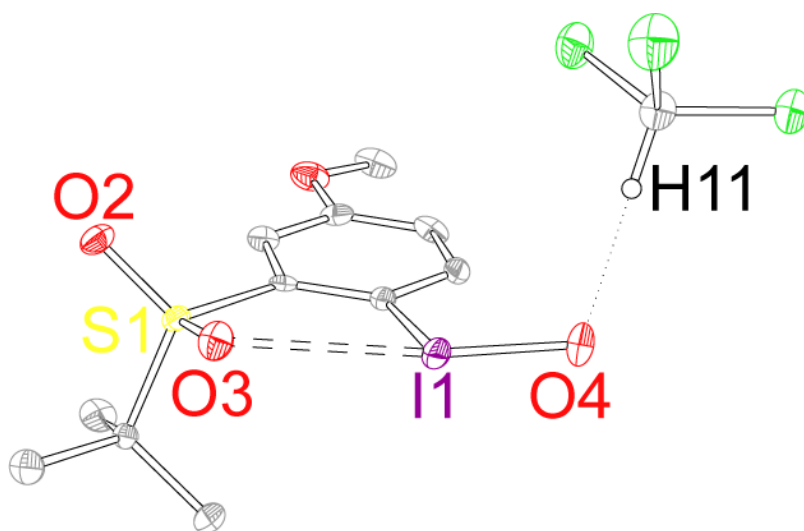


**Figure S19.** Displacement ellipsoid plot of **3** plotted at 50% probability. H-atoms (excluding H11), and co-crystallized solvent (excluding the hydrogen-bonded chloroform) are removed for clarity.

**Table S8.** X-ray experimental details for **3** (CCDC 2176973)

Crystal data	
Chemical formula	C <sub>11</sub> H <sub>15</sub> IO <sub>4</sub> S·2(CHCl <sub>3</sub> )
<i>M<sub>r</sub></i>	608.92
Crystal system, space group	Orthorhombic, <i>Pna</i> 2 <sub>1</sub>
Temperature (K)	110
<i>a</i> , <i>b</i> , <i>c</i> (Å)	15.810(1), 23.950(2), 5.7108(5)
<i>V</i> (Å <sup>3</sup> )	2162.4(3)
<i>Z</i>	4
Radiation type	Mo <i>K</i> α
μ (mm <sup>-1</sup> )	2.33
Crystal size (mm)	0.14 × 0.08 × 0.04
Data collection	
Diffractometer	Bruker <i>APEX</i> -II CCD
Absorption correction	Multi-scan <i>SADABS</i> 2016/2 (Bruker,2016/2) was used for absorption correction. <i>wR</i> 2(int) was 0.0945 before and 0.0619 after correction. The Ratio of minimum to maximum transmission is 0.7533. The λ/2 correction factor is not present.
<i>T<sub>min</sub></i> , <i>T<sub>max</sub></i>	0.562, 0.746
No. of measured, independent and observed [ <i>I</i> > 2σ( <i>I</i> )] reflections	21328, 6468, 5959
<i>R<sub>int</sub></i>	0.041
(sin θ/λ) <sub>max</sub> (Å <sup>-1</sup> )	0.715
Refinement	
<i>R</i> [ <i>F</i> <sup>2</sup> > 2σ( <i>F</i> <sup>2</sup> )], <i>wR</i> ( <i>F</i> <sup>2</sup> ), <i>S</i>	0.063, 0.131, 1.28
No. of reflections	6468
No. of parameters	230
No. of restraints	1
H-atom treatment	H-atom parameters constrained $w = 1/[\sigma^2(F_o^2) + 22.3117P]$ where $P = (F_o^2 + 2F_c^2)/3$
Δρ <sub>max</sub> , Δρ <sub>min</sub> (e Å <sup>-3</sup> )	1.75, -1.49
Absolute structure	Flack <i>x</i> determined using 2263 quotients [( <i>I</i> <sup>+)-(<i>I</i><sup>-</sup>)]/[(<i>I</i><sup>+</sup>)+(<i>I</i><sup>-</sup>)] (Parsons, Flack and Wagner, <i>Acta Cryst.</i> B69 (2013) 249-259).</sup>
Absolute structure parameter	0.219(9)

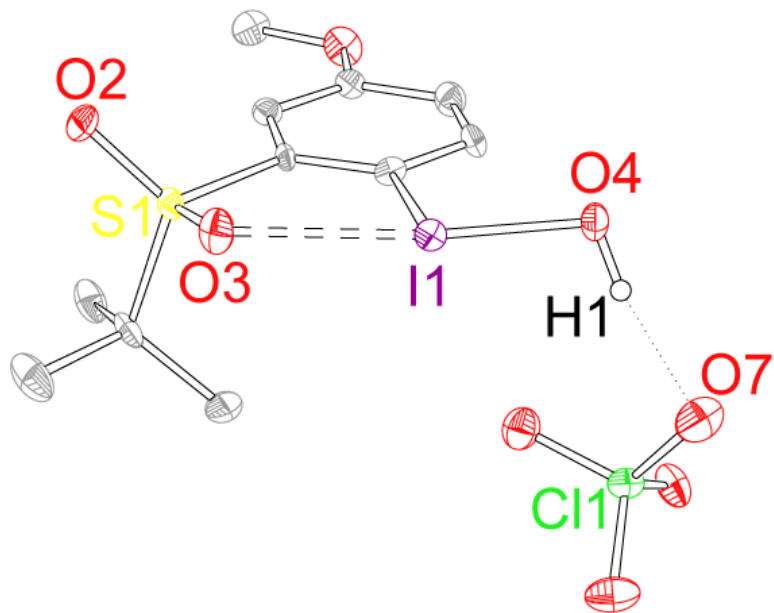


**Figure S20.** Displacement ellipsoid plot of  $3 \cdot \text{HClO}_4$  plotted at 50% probability. H-atoms (excluding H1) are removed for clarity.

**Table S9.** X-ray experimental details for **3·HClO<sub>4</sub>** (CCDC 2176974)

Crystal data	
Chemical formula	C <sub>11</sub> H <sub>16</sub> IO <sub>4</sub> S·ClO <sub>4</sub>
<i>M<sub>r</sub></i>	473.69
Crystal system, space group	Orthorhombic, <i>P</i> 2 <sub>1</sub> 2 <sub>1</sub> 2 <sub>1</sub>
Temperature (K)	110
<i>a</i> , <i>b</i> , <i>c</i> (Å)	5.7361(2), 16.5918(7), 17.3437(7)
<i>V</i> (Å <sup>3</sup> )	1650.6(1)
<i>Z</i>	4
Radiation type	Mo <i>K</i> α
μ (mm <sup>-1</sup> )	2.26
Crystal size (mm)	0.08 × 0.03 × 0.02
Data collection	
Diffractometer	Bruker APEX-II CCD
Absorption correction	Multi-scan SADABS2016/2 (Bruker,2016/2) was used for absorption correction. <i>w</i> R <sub>2</sub> (int) was 0.1389 before and 0.0743 after correction. The Ratio of minimum to maximum transmission is 0.8690. The λ/2 correction factor is not present.
<i>T<sub>min</sub></i> , <i>T<sub>max</sub></i>	0.648, 0.746
No. of measured, independent and observed [ <i>I</i> ≥ 2 <i>u</i> ( <i>I</i> )] reflections	36452, 4881, 4621
<i>R<sub>int</sub></i>	0.077
(sin θ/λ) <sub>max</sub> (Å <sup>-1</sup> )	0.707
Refinement	
<i>R</i> [ <i>F</i> <sup>2</sup> > 2σ( <i>F</i> <sup>2</sup> )], <i>wR</i> ( <i>F</i> <sup>2</sup> ), <i>S</i>	0.043, 0.076, 1.06
No. of reflections	4881
No. of parameters	206
H-atom treatment	H-atom parameters constrained
Δρ <sub>max</sub> , Δρ <sub>min</sub> (e Å <sup>-3</sup> )	1.26, -2.65
Absolute structure	Hooft, R.W.W., Straver, L.H., Spek, A.L. (2010). <i>J. Appl. Cryst.</i> , 43, 665-668.
Absolute structure parameter	-0.01(1)

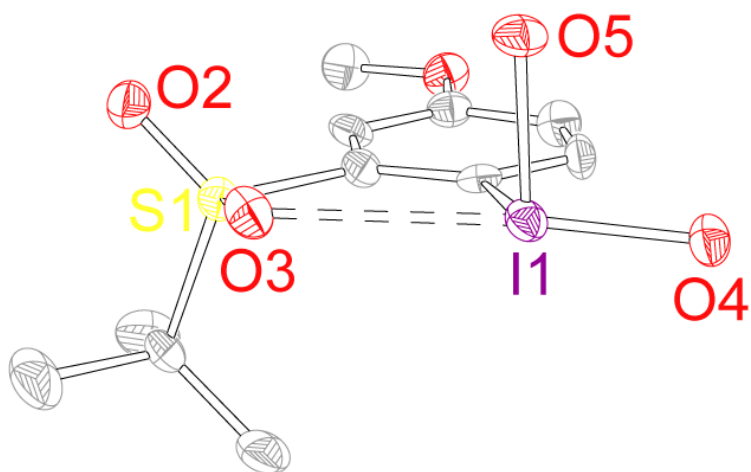


**Figure S21.** Displacement ellipsoid plot of **5** plotted at 50% probability. H-atoms, co-crystallized solvent and the other 4 molecules of **5** are removed for clarity.

**Table S10.** X-ray experimental details for **5** (CCDC 2176975)

Crystal data	
Chemical formula	C <sub>11</sub> H <sub>15</sub> IO <sub>5</sub> S·CH <sub>2</sub> Cl <sub>2</sub>
<i>M</i> <sub>r</sub>	475.17
Crystal system, space group	Triclinic, <i>P</i> 1
Temperature (K)	110
<i>a</i> , <i>b</i> , <i>c</i> (Å)	13.6039(7), 14.7431(8), 23.6714(8)
α, β, γ (°)	84.158(4), 73.474(4), 68.652(5)
<i>V</i> (Å <sup>3</sup> )	4239.2(4)
<i>Z</i>	10
Radiation type	Mo <i>K</i> α
μ (mm <sup>-1</sup> )	2.34
Crystal size (mm)	0.31 × 0.08 × 0.05
Data collection	
Diffractometer	Bruker <i>APEX</i> -II CCD
Absorption correction	Multi-scan SADABS-2016/2 (Bruker, 2016/2) was used for absorption correction. <i>wR</i> 2(int) was 0.1345 before and 0.0688 after correction. The Ratio of minimum to maximum transmission is 0.6974. The λ/2 correction factor is Not present.
No. of measured, independent and observed [ <i>I</i> ≥ 2σ( <i>I</i> )] reflections	166139, 21788, 15053
<i>R</i> <sub>int</sub>	0.131
(sin θ/λ) <sub>max</sub> (Å <sup>-1</sup> )	0.699
Refinement	
<i>R</i> [ <i>F</i> <sup>2</sup> > 2σ( <i>F</i> <sup>2</sup> )], <i>wR</i> ( <i>F</i> <sup>2</sup> ), <i>S</i>	0.062, 0.134, 1.04
No. of reflections	21788
No. of parameters	966
H-atom treatment	H-atom parameters constrained $w = 1/[\sigma^2(F_o^2) + (0.041P)^2 + 18.2321P]$ where $P = (F_o^2 + 2F_c^2)/3$
Δρ <sub>max</sub> , Δρ <sub>min</sub> (e Å <sup>-3</sup> )	2.19, -2.25

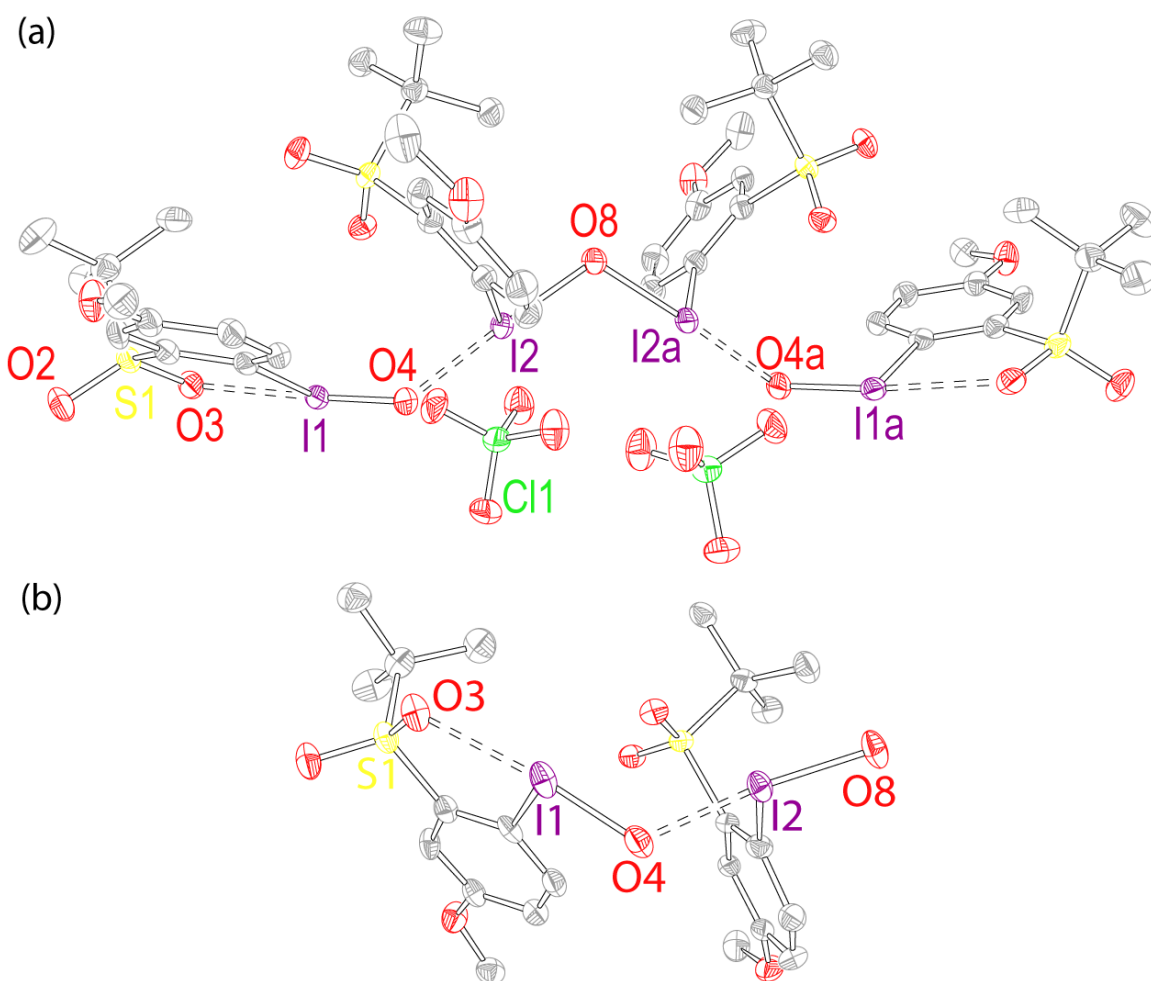


**Figure S22.** (a) Displacement ellipsoid plot of **6** plotted at 50% probability. H-atoms are removed for clarity. O8 sits on a special position with the two halves of the molecule related by a crystallographic  $C_2$ -axis. (b) Displacement ellipsoid plot of the asymmetric unit of **6** plotted at 50% probability. H-atoms and the perchlorate anion are removed for clarity. The quality of the data was such that every proton could be observed in the difference map and there was no evidence of protonation at O4 or O8.

**Table S11.** X-ray experimental details for **6** (CCDC 2189772)

Crystal data	
Chemical formula	C <sub>22</sub> H <sub>30</sub> I <sub>2</sub> O <sub>7.5</sub> S <sub>2</sub> ·ClO <sub>4</sub>
<i>M</i> <sub>r</sub>	831.85
Crystal system, space group	Monoclinic, <i>C2/c</i>
Temperature (K)	110
<i>a</i> , <i>b</i> , <i>c</i> (Å)	33.080(3), 9.9990(9), 20.993(2)
β (°)	121.842(1)
<i>V</i> (Å <sup>3</sup> )	5898.6(9)
<i>Z</i>	8
Radiation type	Mo <i>K</i> α
μ (mm <sup>-1</sup> )	2.42
Crystal size (mm)	0.12 × 0.08 × 0.03
Data collection	
Diffractometer	Bruker <i>APEX-II</i> CCD
Absorption correction	Multi-scan <i>SADABS2016/2</i> (Bruker,2016/2) was used for absorption correction. <i>wR2(int)</i> was 0.0808 before and 0.0593 after correction. The Ratio of minimum to maximum transmission is 0.8962. The λ/2 correction factor is not present.
<i>T</i> <sub>min</sub> , <i>T</i> <sub>max</sub>	0.668, 0.746
No. of measured, independent and observed [ <i>I</i> > 2σ( <i>I</i> )] reflections	49267, 7130, 5742
<i>R</i> <sub>int</sub>	0.055
(sin θ/λ) <sub>max</sub> (Å <sup>-1</sup> )	
Refinement	
<i>R</i> [ <i>F</i> <sup>2</sup> > 2σ( <i>F</i> <sup>2</sup> )], <i>wR</i> ( <i>F</i> <sup>2</sup> ), <i>S</i>	0.034, 0.056, 1.10
No. of reflections	7130
No. of parameters	504
H-atom treatment	All H-atom parameters refined $w = 1/[\sigma^2(F_o^2) + (0.0033P)^2 + 25.6211P]$ where $P = (F_o^2 + 2F_c^2)/3$

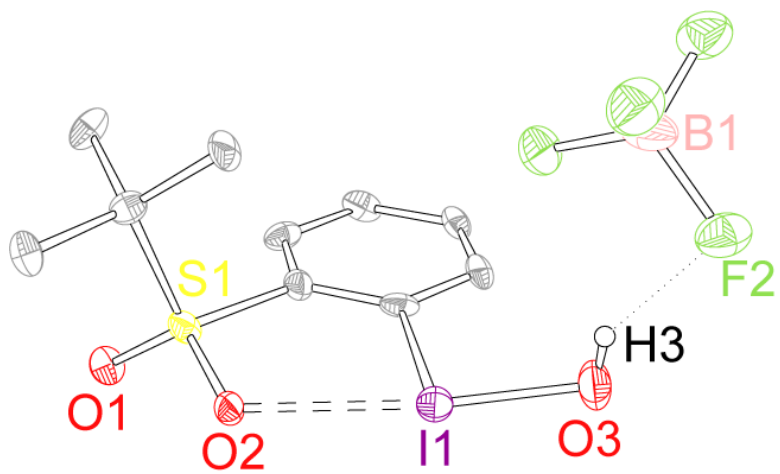


**Figure S23.** Displacement ellipsoid plot of  $\text{S3} \cdot \text{HBF}_4$  plotted at 50% probability. H-atoms (excluding H3) are removed for clarity.

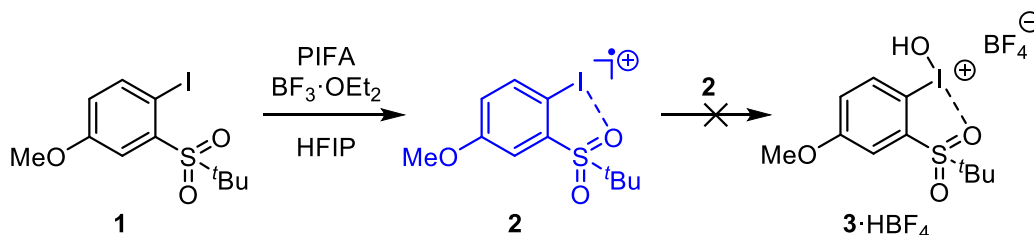
**Table S12.** X-ray experimental details for **S3·HBF<sub>4</sub>** (CCDC 2234041)

<b>Crystal data</b>	
Chemical formula	C <sub>10</sub> H <sub>14</sub> IO <sub>3</sub> S·BF <sub>4</sub>
<i>M<sub>r</sub></i>	427.98
Crystal system, space group	Orthorhombic, <i>P</i> 2 <sub>1</sub> 2 <sub>1</sub> 2 <sub>1</sub>
Temperature (K)	110
<i>a</i> , <i>b</i> , <i>c</i> (Å)	5.647(2), 10.259(3), 24.055(1)
<i>V</i> (Å <sup>3</sup> )	1393.7(6)
<i>Z</i>	4
Radiation type	Mo Kα
μ (mm <sup>-1</sup> )	2.50
Crystal size (mm)	0.05 × 0.02 × 0.01
<b>Data collection</b>	
Diffractometer	Bruker <i>APEX-II</i> CCD
	Multi-scan
Absorption correction	SADABS2016/2 (Bruker,2016/2) was used for absorption correction. <i>wR2</i> (int) was 0.1101 before and 0.0751 after correction. The ratio of minimum to maximum transmission is 0.7082. The λ/2 correction factor is not present
<i>T<sub>min</sub></i> , <i>T<sub>max</sub></i>	0.528, 0.745
No. of measured, independent and observed [ <i>I</i> > 2σ( <i>I</i> )] reflections	7549, 2135, 2048
<i>R</i> <sub>int</sub>	0.060
(sin θ/λ) <sub>max</sub> (Å <sup>-1</sup> )	0.568
<b>Refinement</b>	
<i>R</i> [ <i>F</i> <sup>2</sup> > 2σ( <i>F</i> <sup>2</sup> )], <i>wR</i> ( <i>F</i> <sup>2</sup> ), <i>S</i>	0.054, 0.120, 1.25
No. of reflections	2135
No. of parameters	187
No. of restraints	9
H-atom treatment	H-atom parameters constrained
Δρ <sub>max</sub> , Δρ <sub>min</sub> (e Å <sup>-3</sup> )	1.26, -2.65
Absolute structure	Flack <i>x</i> determined using 730 quotients [( <i>I</i> <sup>+</sup> )-( <i>I</i> <sup>-</sup> )]/[( <i>I</i> <sup>+</sup> )+( <i>I</i> <sup>-</sup> )] (Parsons, Flack and Wagner, <i>Acta Cryst.</i> B69 (2013) 249-259).
Absolute structure parameter	0.06(2)

## F. Additional Data

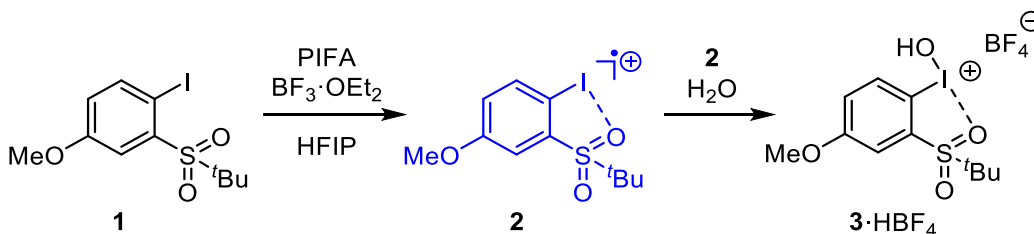
### F.1 Impact of O<sub>2</sub> and H<sub>2</sub>O on the Synthesis of 2

#### Air-Free Synthesis of Iodanyl Radical 2



A 20-mL scintillation vial was charged with 2-(*tert*-butylsulfonyl)-1-iodo-4-methoxybenzene (**1**, 22.3 mg, 63.0 μmol, 1.00 equiv), dry BF<sub>3</sub>·OEt<sub>2</sub>, and dry HFIP (0.75 mL) under an atmosphere of N<sub>2</sub> at 23 °C. To this cuvette was added a solution of PIFA (14.0 mg, 32.6 μmol, 0.517 equiv) dissolved in dry HFIP (0.25 mL). The solution immediately changed from colorless to dark blue then to dark red. The reaction mixture was stirred at 23 °C for 30 min. The reaction mixture was then concentrated *in vacuo*. To the residue was added 1.0 mL of dry MeCN. An aliquot (0.10 mL) of this mixture was taken, diluted with dry CD<sub>3</sub>CN (0.50 mL), and analyzed by <sup>1</sup>H NMR. The spectral data showed the starting aryl iodide **1** with no formation of oxidized product (*i.e.*, 3·HBF<sub>4</sub>).

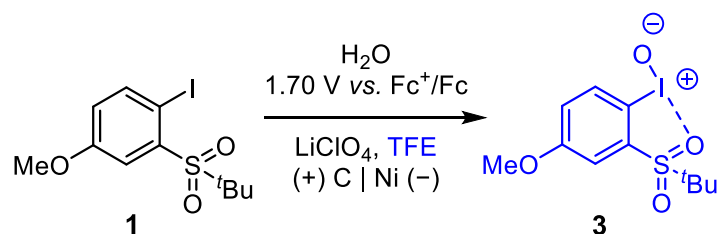
#### Air-Free Synthesis of Iodanyl Radical 2 in the Presence of H<sub>2</sub>O



A 25-mL Schlenk flask was charged with 2-(*tert*-butylsulfonyl)-1-iodo-4-methoxybenzene (**1**, 22.3 mg, 63.0 μmol, 1.00 equiv), BF<sub>3</sub>·OEt<sub>2</sub>, water (2.3 μL, 130 μmol, 2.0 equiv), and dry HFIP (0.75 mL) under an atmosphere of N<sub>2</sub> at 23 °C. To this flask was added a solution of PIFA (14.0 mg, 32.6 μmol, 0.517 equiv) dissolved in dry HFIP (0.25 mL). Upon the addition, the solution immediately changed from colorless to dark blue then rapidly to light yellow. The reaction mixture was stirred at 23 °C for 30 min. The reaction mixture was then concentrated *in vacuo*. To the residue was added 1.0 mL of dry MeCN and mesitylene as an internal standard. An aliquot (0.10 mL) of this mixture was taken, diluted with dry CD<sub>3</sub>CN (0.50 mL), and analyzed by <sup>1</sup>H NMR, which showed the I(III) product 3·HBF<sub>4</sub> in 21% yield with 66% of remaining aryl iodide **1**.

## F.2 Procedure for the Electrosynthesis of **3**, **3**·HClO<sub>4</sub>, and **5**

### Electrosynthesis of 2-(*tert*-butylsulfonyl)-1-iodosyl-4-methoxybenzene (**3**)



A 10-mL glass vial was charged with 2-(*tert*-butylsulfonyl)-1-iodo-4-methoxybenzene (**1**, 44.3 mg, 0.125 mmol, 1.00 equiv), water (4.50  $\mu\text{L}$ , 0.250 mmol, 2.00 equiv), lithium perchlorate (53.0 mg, 0.500 mmol, 4.00 equiv), and TFE (5.0 mL), and was fitted with a graphite anode, nickel cathode, and  $\text{Ag}^+/\text{Ag}$  reference electrode. A constant potential of 1.86 V vs.  $\text{Ag}^+/\text{Ag}$  (1.70 V vs.  $\text{Fc}^+/\text{Fc}$ ) was applied to the reaction mixture with stirring at 400 rpm, 23 °C until 30 C charge (2.5 F/mol) was passed. The electrolysis was then stopped, and mesitylene was added as an internal standard. An aliquot (0.10 mL) of the reaction mixture was taken, diluted with  $\text{CD}_3\text{CN}$  (0.50 mL), and analyzed by  $^1\text{H}$  NMR spectroscopy (52% yield, 42% faradaic efficiency). Spectral data obtained following electrolysis of **1** is well-matched to that obtained for independently synthesized **3** dissolved in TFE.

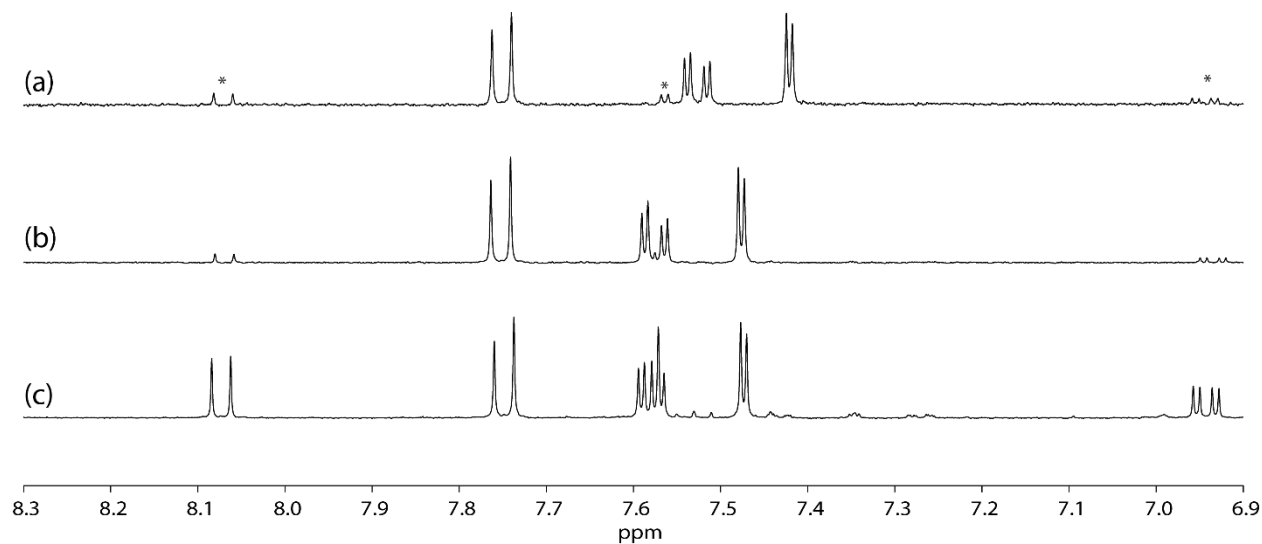
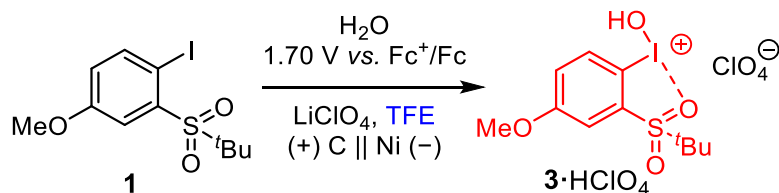


**Figure S24.** NMR spectra (23 °C, 400 MHz,  $\text{CD}_3\text{CN}$ ) of: (a) independently synthesized **3** in the absence of TFE, (b) aliquot of independently synthesized **3** in TFE, (c) aliquot of electrolysis mixture of **1** in TFE. The asterisk (\*) indicates signals associated with aryl iodide **1**.

*Electrosynthesis of 2-(tert-butylsulfonyl)-4-methoxyphenyl(hydroxy)iodonium perchlorate (3·HClO<sub>4</sub>) in TFE using a divided cell*



The anodic cell of a 5-mL divided cell was charged with 2-(tert-butylsulfonyl)-1-iodo-4-methoxybenzene (**1**, 44.3 mg, 0.125 mmol, 1.00 equiv), water (4.5  $\mu$ L, 0.25 mmol, 2.0 equiv), lithium perchlorate (106 mg, 1.00 mmol, 8.00 equiv), and TFE (5.0 mL), and was fitted with a graphite electrode and an Ag<sup>+</sup>/Ag reference electrode. The cathodic cell was charged with lithium perchlorate (106 mg, 1.00 mmol, 8.00 equiv) and TFE (5.0 mL), and was fitted with a nickel electrode. A constant potential of 1.65 V vs. Ag<sup>+</sup>/Ag (1.51 V vs. Fc<sup>+</sup>/Fc) was applied to the reaction mixture with stirring at 400 rpm, 23 °C until 28 C charge (2.3 F/mol) was passed. The electrolysis was then stopped, and mesitylene was added to the anodic cell as an internal standard. An aliquot (0.10 mL) of the reaction mixture in the anodic cell was taken, diluted with CD<sub>3</sub>CN (0.50 mL), and analyzed by NMR spectroscopy (77% yield, 67% faradaic efficiency). The <sup>1</sup>H NMR spectral data of the electrolysis solution is in good agreement with an externally prepared sample of **3**·HClO<sub>4</sub> obtained from mixing **3** (3.7 mg, 0.010 mmol, 1.0 equiv) and HClO<sub>4</sub> (70 wt% solution, 1.5 mg, 0.010 mmol, 1.0 equiv) in CD<sub>3</sub>CN (1.0 mL).

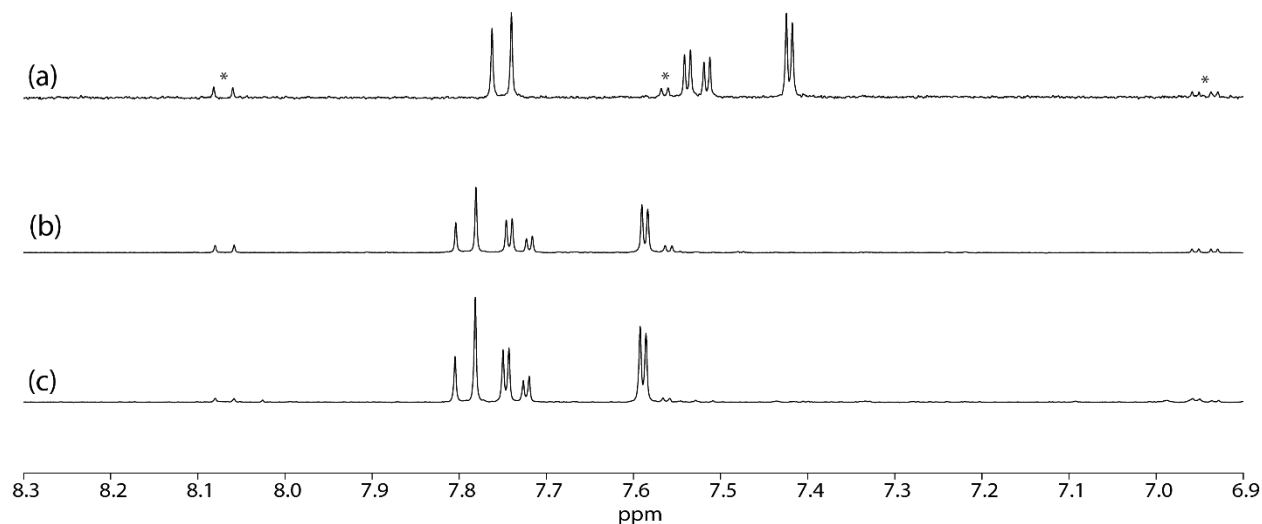
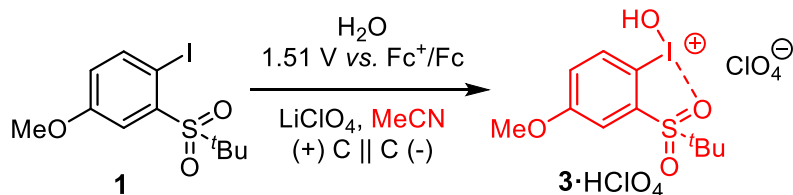


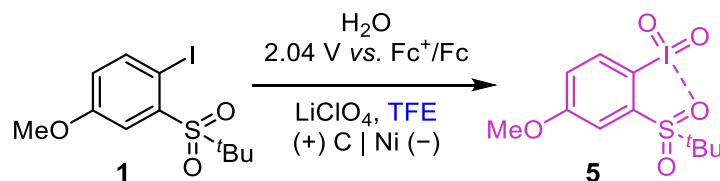
**Figure S25.** NMR spectra (23 °C, 400 MHz, CD<sub>3</sub>CN) of: (a) independently synthesized **3** in the absence of HClO<sub>4</sub>, (b) aliquot of a mixture of **3** and HClO<sub>4</sub> in MeCN, (c) aliquot of electrolysis mixture of **1** in MeCN. The asterisk (\*) indicates signals associated with aryl iodide **1**.

*Electrosynthesis of (2-(tert-butylsulfonyl)-4-methoxyphenyl)(hydroxy)iodonium perchlorate (3·HClO<sub>4</sub>) in MeCN using a divided cell*



The anodic cell of a 5-mL divided cell was charged with 2-(*tert*-butylsulfonyl)-1-iodo-4-methoxybenzene (**1**, 44.3 mg, 0.125 mmol, 1.00 equiv), water (4.5  $\mu$ L, 0.25 mmol, 2.0 equiv), lithium perchlorate (106 mg, 1.00 mmol, 8.00 equiv), and MeCN (5.0 mL), and was fitted with a graphite electrode and an Ag<sup>+</sup>/Ag reference electrode. The cathodic cell was charged with lithium perchlorate (106 mg, 1.00 mmol, 8.00 equiv) and MeCN (5.0 mL), and was fitted with a graphite electrode. A constant potential of 1.65 V vs. Ag<sup>+</sup>/Ag (1.51 V vs. Fc<sup>+</sup>/Fc) was applied to the reaction mixture with stirring at 400 rpm, 23 °C until 27 C charge (2.3 F/mol) was passed. The electrolysis was then stopped, and mesitylene was added to the anodic cell as an internal standard. An aliquot (0.10 mL) of the reaction mixture in the anodic cell was taken, diluted with CD<sub>3</sub>CN (0.50 mL), and analyzed by NMR spectroscopy (72% yield, 63% faradaic efficiency).

*Electrosynthesis of 2-(tert-butylsulfonyl)-1-iodoxy-4-methoxybenzene (5) via sequential anodic oxidation in TFE*



A 10-mL glass vial was charged with 2-(*tert*-butylsulfonyl)-1-iodo-4-methoxybenzene (**1**, 44.3 mg, 0.125 mmol, 1.00 equiv), water (11.3  $\mu\text{L}$ , 0.625 mmol, 5.00 equiv), lithium perchlorate (106 mg, 1.00 mmol, 8.00 equiv), and TFE (5.0 mL), and was fitted with a graphite anode, nickel cathode, and  $\text{Ag}^+/\text{Ag}$  reference electrode. A constant potential of 2.20 V vs.  $\text{Ag}^+/\text{Ag}$  (2.04 V vs.  $\text{Fc}^+/\text{Fc}$ ) was applied to the reaction mixture with stirring at 400 rpm, 23  $^\circ\text{C}$  until 100 C of charge (8.5 F/mol) was passed. Mesitylene was added as an internal standard. An aliquot (0.10 mL) of the reaction mixture was taken, diluted with  $\text{CD}_3\text{CN}$  (0.50 mL), and analyzed by  $^1\text{H}$  NMR spectroscopy (39% NMR yield of **5** and 21% yield of **3**, 23% faradaic efficiency overall). The  $^1\text{H}$  NMR spectral data of the electrolysis solution is in good agreement with an independently synthesized **5** in  $\text{CD}_3\text{CN}$ .

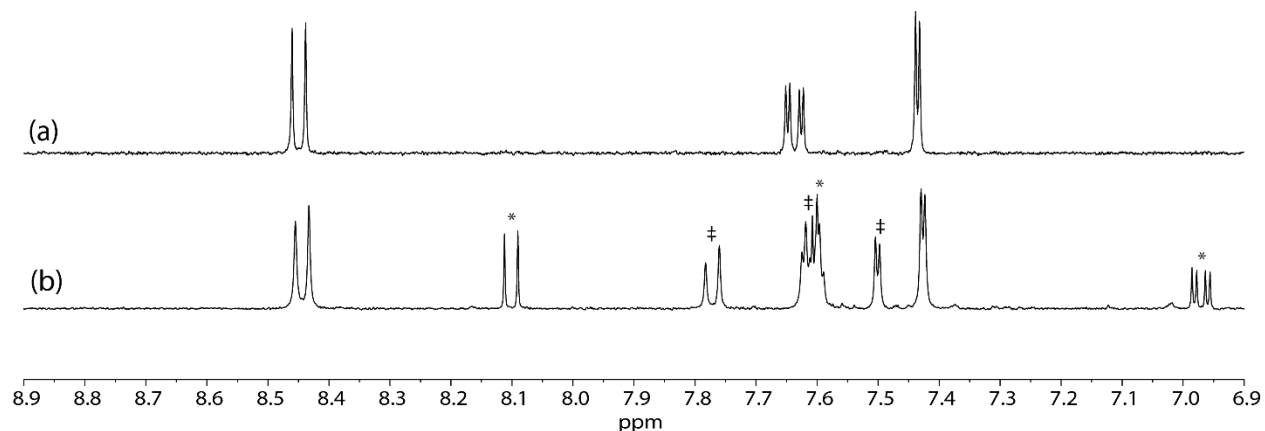
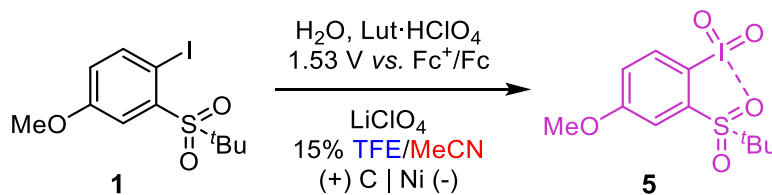


**Figure S26.** NMR spectra (23  $^\circ\text{C}$ , 400 MHz,  $\text{CD}_3\text{CN}$ ) of: (a) independently synthesized **5**, (b) aliquot of electrolysis mixture of **1** in TFE. The asterisk (\*) indicates signals associated with aryl iodide **1**. The double dagger (‡) indicates signals associated with iodosylarene **3**.

*Electrosynthesis of 2-(tert-butylsulfonyl)-1-iodoxy-4-methoxybenzene (5) in TFE/MeCN mixture*



A 10-mL glass vial was charged with 2-(*tert*-butylsulfonyl)-1-iodo-4-methoxybenzene (**1**, 44.3 mg, 0.125 mmol, 1.00 equiv), lutidinium perchlorate (64.9 mg, 0.313 mmol, 2.50 equiv), water (4.50  $\mu\text{L}$ , 0.250 mmol, 2.00 equiv), lithium perchlorate (53.0 mg, 0.500 mmol, 4.00 equiv), MeCN (3.25 mL), and TFE (0.75 mL), and was fitted with a graphite anode, nickel cathode, and  $\text{Ag}^+/\text{Ag}$  reference electrode. A constant potential of 1.68 V vs.  $\text{Ag}^+/\text{Ag}$  (1.55 V vs.  $\text{Fc}^+/\text{Fc}$ ) was applied to the reaction mixture with stirring at 400 rpm, 23 °C until 60 C of charge (5.0 F/mol) was passed. Mesitylene was added as an internal standard. An aliquot (0.10 mL) of the reaction mixture was taken, diluted with  $\text{CD}_3\text{CN}$  (0.50 mL), and analyzed by  $^1\text{H}$  NMR spectroscopy (46% NMR yield of **5**, 37% faradaic efficiency). The  $^1\text{H}$  NMR spectral data of the electrolysis solution is in good agreement with an independently synthesized **5** dissolved in  $\text{CD}_3\text{CN}$ .

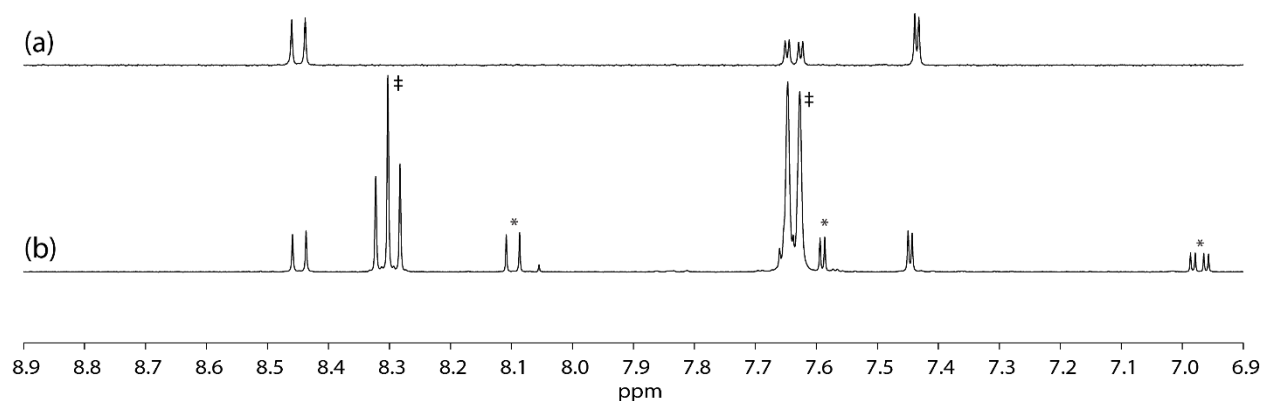
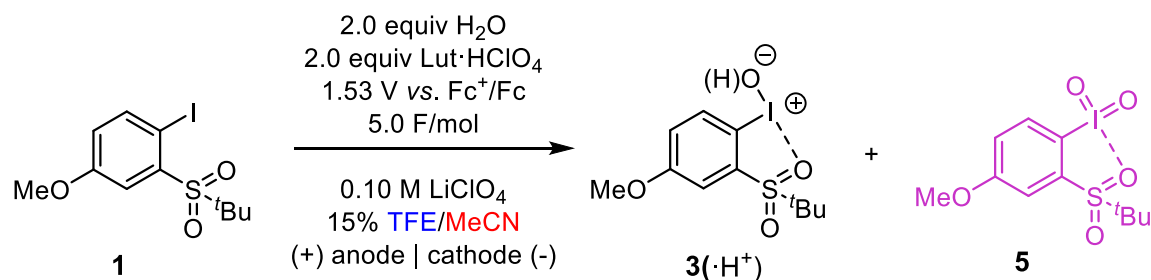


**Figure S27.** NMR spectra (23 °C, 400 MHz,  $\text{CD}_3\text{CN}$ ) of: (a) independently synthesized **5**, (b) aliquot of electrolysis mixture of **1** in 15% TFE/MeCN. The asterisk (\*) indicates signals associated with aryl iodide **1**. The double dagger (‡) relates to signals of 2,6-lutidinium perchlorate.

### F.3 Optimization for the Electrosynthesis of 5

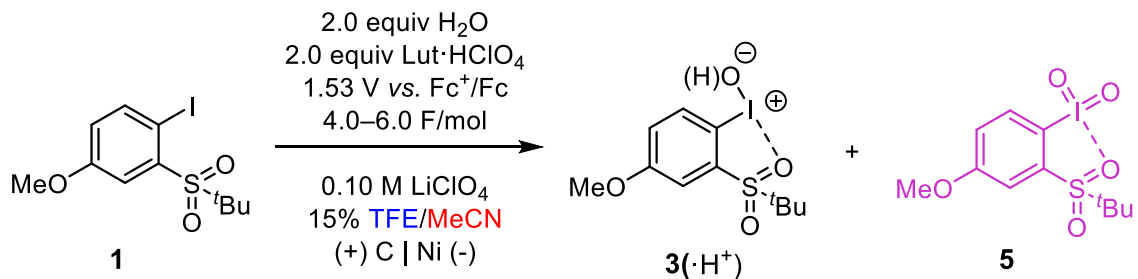
**Table S13.** Optimization of the anode and cathode in the electrochemical synthesis of 2-(*tert*-butylsulfonyl)-1-iodoxy-4-methoxybenzene **5**. Reaction conditions: 0.125 mmol of 2-(*tert*-butylsulfonyl)-1-iodo-4-methoxybenzene **1**, 5.0 mL of solvent, and Ag<sup>+</sup>/Ag reference electrode in an undivided cell setup.



Entry	Anode	Cathode	Yield of <b>3</b> and <b>3</b> ·HClO <sub>4</sub> <sup>a</sup>	Yield of <b>5</b> <sup>a</sup>	<b>5</b> : <b>3</b> ·(H <sup>+</sup> )
<b>1</b>	Graphite	Platinum	10–14%	19–53%	2.7–3.1 : 1.0
<b>2</b>	Graphite	Nickel	17–21%	41–47%	2.2–2.4 : 1.0
<b>3</b>	Glassy Carbon	Nickel	13%	13%	1.0 : 1.0

<sup>a</sup>Determined by <sup>1</sup>H NMR using mesitylene as internal standard.

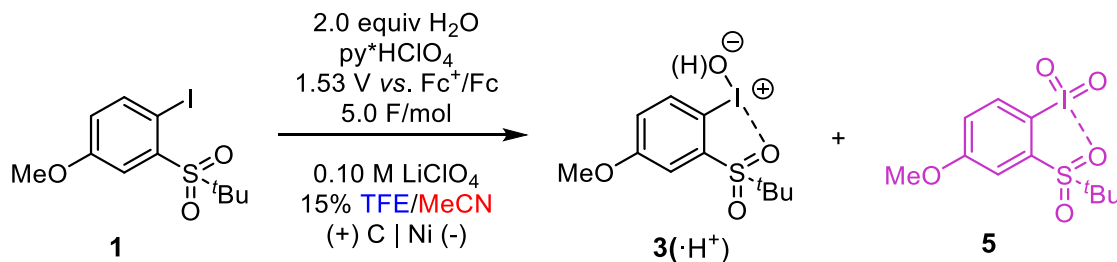
**Table S14.** Optimization of the charge passed in the electrochemical synthesis of 2-(*tert*-butylsulfonyl)-1-iodoxy-4-methoxybenzene **5**. Reaction conditions: 0.125 mmol of 2-(*tert*-butylsulfonyl)-1-iodo-4-methoxybenzene **1**, 5.0 mL of solvent, graphite anode, nickel cathode, and Ag<sup>+</sup>/Ag reference electrode in an undivided cell setup.



Entry	Charge Passed	Yield of <b>3</b> and <b>3·HClO<sub>4</sub><sup>a</sup></b>	Yield of <b>5<sup>a</sup></b>	<b>5 : 3·H<sup>+</sup></b>
<b>1</b>	48 C (4.0 F/mol)	10%	32%	3.2 : 1.0
<b>2</b>	60 C (5.0 F/mol)	18%	42%	2.3 : 1.0
<b>3</b>	72 C (6.0 F/mol)	23%	37%	1.6 : 1.0

<sup>a</sup>Determined by <sup>1</sup>H NMR using mesitylene as internal standard.

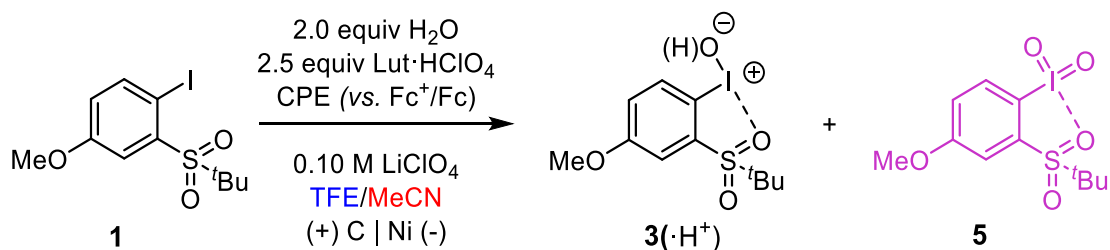
**Table S15.** Optimization of the pyridinium salt in the electrochemical synthesis of 2-(*tert*-butylsulfonyl)-1-iodoxybenzene **5**. Reaction conditions: 0.125 mmol of 2-(*tert*-butylsulfonyl)-1-iodo-4-methoxybenzene **1**, 5.0 mL of solvent, graphite anode, nickel cathode, and Ag<sup>+</sup>/Ag reference electrode in an undivided cell setup.



Entry	Pyridinium salt	Pyridinium Loading	Yield of <b>3</b> and 3·HClO <sub>4</sub> <sup>a</sup>	Yield of <b>5</b> <sup>a</sup>	<b>5</b> : 3(H <sup>+</sup> )
<b>1</b>	pyridinium perchlorate	2.0 equiv	17%	40%	2.4 : 1.0
<b>2</b>	2,6-lutidinium perchlorate	0 equiv	27%	31%	1.1 : 1.0
<b>3</b>	2,6-lutidinium perchlorate	0.5 equiv	20%	36%	1.8 : 1.0
<b>4</b>	2,6-lutidinium perchlorate	1.0 equiv	20%	42%	2.1 : 1.0
<b>5</b>	2,6-lutidinium perchlorate	1.5 equiv	18%	40%	2.2 : 1.0
<b>6</b>	2,6-lutidinium perchlorate	2.0 equiv	18%	42%	2.3 : 1.0
<b>7</b>	2,6-lutidinium perchlorate	2.5 equiv	11%	46%	4.2 : 1.0
<b>8</b>	2,4,6-collidinium perchlorate	2.0 equiv	18%	32%	1.8 : 1.0

<sup>a</sup>Determined by <sup>1</sup>H NMR using mesitylene as internal standard.

**Table S16.** Impact of the TFE:MeCN ratio on the electrochemical synthesis of 2-(*tert*-butylsulfonyl)-1-iodoxybenzene **5**. Reaction conditions: 0.125 mmol of 2-(*tert*-butylsulfonyl)-1-iodo-4-methoxybenzene **1**, 5.0 mL of solvent, graphite anode, nickel cathode, and Ag<sup>+</sup>/Ag reference electrode in an undivided cell setup. The reaction mixture was electrolyzed until the current stopped changing or after 5.0 F/mol of charge was passed. Data are summarized in Figure 5.



Entry	Solvent	Potential (V)	Charge passed (F/mol)	Yield of 3 and 3·HClO <sub>4</sub> <sup>a</sup>	Yield of 5 <sup>a</sup>	5 : 3·(H <sup>+</sup> )
<b>1<sup>b</sup></b>	0% TFE/MeCN	1.51	3.6	10%	0%	<1.0 : 99
<b>2<sup>b,c</sup></b>	0% TFE/MeCN	1.51	2.5	82%	0%	<1.0 : 99
<b>3</b>	5% TFE/MeCN	1.53	3.6	28%	12%	1.0 : 2.3
<b>4<sup>b</sup></b>	5% TFE/MeCN	1.53	5.0	39%	0%	<1.0 : 99
<b>5</b>	10% TFE/MeCN	1.53	5.0	13%	48%	3.7 : 1.0
<b>6</b>	15% TFE/MeCN	1.53	5.0	11%	46%	4.2 : 1.0
<b>7</b>	20% TFE/MeCN	1.53	5.0	8%	44%	5.5 : 1.0
<b>8</b>	25% TFE/MeCN	1.54	4.7	9%	39%	4.3 : 1.0
<b>9</b>	40% TFE/MeCN	1.55	2.9	25%	19%	1.0 : 1.3
<b>10</b>	50% TFE/MeCN	1.56	2.7	33%	11%	1.0 : 3.0
<b>11</b>	75% TFE/MeCN	1.61	3.1	21%	6%	1.0 : 3.5
<b>12<sup>d</sup></b>	75% TFE/MeCN	1.61	2.0	43%	4%	1.0 : 11
<b>13</b>	100% TFE/MeCN	1.70	2.2	23%	5%	1.0 : 4.6
<b>14<sup>d</sup></b>	100% TFE/MeCN	1.70	2.3	51%	1%	1.0 : 51

<sup>a</sup>Determined by <sup>1</sup>H NMR using mesitylene as internal standard.

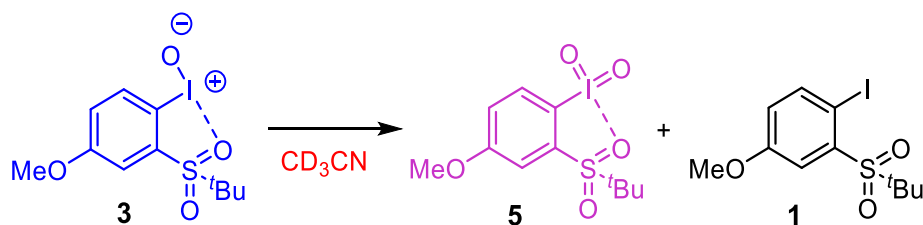
<sup>b</sup>Graphite cathode was used.

<sup>c</sup>Divided cell setup was used.

<sup>d</sup>No lutidinium perchlorate was added to the reaction mixture.

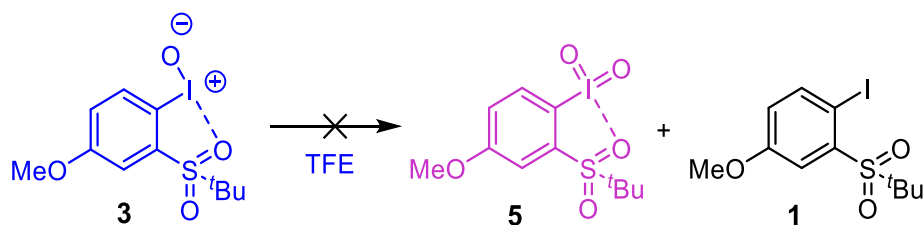
## F.4 Control Reactions

### Disproportionation of **3** in MeCN



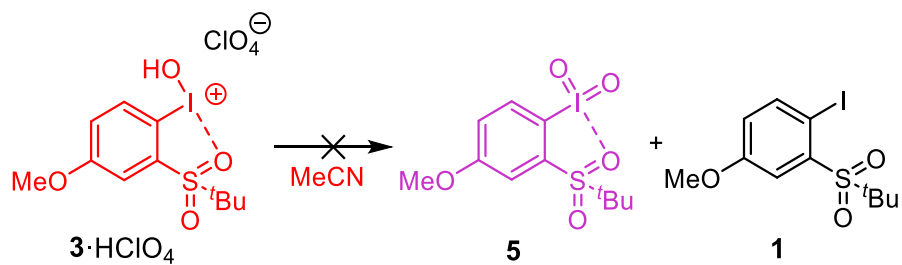
A test tube was charged with 2-(tert-butylsulfonyl)-1-iodosyl-4-methoxybenzene (**3**, 3.7 mg, 0.010 mmol) and  $\text{CD}_3\text{CN}$  (1.0 mL). The solution was filtered through a cotton plug, and the filtrate was analyzed by  $^1\text{H}$  NMR. The sample was allowed to sit for 10 h, and another  $^1\text{H}$  NMR spectrum was taken. The products **5** and **1** were observed to form in 42% and 48% NMR yield, respectively.

### Disproportionation of **3** in TFE



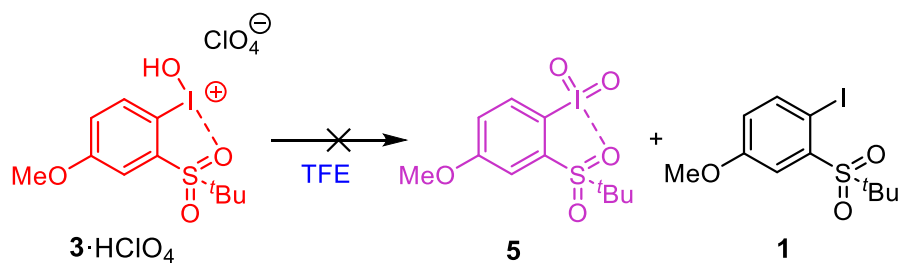
A test tube was charged with 2-(tert-butylsulfonyl)-1-iodosyl-4-methoxybenzene (**3**, 3.7 mg, 0.010 mmol) and TFE (1.0 mL). The solution was allowed to sit for 16 h. An aliquot (0.10 mL) of the reaction mixture was taken, diluted with  $\text{CD}_3\text{CN}$  (0.50 mL), and analyzed by  $^1\text{H}$  NMR. The products **5** and **1** were not observed.

*Disproportionation of 3·HClO<sub>4</sub> in MeCN*



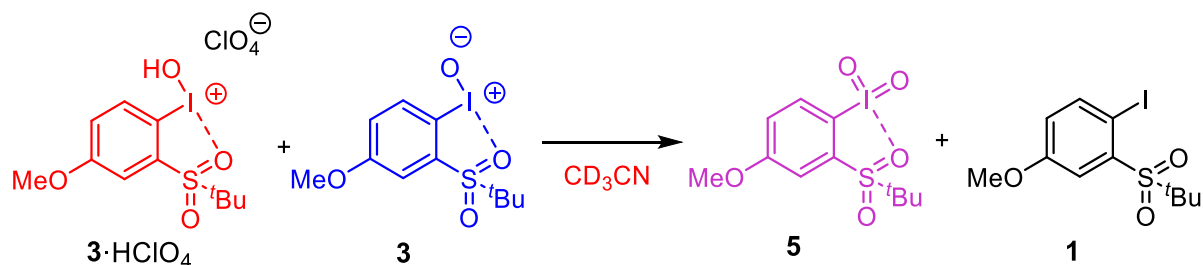
A test tube was charged with **3**·HClO<sub>4</sub> (4.7 mg, 0.010 mmol) and MeCN (1.0 mL). The solution was allowed to sit for 16 h. An aliquot (0.10 mL) of the reaction mixture was taken, diluted with CD<sub>3</sub>CN (0.50 mL), and analyzed by <sup>1</sup>H NMR. The products **5** and **1** were not observed.

*Disproportionation of 3·HClO<sub>4</sub> in TFE*



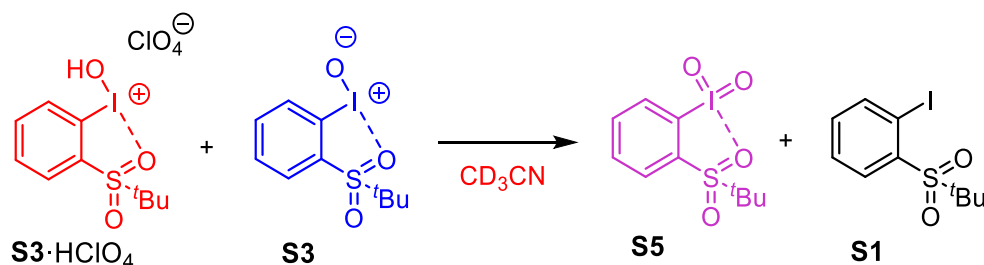
A test tube was charged with **3**·HClO<sub>4</sub> (4.7 mg, 0.010 mmol) and TFE (1.0 mL). The solution was allowed to sit for 16 h. An aliquot (0.10 mL) of the reaction mixture was taken, diluted with CD<sub>3</sub>CN (0.50 mL), and analyzed by <sup>1</sup>H NMR. The products **5** and **1** were not observed.

### Reaction of **3**·HClO<sub>4</sub> and **3**



A 20-ml scintillation vial was charged with **3**·HClO<sub>4</sub> (4.7 mg, 0.010 mmol, 1.0 equiv), **3** (3.7 mg, 0.010 mmol, 1.0 equiv), and CD<sub>3</sub>CN (1.0 mL). The reaction mixture was stirred for 1 h. Mesitylene was added as an internal standard, and a <sup>1</sup>H NMR spectrum of the solution was recorded. The products **5** and **1** were observed to form in 40% and 43% NMR yield, respectively.

### Reaction of **S3**·HClO<sub>4</sub> and **S3**



A 20-ml scintillation vial was charged with **S3**·HClO<sub>4</sub> (4.5 mg, 0.010 mmol, 1.0 equiv), **S3** (3.4 mg, 0.010 mmol, 1.0 equiv), and CD<sub>3</sub>CN (1.0 mL). The reaction mixture was stirred for 1 h. Mesitylene was added as an internal standard, and a <sup>1</sup>H NMR spectrum of the solution was recorded. The products **S5** and **S1** were observed to form in 40% and 48% NMR yield, respectively.

## G. NMR Spectra for New Compounds

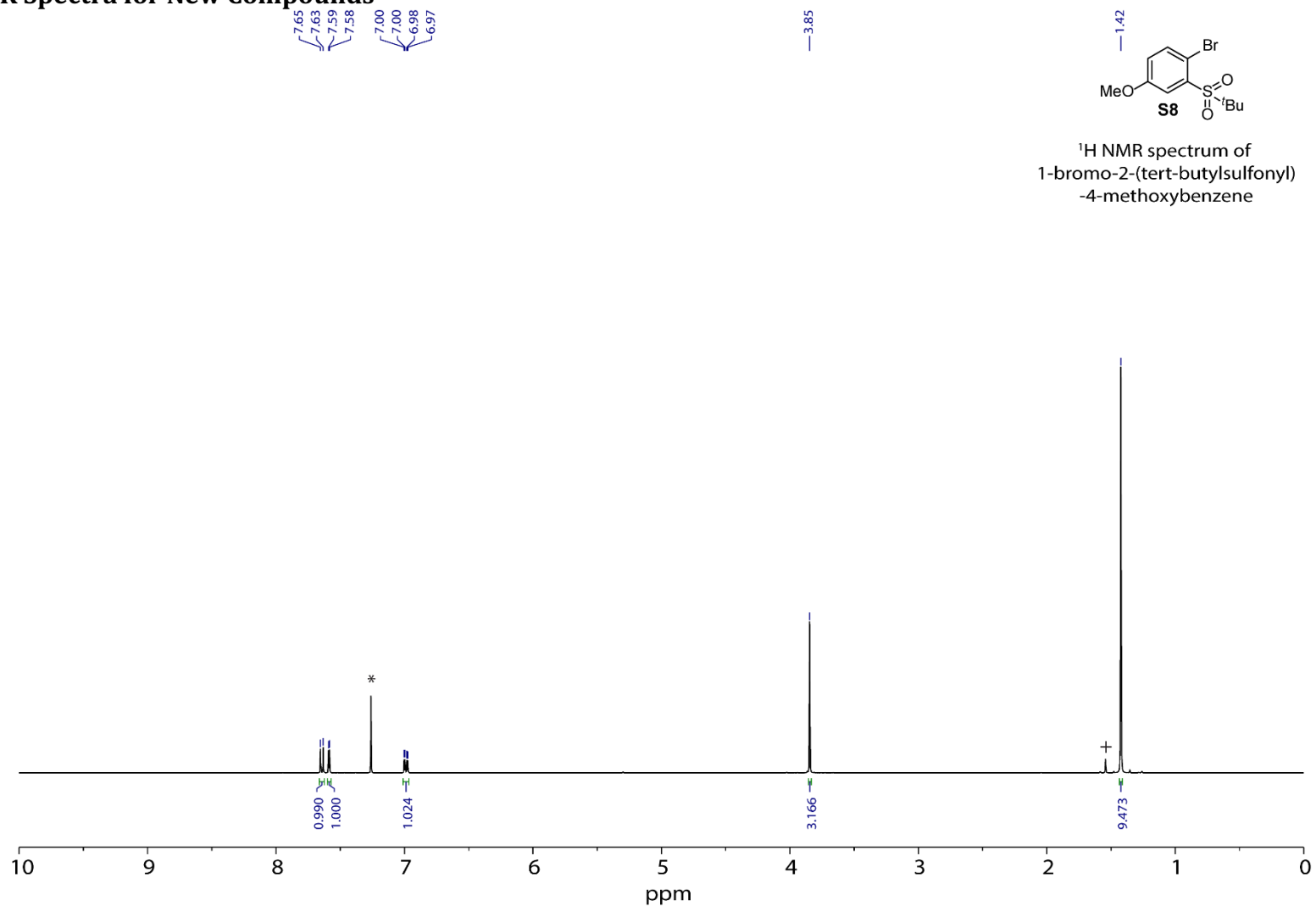


**Figure S28.** <sup>1</sup>H NMR spectrum of 1-bromo-2-(*tert*-butylsulfonyl)-4-methoxybenzene (**S8**) in CDCl<sub>3</sub> (400 MHz) at 23 °C. CDCl<sub>3</sub> solvent peak is marked with \*. Water peak is marked with +.

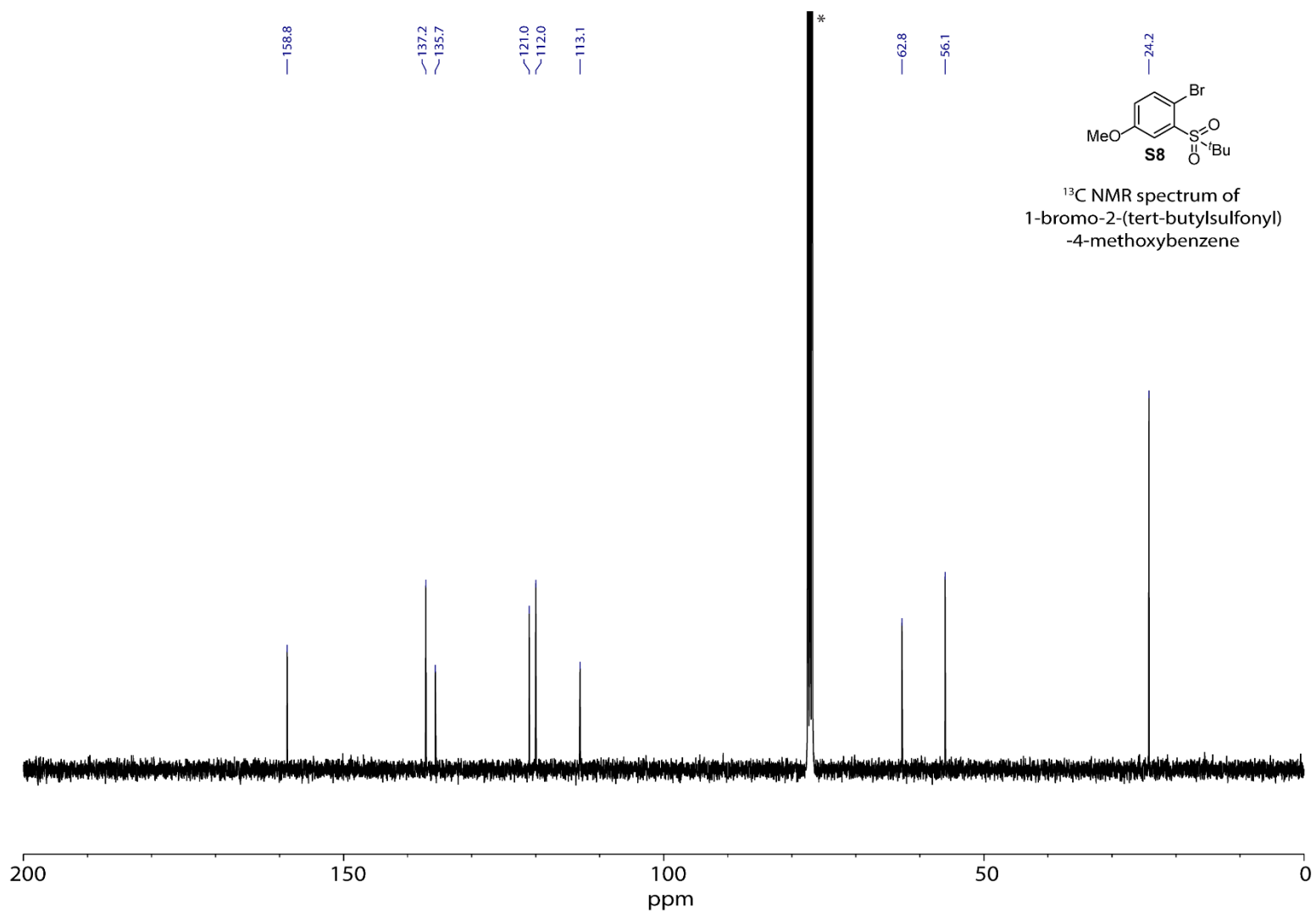


**Figure S29.** <sup>13</sup>C NMR spectrum of 1-bromo-2-(tert-butylsulfonyl)-4-methoxybenzene (**S8**) in CDCl<sub>3</sub> (100 MHz) at 23 °C. CDCl<sub>3</sub> solvent peak is marked with \*.

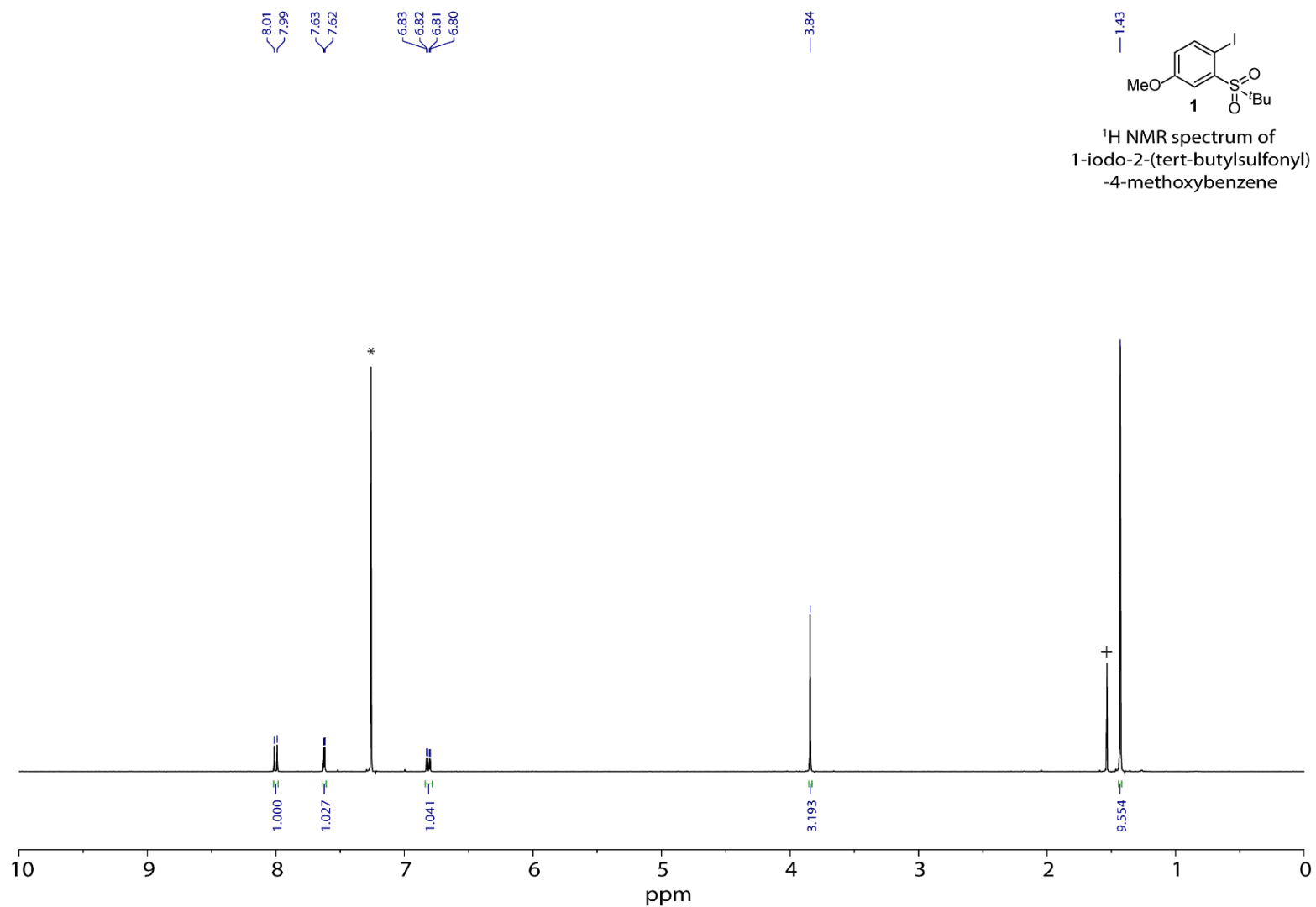


**Figure S30.** <sup>1</sup>H NMR spectrum of 2-(*tert*-butylsulfonyl)-1-iodo-4-methoxybenzene **1** in CDCl<sub>3</sub> (400 MHz) at 23 °C. CDCl<sub>3</sub> solvent peak is marked with \*. Water peak is marked with +.

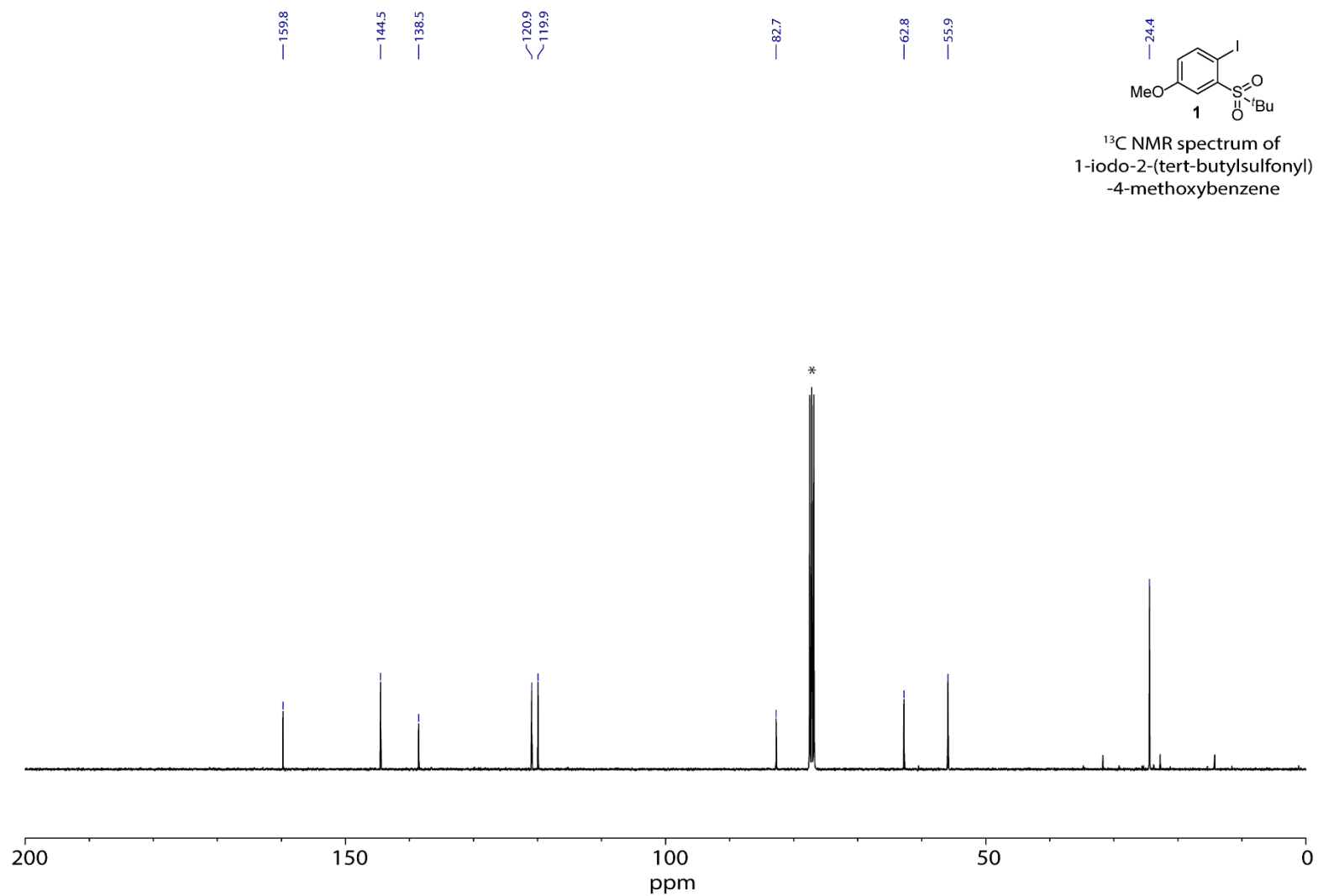


**Figure S31.** <sup>13</sup>C NMR spectrum of 2-(*tert*-butylsulfonyl)-1-iodo-4-methoxybenzene **1** in CDCl<sub>3</sub> (100 MHz) at 23 °C. CDCl<sub>3</sub> solvent peak is marked with \*.

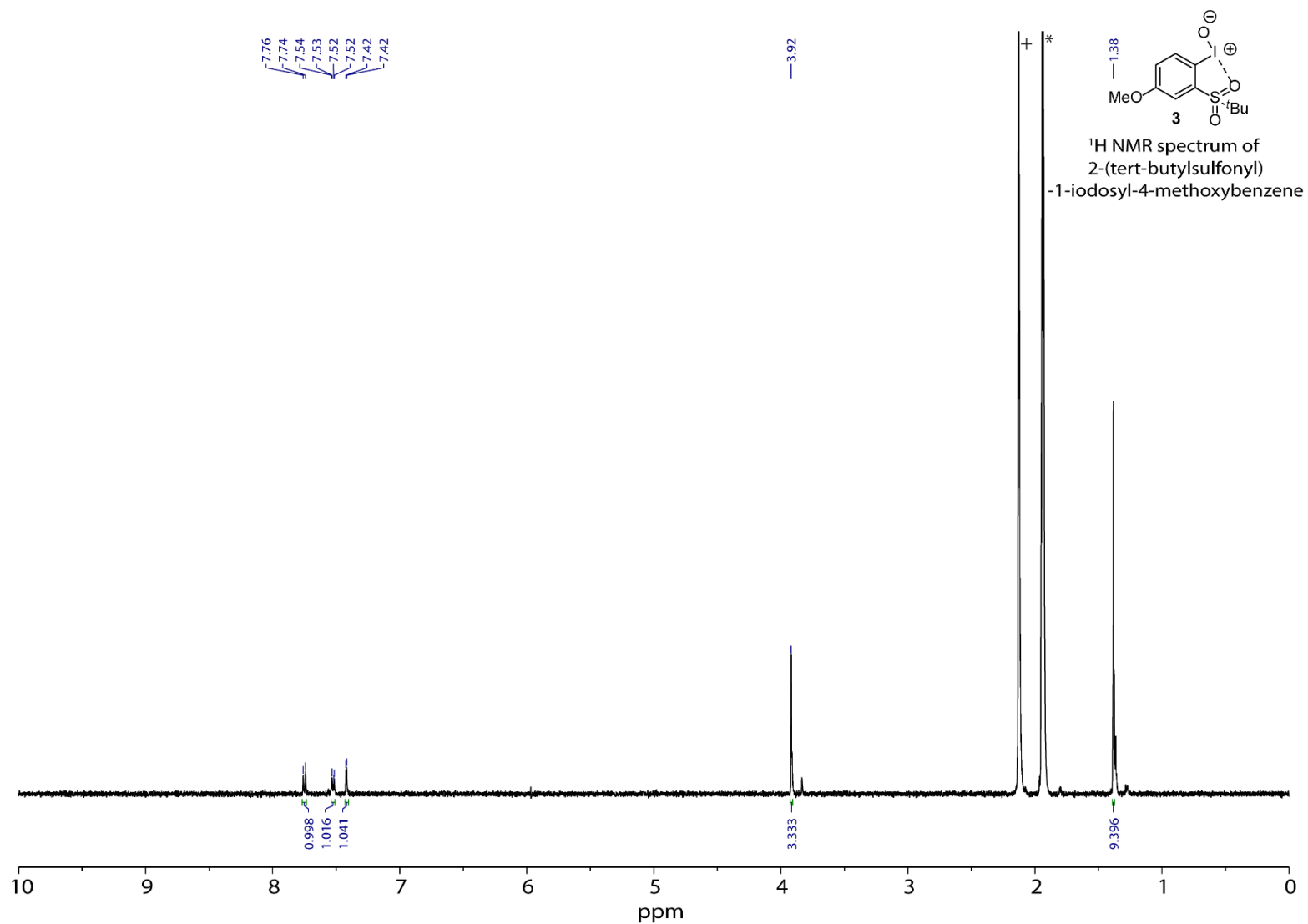


**Figure S32.** <sup>1</sup>H NMR spectrum of 2-(*tert*-butylsulfonyl)-1-iodosyl-4-methoxybenzene **3** in CD<sub>3</sub>CN (400 MHz) at 23 °C. CD<sub>3</sub>CN solvent peak is marked with \*. Water peak is marked with +.

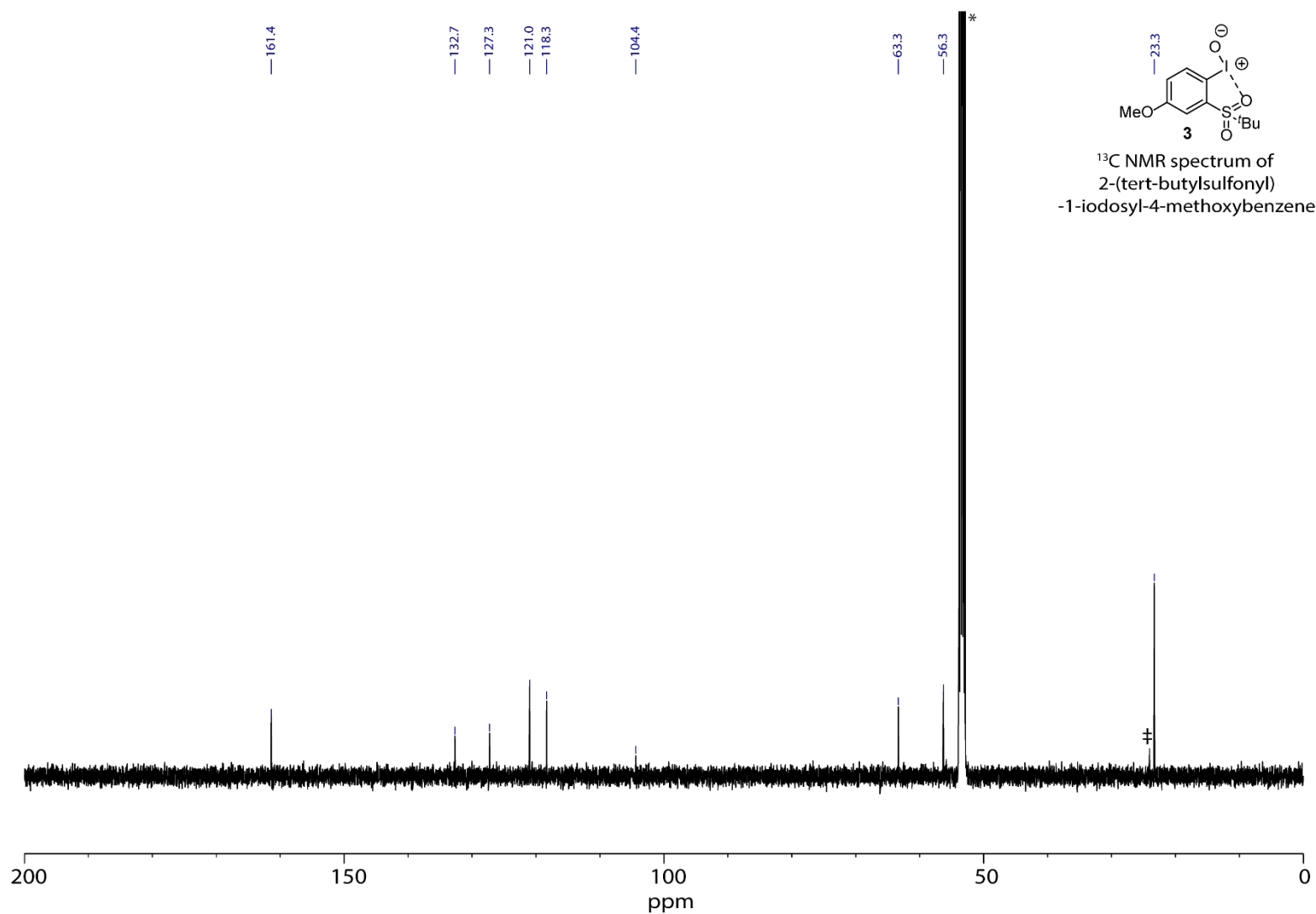


**Figure S33.** <sup>13</sup>C NMR spectrum of 2-(*tert*-butylsulfonyl)-1-iodosyl-4-methoxybenzene **3** in CD<sub>2</sub>Cl<sub>2</sub> (100 MHz) at 23 °C. CD<sub>2</sub>Cl<sub>2</sub> solvent peak is marked with \*. Peak of 2-(*tert*-butylsulfonyl)-1-iodo-4-methoxybenzene **1** is marked with †.

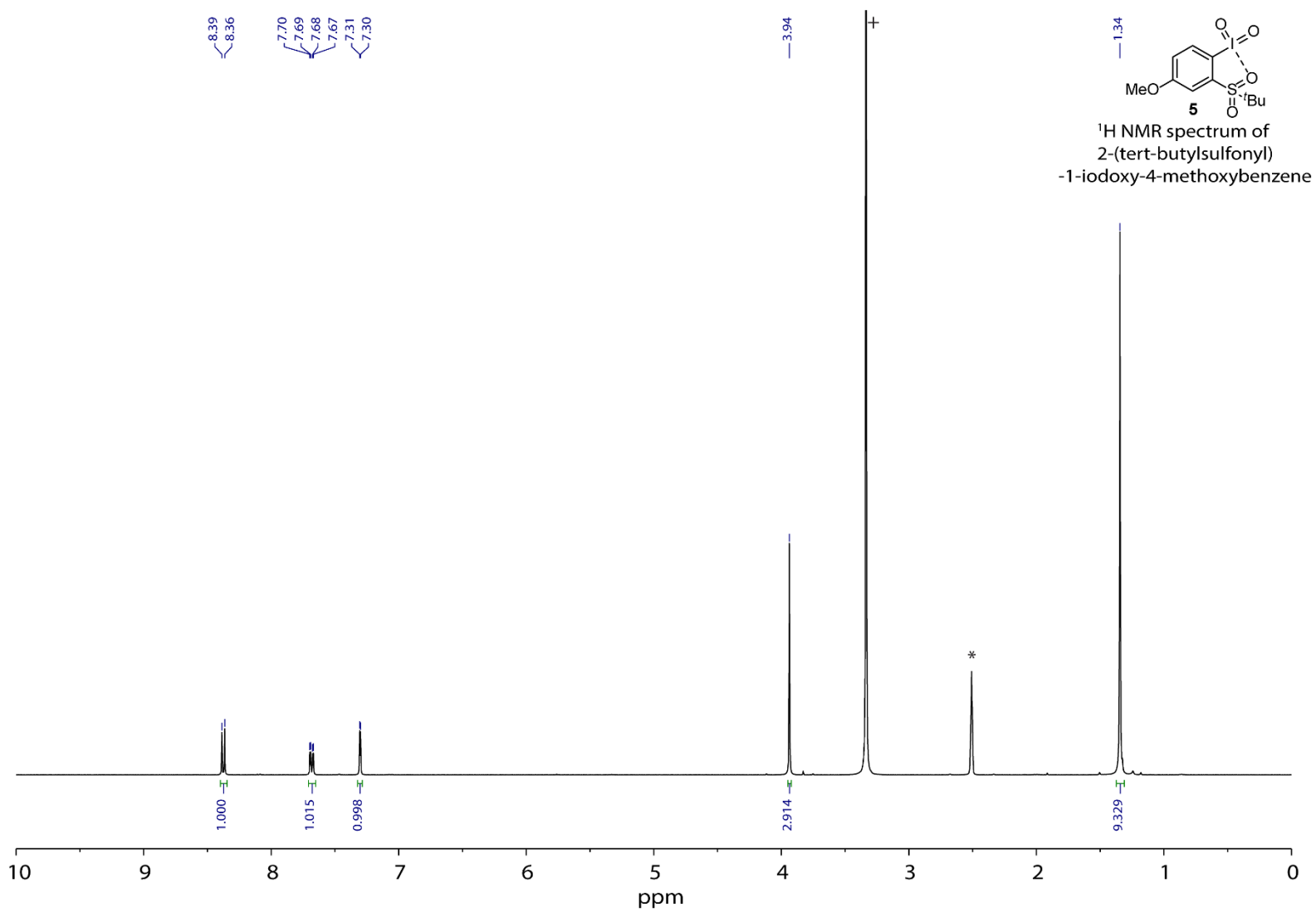


**Figure S34.** <sup>1</sup>H NMR spectrum of 2-(*tert*-butylsulfonyl)-1-iodoxy-4-methoxybenzene **5** in (CD<sub>3</sub>)<sub>2</sub>SO (400 MHz) at 23 °C. (CD<sub>3</sub>)<sub>2</sub>SO solvent peak is marked with \*. Water peak is marked with +.

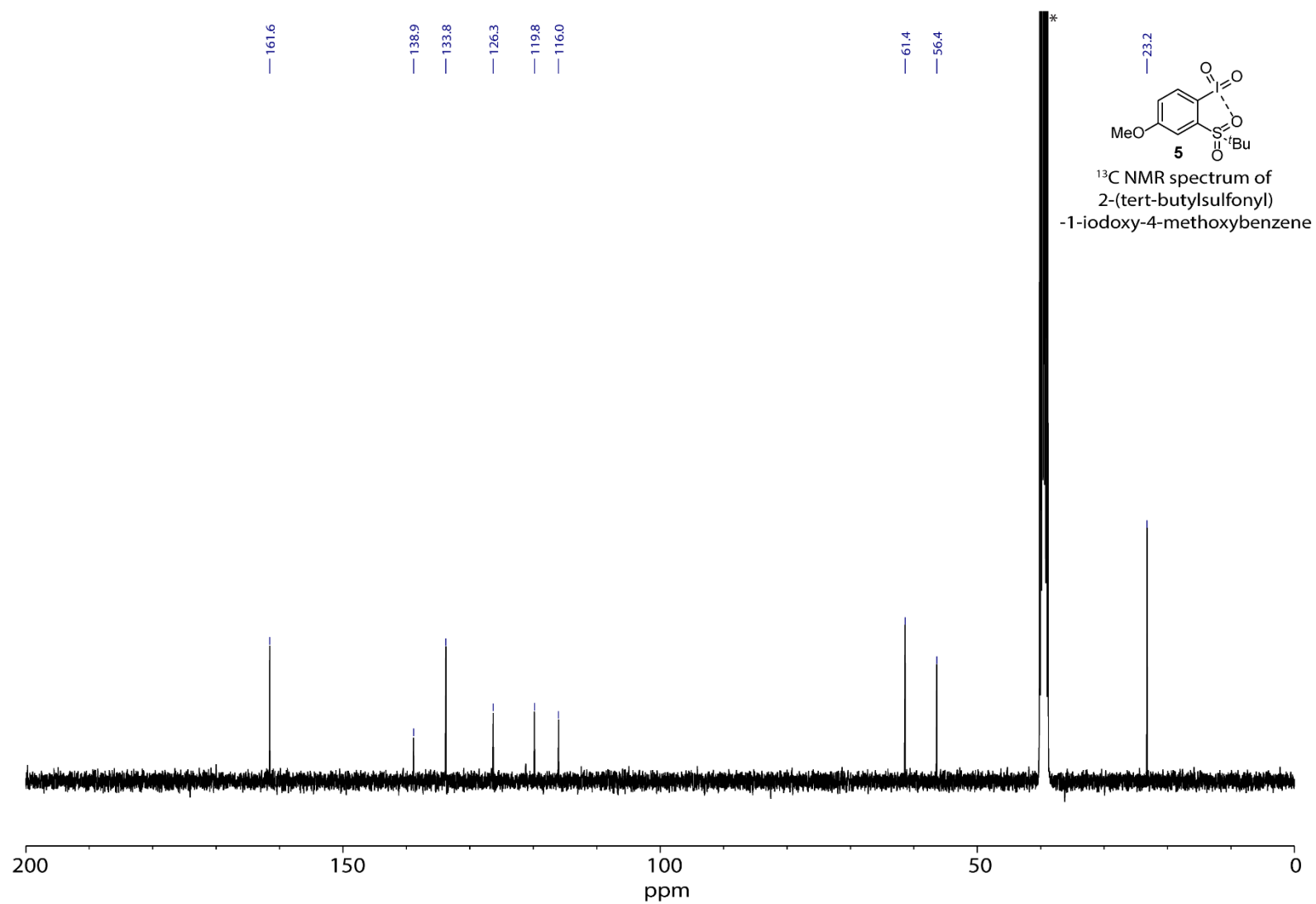


**Figure S35.** <sup>13</sup>C NMR spectrum of 2-(*tert*-butylsulfonyl)-1-iodoxy-4-methoxybenzene **5** in (CD<sub>3</sub>)<sub>2</sub>SO (100 MHz) at 23 °C. (CD<sub>3</sub>)<sub>2</sub>SO solvent peak is marked with \*.

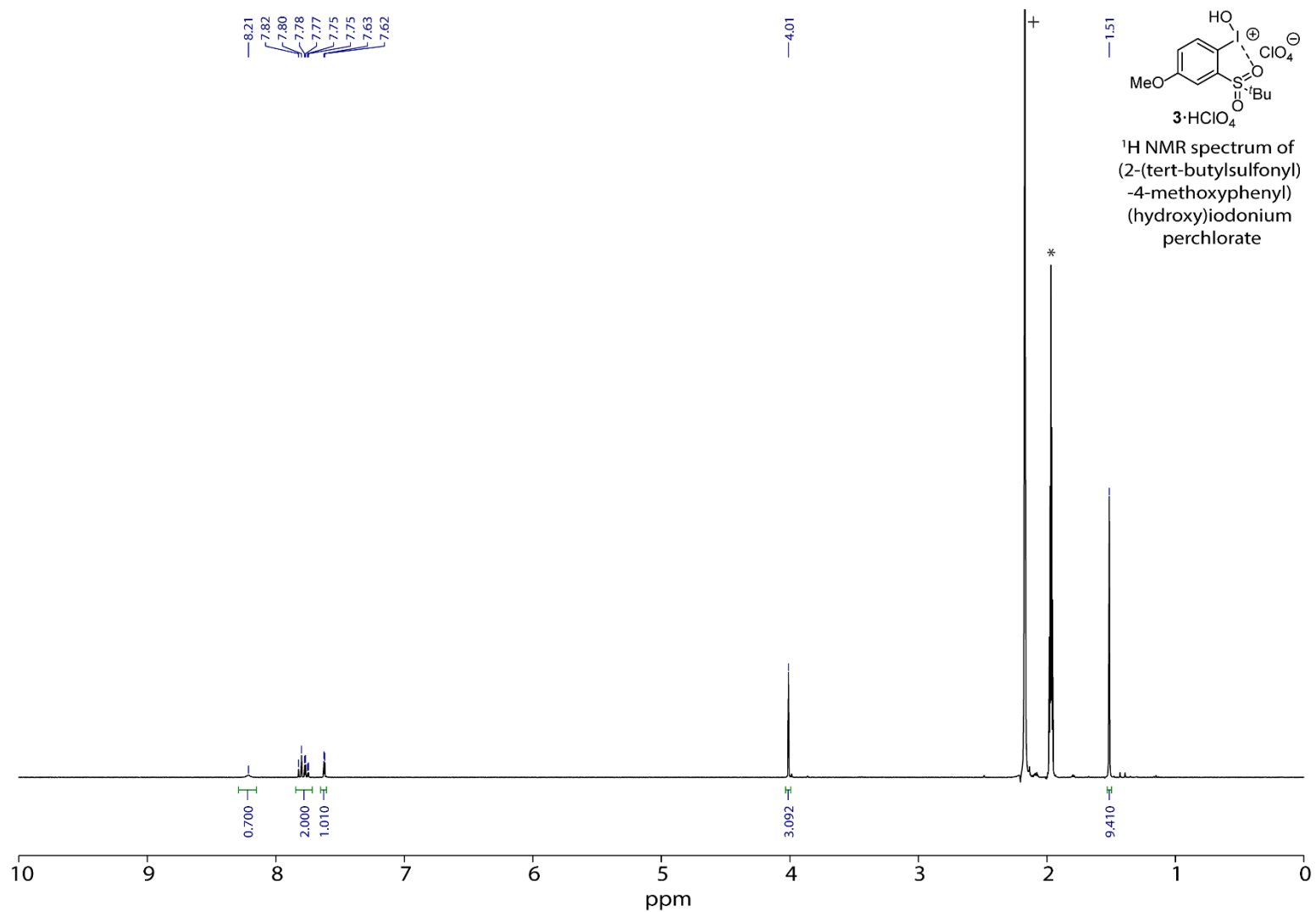


**Figure S36.** <sup>1</sup>H NMR spectrum of (2-(*tert*-butylsulfonyl)-4-methoxyphenyl)(hydroxy)iodonium perchlorate **3**·HClO<sub>4</sub> in CD<sub>3</sub>CN (400 MHz) at 23 °C. CD<sub>3</sub>CN solvent peak is marked with \*. H<sub>2</sub>O peak is marked with +.

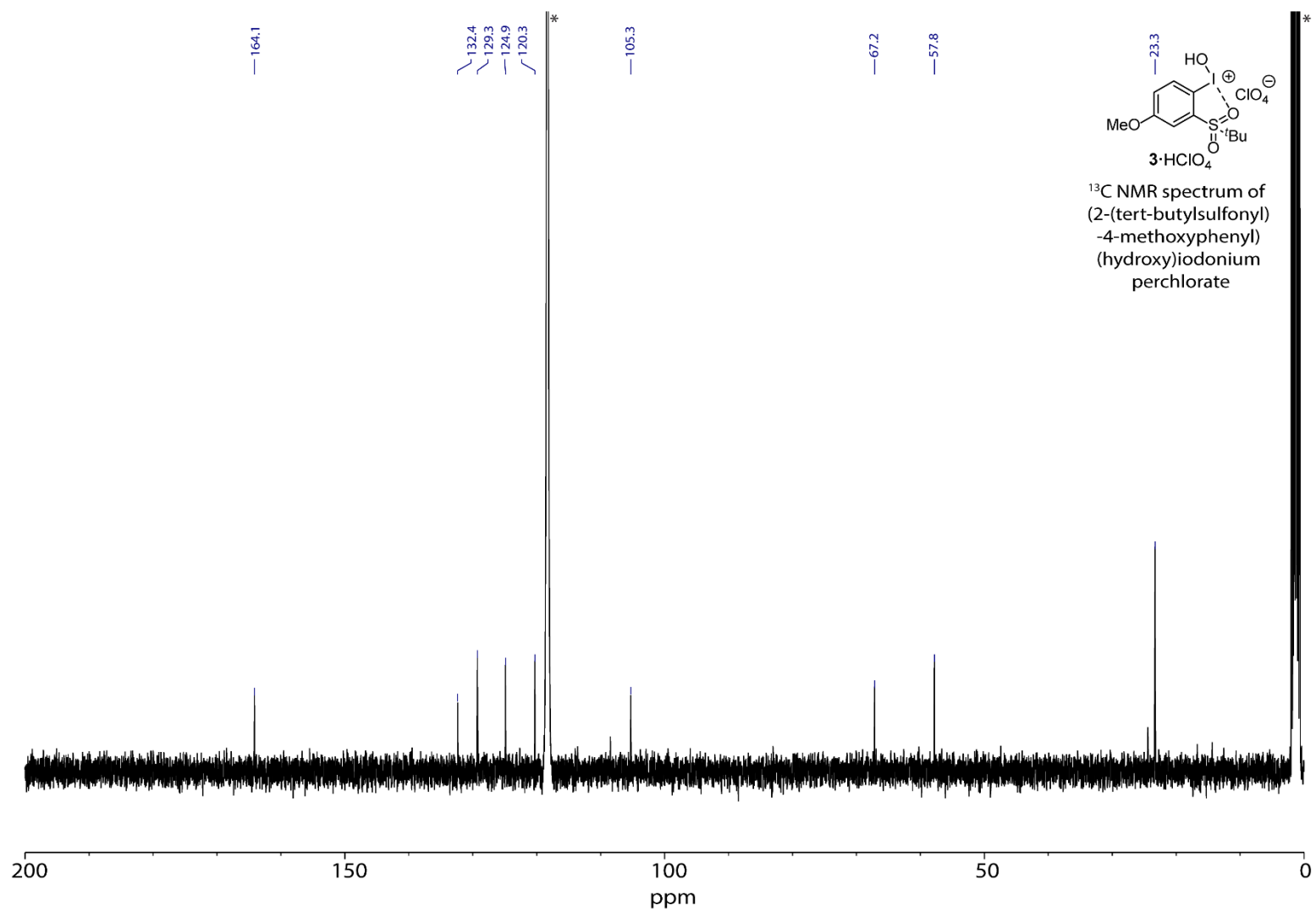


**Figure S37.** <sup>13</sup>C NMR spectrum of (2-(*tert*-butylsulfonyl)-4-methoxyphenyl)(hydroxy)iodonium perchlorate 3·HClO<sub>4</sub> in CD<sub>3</sub>CN (100 MHz) at 23 °C. CD<sub>3</sub>CN solvent peak is marked with \*.

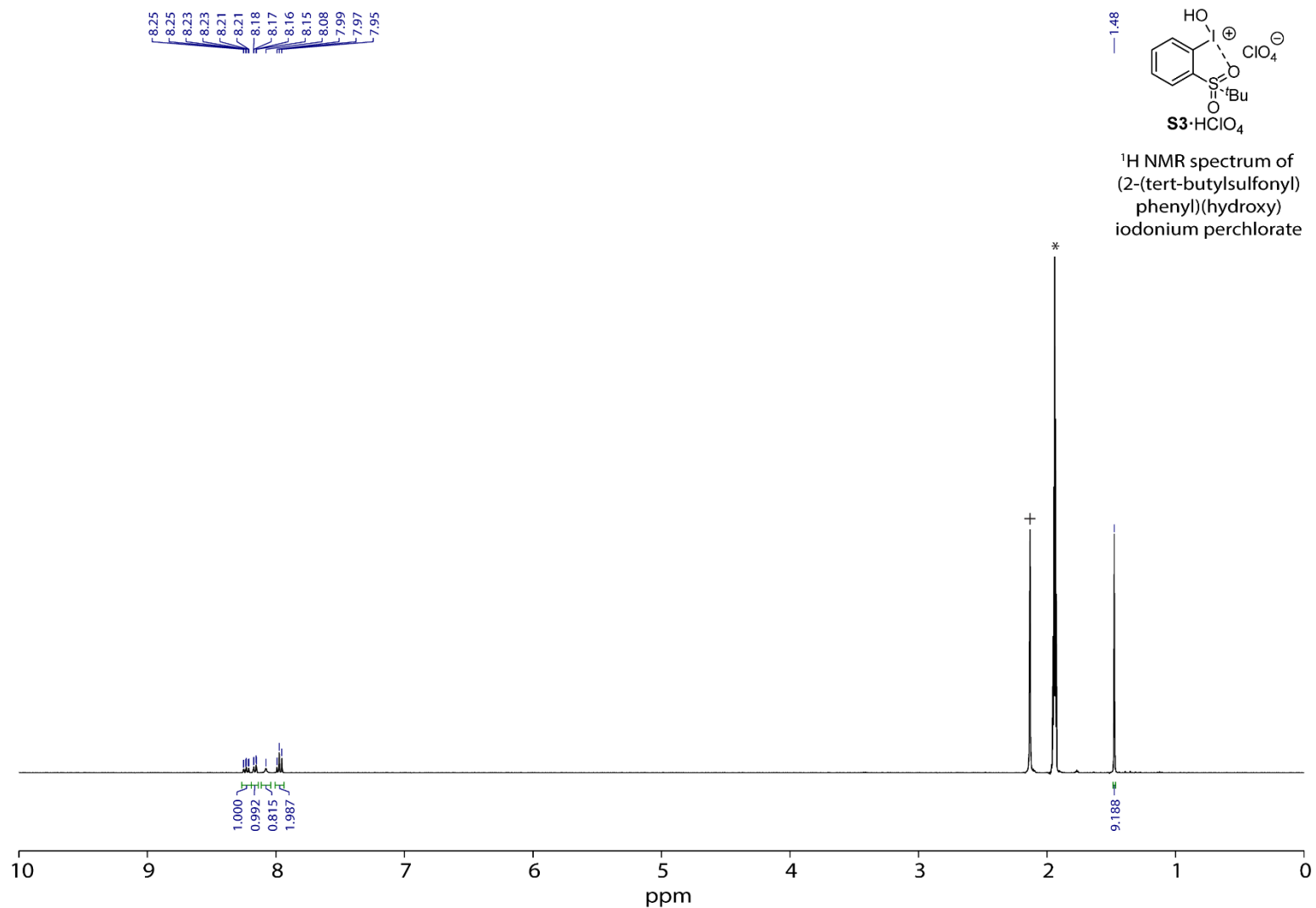


**Figure S38.** <sup>1</sup>H NMR spectrum of (2-(*tert*-butylsulfonyl)phenyl)(hydroxy)iodonium perchlorate **S3**·HClO<sub>4</sub> in CD<sub>3</sub>CN (400 MHz) at 23 °C. CD<sub>3</sub>CN solvent peak is marked with \*. H<sub>2</sub>O peak is marked with +.

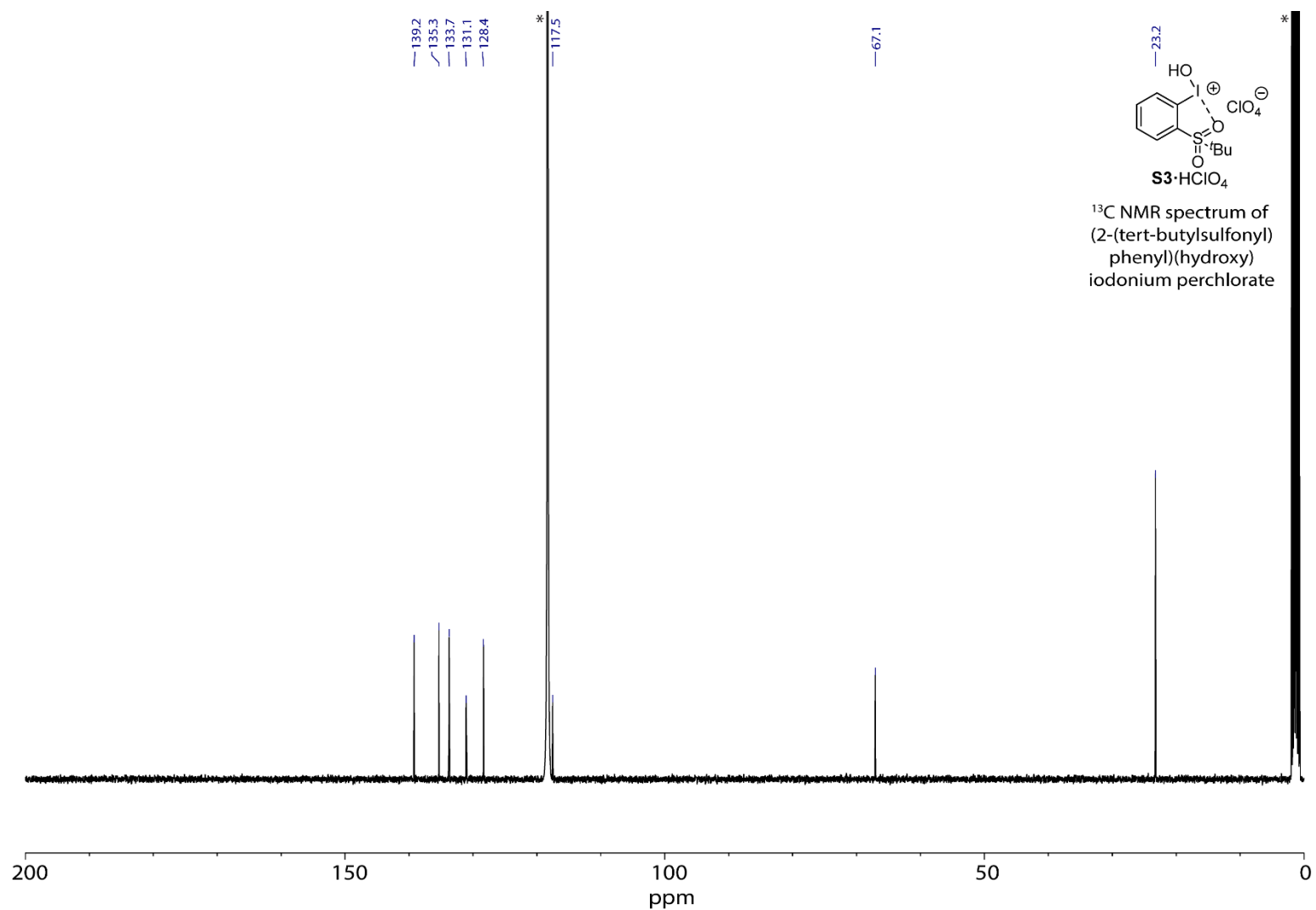


**Figure S39.**  $^{13}\text{C}$  NMR spectrum of (2-(*tert*-butylsulfonyl)phenyl)(hydroxy)iodonium perchlorate **S3**·HClO<sub>4</sub> in CD<sub>3</sub>CN (100 MHz) at 23 °C. CD<sub>3</sub>CN solvent peak is marked with \*.

## H. References

1. X. Li, F. Bai, C. Liu, X. Ma, C. Gu and B. Dai, *Org. Lett.*, 2021, **23**, 7445–7449.
2. A. D. Cardenal, A. Maity, W.-Y. Gao, R. Ashirov, S.-M. Hyun and D. C. Powers, *Inorg. Chem.*, 2019, **58**, 10543–10553.
3. A. Maity, S. M. Hyun, A. K. Wortman and D. C. Powers, *Angew. Chem. Int. Ed.*, 2018, **130**, 7323–7327.
4. C. Mukherjee and E. R. Biehl, *Heterocycles*, 2004, **63**, 2309–2318.
5. Z.-Z. Yang and L.-N. He, Beilstein *J. Org. Chem.*, 2014, **10**, 1959–1966.
6. G. R. Fulmer, A. J. M. Miller, N. H. Sherden, H. E. Gottlieb, A. Nudelman, B. M. Stoltz, J. E. Bercaw and K. I. Goldberg, *Organometallics*, 2010, **29**, 2176–2179.
7. G. M. Sheldrick, *Acta Crystallogr. A: Found. Crystallogr.*, 2008, **64**, 112–122.
8. G. M. Sheldrick, *Acta Crystallogr. C Struct. Chem.*, 2015, **71**, 3–8.
9. O. V. Dolomanov, L. J. Bourhis, R. J. Gildea, J. A. Howard and H. Puschmann, *J. Appl. Crystallogr.*, 2009, **42**, 339–341.
10. M. Frisch, G. Trucks, H. Schlegel, G. Scuseria, M. Robb, J. Cheeseman, G. Scalmani, V. Barone, G. Petersson and H. Nakatsuji, Gaussian 16 Rev. C. 01, Wallingford, 2016.
11. A. D. Becke, Density-functional thermochemistry. I. *J. Chem. Phys.*, 1992, **96**, 2155–2160.
12. C. Lee, W. Yang and R. G. Parr, *Phys. Rev. B*, 1988, **37**, 785.
13. S. Grimme, *J. Comput. Chem.*, 2006, **27**, 1787–1799.
14. S. Grimme, S. Ehrlich and L. Goerigk, *J. Comput. Chem.*, 2011, **32**, 1456–1465.
15. K. A. Peterson, D. Figgen, E. Goll, H. Stoll and M. Dolg, *J. Chem. Phys.*, 2003, **119**, 11113–11123.
16. F. Weigend and R. Ahlrichs, *Phys. Chem. Chem. Phys.*, 2005, **7**, 3297–3305.
17. G. Petersson and M. A. Al-Laham, *J. Chem. Phys.*, 1991, **94**, 6081–6090.
18. A. McLean and G. Chandler, *J. Chem. Phys.*, 1980, **72**, 5639–5648.
19. A. V. Marenich, C. J. Cramer and D. G. Truhlar, *J. Phys. Chem. B*, 2009, **113**, 6378–6396.
20. M. A. Marques and E. K. Gross, *Annu. Rev. Phys. Chem.*, 2004, **55**, 427–455.
21. R. Dennington, T. Keith and J. Millam, GaussView, (Version 6.1.1.), Shawnee Mission, KS, 2019.
22. R. S. Drago, *Physical Methods for Chemists*, Gainesville, FL, 1992.
23. M. C. Leech and K. Lam, *Nat. Rev. Chem.*, 2022, **6**, 275–286.